Gamma Band Oscillation Response to Somatosensory Feedback Stimulation Schemes Constructed on Basis of Biphasic Neural Touch Representation

by

Justin C. Tanner

A Dissertation Presented in Partial Fulfillment
of the Requirements for the Degree
Doctor of Philosophy

Approved July 2017 by the
Graduate Supervisory Committee:

Stephen Helms Tillery, Chair
Marco Santello
Christopher Buneo
Veronica Santos
Bradley Greger

ARIZONA STATE UNIVERSITY

August 2017

ABSTRACT

Prosthetic users abandon devices due to difficulties performing tasks without proper graded or interpretable feedback. The inability to adequately detect and correct error of the device leads to failure and frustration. In advanced prostheses, peripheral nerve stimulation can be used to deliver sensations, but standard schemes used in sensorized prosthetic systems induce percepts inconsistent with natural sensations, providing limited benefit. Recent uses of time varying stimulation strategies appear to produce more practical sensations, but without a clear path to pursue improvements. This dissertation examines the use of physiologically based stimulation strategies to elicit sensations that are more readily interpretable. A psychophysical experiment designed to investigate sensitivities to the discrimination of perturbation direction within precision grip suggests that perception is biomechanically referenced: increased sensitivities along the ulnar-radial axis align with potential anisotropic deformation of the finger pad, indicating somatosensation uses internal information rather than environmental. Contact-site and direction dependent deformation of the finger pad activates complimentary fast adapting and slow adapting mechanoreceptors, exhibiting parallel activity of the two associate temporal patterns: static and dynamic. The spectrum of temporal activity seen in somatosensory cortex can be explained by a combined representation of these distinct response dynamics, a phenomenon referred in this dissertation to "biphasic representation." In a reach-to-precision-grasp task, neurons in somatosensory cortex were found to possess biphasic firing patterns in their responses to texture, orientation, and movement. Sensitivities seem to align with variable deformation and mechanoreceptor activity: movement and smooth texture responses align with potential fast adapting activation, non-movement and coarse texture responses align with potential increased slow adapting activation, and responses to orientation are conceptually consistent with coding of tangential load. Using evidence of biphasic representations' association with perceptual priorities,

gamma band phase locking is used to compare responses to peripheral nerve stimulation patterns and mechanical stimulation. Vibrotactile and punctate mechanical stimuli are used to represent the practical and impractical percepts commonly observed in peripheral nerve stimulation feedback. Standard patterns of constant parameters closely mimic impractical vibrotactile stimulation while biphasic patterns better mimic punctate stimulation and provide a platform to investigate intragrip dynamics representing contextual activation.

ACKNOWLEDGMENTS

Over the years, this project and my progress has been helped in innumerable ways in discussion, support, or active help. My family, who has always encouraged me to do exactly what I want in life and how to maintain passionate optimism with balanced realism. They taught me that success lies in overcoming challenges, not in accumulating accomplishments. I would not be who I am without the patience provided and curiosity developed by my parents and brother.

Working with the Sensory Motor Research Group has been such an incredibly positive personal and professional experience. I cannot imagine accomplishing this alone, without their community of support and insight. Stephanie Naufel introduced me to the first experiments at ASU, and helped guide me. Naomi Newman's persistence in helping design and execute experiments was profoundly helpful. Taylor Hearn has worked closely with me in the recent years, developing analysis procedures and contributing constant feedback to my questions. Cynthia Overstreet was the senior student in the lab when I started and I was continually catching up to what she knew how to do. Rachele McAndrew's efforts in the lab and with RARF are vital to our work, and the humor keeps the lab sane. My mentor, Steve Helms Tillery, has guided me through grad school patiently and intently. What I have learned from him about what it means to be a researcher, choosing your goals, and preserving curiosity will persist in who I am continuously.

My undergraduate advisor, Dr. David Lin, once provided an opportunity for our BMES chapter to observe a talk on neuroprosthetic sensory feedback and have a subsequent class discussion with the presenter. This was the initial spark the drove me here, rekindled by Dr. Howard Davis when in doubt – who assured me that there was so much left to be done.

Jonathan Cheng and Ed Keefer of Nerves Incorporated have been a pleasure to work with, and have made the peripheral experiments possible with technical designs and surgical experience.

This work would not be possible without DACT ensuring our animal subjects have healthy, enriched lives, with successful surgeries and recovery. I would also like to thank Kringle, Tiberius, and River for being so incredibly helpful and patient.

Finally, the work presented in this thesis was partially funded by both the National Science Foundation Cyber Physical Systems and DARPA HAPTIX programs.

TABLE OF CONTENTS

Page

Page

PAGE

INTRODUCTION

In this dissertation, it is argued that the tactile input during grip is largely modulated by biomechanical factors occurring at object interaction and can be mimicked for sensory feedback for peripheral nerve stimulation. During grip, the coactivation of tonic and phasic mechanoreceptors provide a highly variable and sensitive framework that informs grip adjustments. The neural representation of this can appear sensitive to multiple variables, but can be explained by complex variation in a single variable's space. This sensitivity within grip is argued to be referenced internal to the grip biomechanics, not due to external factors that would require large amounts of multisensory integration. Recordings of somatosensory cortex representations during active grip conditions mimic the distal sensory coactivation in terms of dynamic onsets and sustained responses. For multimodal cells, the joint sensitivities are explained in terms of increased components of this activation. Use of a physiological mimic as an input model for peripheral nerve stimulation is evaluated in terms of intracortical local field potential dynamics of somatosensory cortex. In comparison to basic stimulation paradigms, the mimic demonstrates responses similar to normal mechanical activation.

ARRANGEMENT OF SOMATOSENSORY CORTEX.

Sensorimotor cortex is well described in terms of structures that possess some degree of specialized functions. The relationships and functions of these structures are intimately related and the cortices are architectonically connected. With regards to substructures of somatosensory cortex, area 1 and 3b are in the rostral bank of the postcentral gyrus, with area 3a at the fundus of the central sulcus. Motor area 4 is rostral adjacent to 3a in the precentral gyrus. Area 3b projects to areas 1 and 2, area 3a reciprocally links to area 1, and area 2 reciprocally links to area 4. Area 3a is suggested to be so intimately connected to motor area 4

that it should be not be considered a separate entity (E. G. Jones, Coulter, & Hendry, 1978).

Somatotopic representations of the hand are present, but not exclusively so, in area 1, 2, 3b, and 4. The hand portion of these representations are rostral and just medial to the terminus of the intraparietal sulcus, all on the surface except area 3b and 4, with 3b between 3 and 8 mm deep into the post central gyrus of *Macaca mulatta*. In both humans and *Macaca mulatta*, areas 1, 2, and 3b have consistent lateromedial digit organization, from digit 1 to digit 5 (Geyer, Schleicher, & Zilles, 1999; Pons, Garraghty, Cusick, & Kaas, 1985; Pons, Wall, Garraghty, Cusick, & Kaas, 1987). Small receptive fields to cutaneous stimulation are also present in both humans and *Macaca mulatta* area 3b, with experienced induced plasticity based on the subjects' environment (Xerri, Coq, Merzenich, & Jenkins, 1996). Increase complex use of the hand increases the cortical representation and spatial resolution of the cutaneous palmar surface. Area 4, while predominantly representing motor activity, also possessed two distinct sensory representations with large receptive fields: one caudal with cutaneous responses and one rostral with deep sensory responses (Strick & Preston, 1982a, 1982b).

Physiological connections and somatotopic similarity begin to illustrate the functional relationships between structures. Encoding reinforces this relation as tactile location information is almost simultaneously represented in areas 3b and 2 (Nicolelis et al., 1998). From lesion studies, area 3b and/or 3a ablation removes general responsivity of area 1 (Garraghty, Florence, & Kaas, 1990). The psychophysical limitations of these lesions elucidates the functional purpose of the structures inputs. Area 3b ablation eliminates texture and shape discrimination, area 1 ablation eliminates just texture discrimination, and area 2 ablation eliminates tactile angle discrimination (Randolph & Semmes, 1974). This coincides with studies

showing area 3b encodes spatial properties such as texture while area 2 encodes tactile curvature and the shape of stimulus features (DiCarlo & Johnson, 2000; DiCarlo, Johnson, & Hsiao, 1998; Yau, Connor, & Hsiao, 2013).

Single-unit responses across somatosensory cortices are thoroughly explored in response to precision grip tasks (Salimi, Brochier, & Smith, 1999a). Areas 3b, 1, and 2 exhibit activity across a spectrum of static sustained spiking with some adaptation, dynamic rates of spiking that show higher activity at the onset and release of grip or changes within the grip, and even pre-grip firing properties. This activity mimics varied activation of the afferent mechanoreceptor inputs, possessing similar onset-release, sustained, and intragrip patterns of spiking. Receptive fields are specific to individual digits for area 3b, but areas 1 and 2 can show receptive fields for single or multiple digits at once. Areas 1 and 3b are the ideal locations to investigate the responses of textures, with both show area 1 likely showing complex responses to additional grip aspects as it is more intrinsically connected and evidenced to have tactile modulation during arm movement (Song & Francis, 2013).

CONTEXTUAL PERCEPTION BASED IN BIOMECHANICS

Texture Perception. Roughness estimation depends on properties of the texture and the tactile action involved, invoking parallel spatial and vibrational models of information. In a series of experiments, roughness estimation was evaluated using machined aluminum textures with varying groove width and land width from 125 μm to 1.25 mm. Roughness estimation was shown to be a direct function of groove width and an inverse function of land width (Lederman, 1974). A static spatial model of skin displacement from the stimulus features efficiently predicts the roughness estimations; increased groove width displaces more skin and increased land width reduces the amount of grooves and therefore reduces displacement (Taylor & Lederman, 1975). For low spatial periods and when groove

widths become wider than ~3mm, the roughness estimation decreases as the spatial variation of skin displacement is low, i.e. the skin does not fit into the narrow grooves. With high spatial periods, the skin is functionally touching the smooth base of the groove and receiving little spatial displacement (Connor, Hsiao, Phillips, & Johnson, 1990). Reinforcing that perception of these textures is composed of spatial information rather than temporal: the estimations were independent of finger scanning speeds and undisrupted by vibrational adaptation (Lederman, Loomis, & Williams, 1982).

Features with spatial periods below 125 μm induce little skin displacement and are therefore reported as smooth. Feature detection and texture discrimination within these ranges becomes possible with the introduction of temporal properties. Using a scanning motion, stimulus features of 2 μm can be detected and roughness estimation can be accurate for textures possessing a spatial period of less than 125 μm (Hollins & Risner, 2000). Unlike the coarse texture estimation, fine texture estimation is disrupted via vibrational adaptation. Direct and indirect exposure to vibrations pre-estimation decreases the perceived roughness of the texture. This is likely because the fine texture roughness estimation is a function of the vibrations induced by the skin-texture scanning interaction and the adaptation of perceived vibration is well established. Peak induced frequency is inversely related to the spatial period, implying that smoothness is perceived via higher generated frequency from scanning (S. BensmaÏa, Hollins, & Yau, 2005; S. J. BensmaÏa & Hollins, 2003).

Texture Encoding. Tactile transduction starts with a suite of mechanoreceptors specialized to specific stimuli, with high density on the finger pads. Based on the properties of the response, receptors are grouped into categories as tonic slow adapting, Merkel-neurite complexes (SA1) and Ruffini corpuscles (SAII), or phasic fast adapting, Meissner corpuscles (FAI) and Pacinian corpuscles

(PC). (Chapter 2, Table 1) Tonic responses are consistent over the period of the stimuli, with little adaptation. Phasic responses respond more to the change in the stimuli, rather than the presence. For this reason, tonic receptors are more responsive to static stimuli and phasic receptors to dynamic stimuli, like vibrations. For a succinct summary of the response properties and receptive fields of these receptors, refer to Table 1 (Kenneth O Johnson, 2001; Klatzky, Lederman, Hamilton, Grindley, & Swendsen, 2003; Wolfe et al., 2008).

Spatial and temporal mechanisms have been established for perception of coarse and fine surfaces, respectively. Spatial systems rely on skin deformations and temporal systems rely on the vibrational power generated during scanning or manipulation. Obvious implications arise while attempting to associate response properties of the mechanoreceptors to the mechanisms. With respect to textures and using coarse variations in raised dot patterns, the activity of spatial variance of firing activity, especially for SAI, accounted for the psychophysical results of roughness estimation while temporal spiking information provided little information (Connor & Johnson, 1992; K. O. Johnson, Yoshioka, & Vega-Bermudez, 2000; LaMotte & Whitehouse, 1986; Srinivasan, Whitehouse, & LaMotte, 1990). Eliminating the SAI terminal endings, the Merkel-neurite complex, via genetically engineered mice show a profound inability to discriminate coarse textures with their feet (Maricich, Morrison, Mathes, & Brewer, 2012).

Selective activation of the SA1 system decreases as static surface features become more difficult to detect. Eventually, only PC system activation is present for minimally detectable microgeometries (LaMotte & Whitehouse, 1986). Within this fine texture range, detection was associated with the peak vibrational power generated from scanning movements, and the vibrational power spectra is consistent across subjects for a single texture (S. J. Bensmaia & Hollins, 2003). Since the PC

system activity is the only mechanoreceptor system active within these ranges, a frequency sensitivity model can be constructed to predict the systems discriminability. These vibrational powers generated during scanning align with PC frequency filter from the model (Bensmaïa & Hollins, 2005; S. Bensmaia et al., 2005). Conceptually, the temporal component of texture recognition is separated from spatial "roughness" and termed "textural timbre."

Cortical areas 1, 2, and 3b possess representations sensitive to the spatial and temporal components associated with texture perception. Discriminating between spatiotemporal variation in a passive texture presentation, all areas produce phasic and tonic responses (Tremblay, Ageranioti-Belanger, & Chapman, 1996). Responses proportional to coarse groove width and stroke velocity demonstrates both tonic and phasic activity, respectively sensitive to force and velocity. That is, individual representations of tactile information of texture included both spatial and temporally sensitive components (Sinclair & Burton, 1991). In a series of lift and hold tasks, somatosensory cortex shows multimodal sensitivity to texture along with force loading, again showing a spectrum of tonic and phasic activity. While two main systems encode texture in separate spatiotemporal models, the perception of texture is represented by conjoined cortical activity.

Static and coarse information are explained through the SAI system via constant skin indentations that activate the Merkel mechanoreceptors. These provide consistent peripheral activation with little adaptation to the stimuli or vibrational disruptions. Discrimination and detection of finer textures can be explained thoroughly by the vibrational power generated during scanning motions and the PC system sensitivity to the associated range of frequencies. Cortical representations of conjoined dynamics indicate that complete perception incorporates the information from both simultaneously. Again, the systems are not mutually exclusive, but use

separate competing and complementary mechanisms to explain subtle differences in texture and touch.

Tactile Properties of Precision Grip. Precision grip consists of the first and second digits' distal phalanges pressing on an object with opposing force; how you might pick up a cherry or marble. Distinguishing between the two objects requires determination of obvious properties like texture, weight, and firmness. Perception of these properties within an active grip relies on reactive properties to biomechanical information of the skin. Response properties of this grip are well documented, and can vary greatly with grip or object context. This highlights the dynamic nature of grip, and the self-structuring nature of grip stability. By self-structuring, it is meant that sensory information and contextual state of a task can change the action of the task. The system adapts with the results of its own actions in a way that primarily preserves the safety margin for stability (Westling & Johansson, 1984).

Perturbations in grasp induce force responses that are modulated by properties of the grasp itself, and scaled to maintain an appropriate safety factor. Load forces distal and proximal to the hand during precision grip induce proportional grip responses, inversely scaled to coarseness of the object (L. A. Jones & Hunter, 1992). Similarly, unexpected loading forces distal to the grip and with the direction of gravity induce increased force magnitude and decreased force latency, e.g. faster and stronger responses in dangerous directions. Inverting the hand maintains this pattern, implying that both body and environmental references inform grip response (Häger-Ross, Cole, & Johansson, 1996). Even unexpected rotational perturbations pulling the object away from the precision grip induced stronger responses than perturbations rotating the grip along the distal-proximal axis (De Gregorio & Santos, 2013). These contextual and anisotropic responses indicate complex sensory activation during precision grip that allows for precise and useful reactive responses.

Short latencies of grip responses to unexpected movements suggest spinal or subspinal reflexive circuits, meaning on-line perception is likely not the primary mechanism for reactive grip structuring. However, the cognitive perception of grip properties is used to learn future grip responses. Information gleaned from previous grips or early in a grip can be used in intentional adjustments. Normally in an unperturbed grip, thumb and index act in phase with each other, providing symmetrical force fluctuations (R. S. Johansson & Westling, 1988; Rearick & Santello, 2002). Using sensory memory and expectation, subjects employ anticipatory loading or alternative digit placements to compensate (Forssberg et al., 1992; Fu, Zhang, & Santello, 2010; R. S. Johansson & Westling, 1984). If this anticipatory planning is perturbed with an expected condition, the sensory information overrides the plan and informs the necessary adjustment (R. S. Johansson & Westling, 1988). In short, the perception of reactionary responses that self-structure the task are used for future tasks, but on-line sensation can override the sensory memory. The perceived, reactive, and remembered responses can all result from a limited variable space input, primarily of dynamic mechanoreceptor activation.

In the inverted grip example, the response is claimed to partially reference the external influence of gravity, but reducing environmental gravity does not reduce the ability to appropriately couple force to the required load. Therefore, that environmental information is not necessary for accurate grasp actions, just grasp scaling (Augurelle, Penta, White, & Thonnard, 2003). In both grip cases, gravity is acting on an axis of increased sensitivity due to the biomechanical properties of the skin. Deformation of the finger pad is anisotropic as the skin's Young's Modulus is a function of the papillary ridge direction: the skin is stiffer along the ridges than across (Wang & Hayward, 2007). The very tips of the finger pad have papillary ridges perpendicular to the distal-

proximal axis but the center of the finger pad typically has papillary ridge arches or whorls, mostly perpendicular to the ulnar-radial axis (Neumann, Evett, Skerrett, & Mateos-Garcia, 2012). Hence, the center of the finger pad will be most deformable in the ulnar-radial axis. Magnitude of deformation is then a function of both tactile direction and contact site, which largely varies between grips and tasks.

These biomechanical variations can contribute to explanations of contextual reactionary responses and perceptions. Maintaining the appropriate safety margin is the primary goal of grip adjustment. Conceptually, this means ensuring frictional force between the fingers and the object exceeds the forces from gravity, movement, or other external factors that would pull the object out of the grip. This frictional force acts tangential to the finger pad, which would induce shear and stretch dependent on the load direction and contact site. The information from these deformations controls how much grip force is required. Increasing object weight would increase the lateral stretch until the object slipped, so grip force would increase to maintain the necessary frictional force. Similarly, increasing the frictional coefficient would show a superfluous deformation, allowing grip force to reduce, economizing the frictional force. Therefore, gravity and other external factors are not referenced in grip, but are inputs to the mechanism of detection. In a precision grip task using the center of the finger pads, movement in the ulnar-radial axis would likely produce more deformation, and therefore stronger responses or higher sensitivities. To reinforce this, a rotation condition with gravity and the ulnar-radial axis orthogonal would differentiate the dominant reference between biomechanical or environmental.

With regards to afferent information, all mechanoreceptors activate at some point within precision grip (Westling & Johansson, 1987). FAI, FAII, and SAI all possess temporally dynamic responses and SAII has solely tonic responses. FA cells activate at onset and release and FAI maintain activity throughout, especially

responding to physiological muscle tremor. FAII intragrip responses are due to force loading changes during grip, firing on directional changes and movement cessation. SAI sustains activity, with eventual adaptation at rates explained by the mechanical relaxation of tissue (Wang & Hayward, 2007). In addition, there is direct evidence that these afferent systems are utilized in the adjustment of the safety factor of precision grip after external cues. In response to electrically induced tactile events, detectable vibration events, and even undetectable vibration events, SAI and FA activity is associated with increased grip responses (R. S. Johansson & Westling, 1987). Portions of FA and SA systems are shown to inform response to unexpected force loads, respectively representing force loading rate and force load magnitude (Macefield, Häger-Ross, & Johansson, 1996). At the tip of the finger, cells demonstrate neural tuning to directional loading without slip: the FA system tuned to loading along the papillary ridges and the SA systems across the ridges. The center of the finger pad typically has papillary ridges perpendicular to the ulnar-radial axis, and one would expect neural tuning to adjust accordingly (Birznieks, Jenmalm, Goodwin, & Johansson, 2001). The FAII system also fires heavily to movement across the finger pad, similarly seen in the previously discussed temporal component of texture recognition (Roland S. Johansson & Vallbo, 1983). In total, the activity produced within these systems provides the contextual and temporal information necessary for the complex responses. Texture, weight, directional loading, and even slip are relayed in this internal variable space.

Cortically, precision grip tasks show robust multimodal biphasic activity over multiple areas of somatosensory cortex. In a series of lift-and-hold tasks, sensitivity to combinations of object weight, frictional stickiness, and texture can be seen in areas 1, 2, and 3b. The single cell responses possess a spectrum of timing activity, typically a combination of both sustained and onset-offset spiking. These papers

investigate sensitivity to weight, texture, and movement; conditions with afferent information explained by the mechanical interactions above. The phasic and static components of mechanoreceptor response seem to be represented in the single cell responses of somatosensory cortex.

SOMATOSENSORY FEEDBACK

The Importance of Somatosensation. In order to achieve desired motor function, basic control theory introduces the importance of error correction. Commonly, the lack of feedback in a dynamic system results in instability and error. Physiologically, we have multiple levels of feedback to guide and correct our actions. Proprioception considers our posture and spatial position, but is deficient in environmental information without the supplementation of tactile information, especially in studies of spatial resolution. In reporting grip aperture or hand position, the addition of tactile information significantly reduces the error in estimation (Rincon-Gonzalez, Buneo, & Tillery, 2011). Tactile sensations must inform us of critical effector-object information for us to effectively and efficiently interact with our environment. Vision provides a lot of redundant information about our own body, environment, and interactions, typically at lower spatial and temporal acuity than the former two senses. While vision is useful in correction and predictive contact properties, a high demand is placed on vision in many other fashions than effector-object relationships. In competing scenarios, bimodal tactile and visual cues provide evidence for neural summation within reaction times, but attention is prioritized to tactile sensation and visual information is disrupted by somatosensation. (Forster, Cavina-Pratesi, Aglioti, & Berlucchi, 2002; Ide & Hidaka, 2013; Miller, 1993). Realistically, most motor/tactile tasks are carried out sans vision, only utilizing it in novel or failure situations.

Observing subjects with complete sensory deafferentation, while possessing intact motor functions, clarifies the importance of somatosensory feedback. Even maintaining vision, the deafferentation of the upper limb causes ubiquitous issues in a subject's daily tasks. In these cases, subjects can retain the ability to perform previously known motor tasks, but at cost of efficiency and increased difficulty. Driving remains possible, drinking and eating become laborious, dressing and buttoning become impossible. While the subject is capable of position and pressure maintenance using visual feedback, the stability quickly deteriorates in its absence. As the manipulation or interaction's requirement for precision increases, more tactile information is necessary, and the subject's ability to rely on predefined motor programs and visual feedback decreases significantly (Marsden, Rothwell, & Day, 1984).

Deafferentation case studies may provide a general sense of the need for somatosensory feedback, especially in finer actions, but the actual contributions of cutaneous sensations in grip tasks has been quantified (Witney, Wing, Thonnard, & Smith, 2004). Slight object movements require slight responses, which are activated and scaled due to intact sensory information. Grip force magnitude and timing responses rely on details such as object movement direction, object texture, gravity, or object (Augurelle, Penta, et al., 2003; Häger-Ross et al., 1996; L. A. Jones & Hunter, 1992; Westling & Johansson, 1984). However, all of these conditions can be reduced to the necessary grip force – load force ratios, where a certain safety factor of higher grip force must be maintained to not allow slip. Texture, weight, direction, and gravity affect the magnitude of this safety factor and somatosensation is how that information is received

As would be expected with the importance of the afferent systems, artificially induced or pathological deficits in afferent activity demonstrate profound reductions

in grasp adjustment ability due to the lack of sensory input (Augurelle, Smith, Lejeune, & Thonnard, 2003; Nowak & Hermsdörfer, 2003; Thonnard, Saels, Van den Bergh, & Lejeune, 1999). Consistently, the deficient subjects over exaggerate the grip safety margin in order to avoid failure as the appropriate cycling grip responses lag the loading force. The increased safety margin allows them to still initialize simple volitional actions by coupling grip force to arm movements, but eventually grasp failure occurs. This supports the notion that sensory memory is used in execution, but on-line sensory input is prioritized for grip adjustment. Under artificial localized cortical lesions of somatosensory cortex, the ability to perform these grip tasks is similar to the peripheral deficits in terms of exaggerated safety margins, without any increased deficits in performance (Brochier, Boudreau, Paré, & Smith, 1999).

Prosthetic users possess many of the same daily difficulties seen in deafferentation, with the added lack of complete motor function, contributing to a high abandonment rate of devices (Biddiss & Chau, 2007). Restoring motor function is steadily being improved, especially with the use of brain-machine interfaces (BMI) and an increased understanding of the necessary cortical encoding and decoding. Using BMIs for motor control has allowed users to operate devices with high degrees of freedom with relative ease. However, the lack of BMI somatosensory feedback presently hinders these patients into error prone and cumbersome actions. Subjects have long recognized these limitations and highly prioritize graded device actuation and the reduction of visual dependency, both which require practical tactile feedback to manage appropriately (Atkins et al., 1996; Biddiss & Chau, 2007; Peerdeman et al., 2011).

The use of some form of tactile feedback with prostheses has been explored in many ways. Electro-tactile, vibro-tactile, intracortical, and peripheral stimulation

have all yielded positive results, with varying levels of improvement. Graded vibrotactile feedback can partially restore proprioception as it has been used to improve the precision and accuracy of joint movements of a prosthetic limb (Mann, 1973). Delicate object manipulation improves when using punctate force feedback that is graded with the grip force, although it does not restore handling success to natural levels (Meek, Jacobsen, & Goulding, 1989). The introduction of basic stimulation patterns to the peripheral nerves can even be used to successfully indicate object deformation or joint position in active prosthetic tasks (Dhillon & Horch, 2005). In more recent studies, chronic medial and ulnar nerve stimulation during graded grip actuation of a prosthetic has allowed for successful handling of delicate objects in both sighted and non-sighted trials – achieving two high priority facets of prosthetic acceptance (Raspopovic et al., 2014; D. Tan et al., 2014).

Physiologically, our motor and sensory systems are interdependent and successful actions require adaptive feedback. Without tactile or proprioceptive senses, tasks become entirely too arduous and even impossible. Motor tasks rely greatly on feedback to function appropriately with respect to force and timing, often unobservable by other senses. Vision can supplement our actions with redundant or predictive information, but cannot entirely nor adequately replace somatosensation. Prosthetic acceptance depends on achieving user desires, to a point where patients express missing the ability when not actively performing experiments.

Current Stimulation Tactics. While the benefits are clear, our goal is not only to replace somatosensory feedback functionality, which can be achieved to varying degrees detailed above. We also mean to make that feedback easy to interpret by way of natural and practical sensations. Creating sensations that match modality and location to natural actions has been explored with some success. However, the stimulus patterns used are not organic nor physiologically driven,

potentially relying on high level processing's ability to classify abnormal patterns to established experiences. Largely, the percepts elicited are not analogous to normal tactile tasks.

As a major component of the strategy, the invasive level of stimulation must be justified. Intracortical microstimulation (ICMS) can be used for artificial texture detection and comparison, even though the patterns used are basic frequency trains (O'Doherty et al., 2011; O'Doherty, Lebedev, Hanson, Fitzsimmons, & Nicolelis, 2009). ICMS can even be used to guide reaching movements with the task error being comparable to reaching with solely visual feedback (Dadarlat, O'Doherty, & Sabes, 2015). However, the topographical organization of somatosensory cortex presents two major issues in scale and invasiveness. Representations of the hands within areas of 1 and 3b, respectively possessing broad and fine cutaneous receptive fields, are located along ~8mm of the postcentral gyrus in *Macaca mulatta* cortex (Friedman, Murray, O'Neill, & Mishkin, 1986; E. G. Jones et al., 1978; Pons, Garraghty, & Mishkin, 1988; Pons et al., 1987). S1 may be on the surface, but 3b is located within the central sulcus, traversed by blood vessels and the arachnoid membrane (Matsuo et al., 2011). Accessing this cortex requires either deep electrode penetrations or subdural intrasulcal arrays. Competitively enticing, peripheral nerves are organized within fascicles and, at the forearm, are composed of mostly afferent fibers. Ulnar and medial nerves separately innervate halves of the palm and specific digits, establishing the importance of stimulation on both and the additional organization. Choosing the peripheral stimulation path greatly reduces the degree of invasion and discrete organization is still partially maintained all accessible via well documented branching topography (Delgado-Martínez, Badia, Pascual-Font, Rodríguez-Baeza, & Navarro, 2016). It also allows physiological filtering and distal processing the still act on the input signal.

Second, the sensations evoked by stimulation need to be distinct, scaled, and natural. Standard strategies have limited success using exploratory stimulation tactics, but the response is not always robust or practical (Clippinger, Avery, & Titus, 1974; Walker, Lockhead, Markle, & McElhaney, 1977). Strategies explored have long consisted of constant parameter trains delivered on single channels. Discrimination of percept location is repeatedly achieved by stimulating separate electrodes, which ideally recruit nerve populations innervating distinct areas of the hand (Dhillon 2005, Tan 2015, Clark 2014, Gasson 2005, Raspopovic 2014). Minimizing percept overlap is necessary to exploit maximum discerning ability for practical tasks. As electrode technology advances, we will be able to recruit finer nerve populations, and therefore percept areas will become more distinct and finite. As true object interaction incorporates more than one active contact, which can vary in size, the demand to create encompassing and variable sensations increases.

Standard stimulation strategies consist of repeating charge-balanced, square pulses at defined magnitude, pulse width, and frequency. Sensations can be manipulated by varying these stimulus characteristics. At lower frequencies, sensations are reminiscent of tingling/paresthesia. Increasing frequency progresses the subject through tapping, pulsing, vibration, possible pressure, and eventually pain responses (Clippinger et al., 1974; Gasson, Hutt, Goodhew, Kyberd, & Warwick, 2005; Walker et al., 1977). Within comfortable ranges identified by a subject, the frequency can be modulated to change sensation intensity to limit error in graded device actuation. Using these cues greatly enhances prosthetics, allowing users to carefully manipulate delicate objects with practical purposes (Dhillon & Horch, 2005). Percept area size depends proportionally on both pulse width and pulse amplitude. When either increases, the delivered charge is raised and broader nerve population recruitment occurs. Time varying pulse width can create a varying intensity stimulus

which results in a sensation described as "natural as could be," achieving familiar pressure, rubbing, and pulsing responses (D. Tan et al., 2014; D. W. Tan, Schiefer, Keith, Anderson, & Tyler, 2015). Varying current intensity as a function of an active pressure sensors allows for graded prosthetic activation and basic object recognition (Raspopovic et al., 2014). Recognizing a time variant stimulus as natural may tie to the fact that natural interactions are hardly spatiotemporally constant and fluctuating pulse width causes percept size and/or nerve recruitment fluctuations. A second potential explanation arises from the benefit of stochastic resonance seen in electrotactile and intracortical stimulation, where subthreshold signals can enhance the detection of a primary signal (Iliopoulos, Nierhaus, & Villringer, 2014; Medina, Lebedev, O'Doherty, & Nicolelis, 2012). The fluctuation of charge may be providing the subthreshold resonance at the edge of the theoretical isopotential sphere, thereby enhancing the stimulation's detection or sensation.

Stimulation strategies need to represent topographically dynamic sensations consistent with the variant activation of natural tasks. Practical information requires modulation of the available percepts, in size or intensity. Stimulation patterns are typically not derived from any sort of physiological source or model and consist of pulses with constant parameters. Resulting percepts are typically not congruous with useful and recognizable feedback. The knowledge gap exists in understanding the neural response to temporally variant stimuli similar to physiological representations of touch.

Many factors go into the suggestion that grip induced peripheral dynamics can be efficiently used as sensory input schemes. First, precision grip varyingly activates tonic and phasic mechanoreceptor systems, providing contextual reaction and perception responses. Second, the cortical representation of touch possesses dynamics that are preceded by afferent mechanoreceptor dynamics during these

active tasks. These can include sustained intragrip activity and a onset-release bursts. Third, grip ability fails on comparable levels with peripheral or central lesions, suggesting complex dynamics in the periphery before cortical input. Fourth, the importance of time variant stimulation is inferred from its ability to elicit "natural as could be" pulsing and pressure sensations. From these assumptions, construction of physiologically representative peripheral nerve stimulations can be well justified. Incorporating the phasic onset-release response mode and the tonic sustained response mode can provide a composite stimulation scheme that mimics the variant dynamics, herein termed "Bimodal Biomimetic." Comparing the cortical dynamics of mechanically stimulation to standard and Bimodal Biomimetic stimulation patterns can pave the way for psychophysical explorations of practical sensations.

Cortical Metrics of Perception: Evoked Potentials. Evoked potentials are measures of voltage activity aligned on an event, implying the event evoked the response. Typically, they are reported as positive or negative inflections at a specific time point, e.g. P100 for a positive inflection at 100ms. A heavily investigated evoked potential in EEG is P300, occurring anywhere from 250 to 500 ms and proposed to be specifically important in high level cognitive thinking that demonstrates strong top-down processing traits (Donchin, Kubovy, Kutas, Johnson, & Tterning, 1973; Duncan-Johnson & Donchin, 1982; Polich, 2007). This evoked potential can scale to complex cognitive loads such as self-esteem and self-relevance (Gray, Ambady, Lowenthal, & Deldin, 2004; Yang & Zhang, 2009).

Basic tactile information of unattended indentation and scanning velocity exhibits slightly shorter latencies occurring just after 125ms, which evidences processing closer to bottom up. Vibration of the knuckle also showed similar scaled activation of evoked potentials, with the additional trait of latent synchronization to stimuli. The modulation of this potential follows psychophysical perception curves of

respective stimuli, but are not necessarily mechanistically correlated (D. Johnson, Jürgens, Kongehl, & Kornhuber, 1975; D. Johnson, Jürgens, & Kornhuber, 1980b, 1980a). However, under a detection task that requires a cognitive judgment, tactile and electrotactile stimuli produce P300 responses (Yamaguchi & Knight, 1991). The understanding of a tactile stimuli pushes the evoked response into the cognitive processing P300 range, implying that perception requires time to process and defining a latency point of perception.

With median nerve stimulation induced non-painful stimuli, the presence of short latency evoked potentials is present as quickly as P20 and nearly coincide with the tactile range at P170. With painful stimuli, similar evoked potentials are produced with the addition latent P200, bridging the latency of bottom up and processing potentials (Babiloni et al., 2001).

Cortical Metrics of Perception: Gamma Phase Locking. The term natural sensation is frustrating, as most sensations elicited from cortical or peripheral stimulation are definable, but not appropriate in task context. We all feel vibration and pulsing sensations, but are typically not using these as cues in everyday tactile tasks. Pressure or skin deformation produces tactilely practical sensations, while even natural vibration cues are minimally beneficial. Isolating specific aspects of the neural response that distinguish between practical and impractical percepts provides the opportunity to resolve the differences between the two. Delivering time variant stimulation patterns, and therefore varying charge intensity, is evidenced to feels natural in some cases, but what aspect of the neural signal means the sensation was tactilely practical? Frequency dynamics are proposed to indicate the perceptual recognition of stimulus.

Classically, frequency bands are divided into three levels: alpha at 8-12Hz, beta at 14-28Hz, and gamma at 30-100Hz. Activation or suppression of these bands

has been well quantified in somatosensory cortex in response to both tactile stimuli and electrical stimuli (Engel, Moll, Fried, & Ojemann, 2005; Fukuda et al., 2008). However, the electrical stimuli is typically 1Hz with a single pulse representing a single trial. Literature has also included additional ranges for high gamma at 100-250Hz, and very high gamma at 250-700Hz (Curio et al., 1997; Hashimoto, Mashiko, & Imada, 1996). The first signals to onset after stimuli are gamma bands, starting with very high frequencies within 20ms and associated with primary cortical processing (Fries, 2009). The signal gradually slows and descends through the gamma levels for about 100ms. Following the onset of gamma is, in order, beta augmentation, alpha augmentation, beta attenuation, and finally alpha attenuation. Not only is the level of gamma activation time dependent, the proportion of non-phase locked gamma is also dynamic and is shown to waver and eventually dominate the gamma signal in response to peripheral nerve stimuli (Fukuda et al., 2008).

Gamma can also be segregated in terms of phase. Phase locked gamma signals are consistent in latency, locked to stimuli across trials with little variance. Calculating the average Phase Lock Value (PLV) between trials (Lachaux, Rodriguez, Martinerie, & Varela, 1999; Rodriguez et al., 1999) for the gamma band dissects it into separate phase locked components. Significant PLV in the time domain indicates the signal is locked to stimuli, while PLV below threshold can be inferred as non-phase locked and therefore possesses jittered latency between trials (Gross, Schnitzler, Timmermann, & Ploner, 2007; Roach & Mathalon, 2008; Tallon-Baudry & Bertrand, 1999; Zhang, Hu, Hung, Mouraux, & Iannetti, 2012). It is important to distinguish between phase locking between trials and phase locking between channels. The calculation can be performed in either dimension, and the across-channel phase locking seems to be directly correlated to detectability. Typically

referred to as "synchronization," it represents cortical structures aligning in activity while "phase-locking" refers to a single cortical structures consistency to stimuli.

Gamma oscillations' role in perception and perception recognition promises interesting results. One of the first reports of gamma frequency activity during somatosensation is observed in *Macaca mulatta* somatosensory cortex during vision occluded exploratory searches that required the NHP to utilize touch information to find a reward (Murthy & Fetz, 1992). However, the gamma band dynamics and attendance to stimuli can reveal multiple aspects of perception across sensory systems. A common investigation of perceptual recognition of a task involves a naïve subject receiving an untrained stimulus. In both the auditory and visual system, the presence of immediate phase locked gamma is consistent in trained and untrained trials. However, a later positive component of non-phase locked gamma occurs at approximately 250ms in the P300 range (Goffaux, Mouraux, Desmet, & Rossion, 2004; Jokeit & Makeig, 1994; Tallon-Baudry & Bertrand, 1999; Tallon-Baudry, Bertrand, Delpuech, & Pernier, 1996, 1997). In similar tasks with a distraction stimulus, subjects had to pay attention and respond to a specific stimulus. The non-phase locked P250 response is present for both relevant and irrelevant stimuli, but augmented for the attended trials, even in tactile tasks (Gurtubay, Alegre, Labarga, Malanda, & Artieda, 2004a; J, V, & T, 1997). Only in nociceptive laser induced sensations is the early phase locking gamma component not seen, but the non-phase locked P250 gamma coincides with pain rating (Roach & Mathalon, 2008; Zhang et al., 2012). As mentioned, non-painful median nerve stimuli produced P20 to P170 evoked potentials and painful median nerve stimuli produced the same with P200 in addition. A companion study investigating the phase locking properties of the data show the early evoked potentials are phase locked between both conditions, but the painful P200 is also phase locked (Babiloni et al., 2002).

Clearly, this non-phase locked P300 gamma is involved in the top-down perceptual recognition of these stimuli. Evoked potentials and phase-locked gamma can be present regardless of perception, representing the input of information. The only occurrence of latent phase locking is in the nociceptive peripheral nerve stimulation. Utilizing these dynamics will be pivotal in understanding the perception of any artificially generated sensations. If we can identify how the brain distinguishes practical and impractical sensations, we can develop stimulation strategies that are based in achieving a specific neural metric rather than the exploratory processes that are presently implemented. Dynamic proportion of non-phase locked versus phase locked gamma bands, the varied temporal and contextual activation of gamma subdivisions and other frequency bands, and the timing of the gamma proportion versus the dominant band of the signal provide a sensation framework that should be very strongly considered.

Function of Stochastic Masking. Signal noise and random external noise can summate to increase the perception of a signal in a phenomenon recognized as stochastic facilitation (Benzi, Sutera, & Vulpiani, 1981). Supplementing systems with subthreshold noise at specific levels provides increases system responses and detections. The presence of this subthreshold noise enhances information transfer in cortex can enhance sensory detection of subthreshold tactile events (Collins, Imhoff, & Grigg, 1997). Interestingly, suprarthreshold noise masks previously strong tactile events, implying a specific level will provide maximum benefit. Varying the level of neural noise in a tactile detection task affects the gamma synchronization in conjunction with tactile detection. At an optimal noise level both are enhanced, but further increased noise causes desynchronization and decreased performance (Ward, Doesburg, Kitajo, MacLean, & Roggeveen, 2006). A model for predicting optimal subthreshold noise to benefit a system can be constructed around probability

distributions of a signal and the associate detection level (Gong, Matthews, & Qian, 2002).

Adapting the sustained portion of the proposed Bimodal Biomimetic stimulation scheme to include time variance in terms of interpulse stochasticity is somewhat similar to the information gleaned from the stochastic facilitation principle. However, the goal of stochastic addition in this experiment is not to enhance underlying signals, but provide sustained physiologically similar stimulation that is not phase locked to stimuli. While not determined in somatosensory experiments, there is evidence that attended acoustic stimuli in subjects exhibiting pathologic neural noise incur significantly less onset phase locked gamma (Roach & Mathalon, 2008; Winterer et al., 2000). A gap in information is present but the assumption is made that stochastically induced neural noise and pathological noise can equate in terms of response effect. Since median nerve stimulation induces undesired latent phase locking, the utilization of latent stochastic noise may mask undesired latent phase locking.

SUMMARY OF UPCOMING CHAPTERS

It is the goal of this dissertation to provide support that perception relies on internal information, the contextual properties are represented within this biphasic space, and that the stimulation patterns based on such patterns are better in terms of the cortical response. In the successive chapters, three experiments will be described that culminate in support of this goal.

In the first experiment, the aim is to investigate sensitivities to movement in different directions and if that sensitivity is referenced to the external factors such as gravity. While an object is held within precision grip, a two alternative forced choice task requires subjects to discriminate between two directional perturbations. An initial quick 1cm perturbation is in the distal, proximal, ulnar, or radial direction. After returning to the initial point, a secondary perturbation follows within a small window of first. Subjects respond whether the direction was the same or different, and the minimal angular difference of discrimination is determined for each initial perturbation. After rotating the grip into a vertical orientation, where the ulnar-radial axis is perpendicular to gravity instead of parallel, the task is repeated to investigate the effect of orientation. Significant sensitivities are observed as lower thresholds of directional discrimination in the ulnar and radial directions, which follow the rotation of the hand. From this, it can be argued that the sensitivities rely on internal information rather than external, likely explained by the anisotropic deformations of the finger pad.

In the second experiment, the aim is to investigate the cortical responses to precision grip conditions and attempt to explain them in terms of these deformations. Precision grip activates both slow adapting and fast adapting classes of mechanoreceptors during these deformations, providing static and dynamic patterns of activity that are similarly seen in the cortical response. While recording single unit

cells of somatosensory cortex area 1, a nonhuman primate performs a reach-to-precision-grasp task on an instrumented manipulandum with varied presentation angles, rotational perturbations, and textures. After eliminating cells with force significance between conditions, bimodal sensitivities of firing rate are observed in response to combinations of the stimulus parameters. Sensitivities appear to align with biomechanical activation and deformation. To start, the cells sensitive to different textures could be explained by varied slow adapting versus fast adapting activity associated with texture recognition. Cells sensitive to orientation conditions all show higher firing rates for the horizontal orientation, conceptually inducing more of a tangential load on the finger pad. Cells with bimodal sensitivity to both texture and perturbations follow patterns associated with biomechanical activation. From literature, it is known that fast adapting receptors associate with fine texture detection and fire during loading changes while slow adapting receptors associate with the complements. In these bimodal sensitivities, cells sensitive to movement are also sensitive to the smooth texture, suggesting common fast adapting activity. In contrast, these bimodal cells sensitive to static conditions lacking temporal information are also sensitive to the coarser texture, suggesting increased slow adapting activity. This experiment, while limited in investigative scope, strongly suggests the cortical biphasic activity is related to variable biomechanical activation of the mechanoreceptors in the finger pad. At this point, it is arguable that this representation, and how it varies, is intrinsic to the contextual and prioritized somatosensory information necessary for adequate feedback.

The third experiment compares and contrasts the somatosensory cortex gamma band dynamics to mechanical stimulation on the fingertips and peripheral nerve stimulation patterns. In typical sensory activation, gamma band phase locking can be associated with sensory input and should only occur within the first 100ms after

stimulation. Also in these typical patterns, latent gamma activity should not be phase locked and should grade with stimulus intensity and attention. Violation of these rules occurs in atypical sensations from median nerve and electrotactile stimulations, representing non-ideal sensory activation. After identifying gamma patterns induced by practical punctate sensations and impractical vibratory sensations, ideal responses are defined and compared to peripheral nerve stimulation patterns. Using both standard constant parameter schemes and time variant patterns based on biphasic representations, median nerve stimulation is delivered and the responses compared. Standard stimulation schemes consistently violate the defined rules by inducing latent and persistent phase locked gamma. Time variant patterns, especially the biphasic inspired pattern, approach the representations induced by practical punctate sensations. Mimicking physiological activity associated with the somatosensory perception provides a viable and beneficial scheme for peripheral nerve stimulation feedback, and provides a platform for interesting future research.

Anisotropic Psychophysical Sensitivities in the Perception of Tactile Direction in a Precision Grip

Abstract

Some of the tactile cues which arise from interactions with objects have a sense of directionality. These cues can inform grasp intent and modulation as reactive properties or as perceived traits. Low latency responses to varied grip perturbations indicate that grasp safety margins are exaggerated in certain directions and conditions. In an ulnar-radially vertical grip, evidence proposes that orthogonal distal and downward directions are more sensitive to task parameters and safety margin maintenance. This suggest a bimodal reference frame of the grip to the hand and to the environment. In this psychophysical experiment, human sensitivities to the direction of tactile movement are examined in the context of precision grip in gravity-orthogonal and gravity-parallel grip orientations. Subjects performed a two-alternative-forced-choice task involving a textured cube moving orthogonal to their grip axis. Subject arms were placed mount that allowed for digital movement, but restrained the wrist to eliminate induced wrist, elbow and shoulder movement. Movement of each joint was monitored via PhaseSpace motion capture. The subject was presented with a 2”x2” textured object and instructed to use two grips: loaded, as if to control the object, and unloaded, as if the object were slipping. In each trial the object is translated 1 cm in 0° (proximal), 90° (ulnar), 180° (distal), and 270° (radial) and returned to its origin. This reference stimulus is immediately followed by a 1 cm test stimulus at a random 5° interval between -30° and 30° of the reference. Response from the subject after each pair of stimuli indicated whether the direction felt the same or different. Using the response curve modelling generates a point of subjective verticality for deviations from each reference stimuli. Lower thresholds, indicating enhanced perception, exist in the ulnar-radial axis even when

the respective axis is orthogonal to gravity. Contribution to the anisotropic thresholds from digit displacement and proprioceptive systems can be eliminated as digit displacement does not coincide with increased sensitivity. Anisotropic stiffness of the finger pad is much lower in this axis, and the increased perceptual sensitivity seems to be explained by the biomechanical properties.

INTRODUCTION

Achieving success in motor tasks requires viable and interpretable somatosensation, especially as the task's nature becomes finer. Removing somatosensation entirely severely hinders motor ability, leaving a person to rely on visual feedback or learned motor patterns, both incurring high levels of error (Marsden et al., 1984). Even with complete somatosensory functionality, there are limits in perceptual abilities associated with fine tasks. Understanding these perceptual limits will help identify the level of somatosensory feedback necessary to produce accurate movements.

A key aspect of successfully performing these movements is discriminating finite differences between movements across fingertips. The directional element of tactile input is useful in informing grasp intent, adjustment, and response. This ability to identify an object's direction of movement across the skin, Tactile Direction Discrimination (TDD), plays an important role in catching falling objects and adjusting grip on moving objects. In a study of 1,575 individuals with upper limb loss, the four most commonly requested actions included using a spoon or fork, fastening a button, tying shoelaces, and operating a doorknob, all of which require TDD for the individual to perform the fine motor adjustments necessary to maintain precise control (Atkins et al., 1996).

To date, studies of small movements have concentrated on the limits of TDD using passive poses (Webster, Murphy, Verner, & Okamura, 2005). These investigated the absolute threshold of directional discrimination in the coronal plane utilizing a passive touch in which subjects placed their index fingers on a rotating ball device. This device's direction varied in 5^{o} increments and subjects identified the direction as either "angled" or "straight." The average least noticeable angular difference in slip direction was determined to be between 20^{o} and 25^{o}. A similar study incorporating various textures found this least noticeable angular difference to be between 3.6^{o} and 11.7^{o}, depending on the surface texture. In addition, it has been shown that proprioception from large arm movements affects the ability to determine slip speed, so it is important to limit the inclusion of proprioceptive information as much as possible by limiting movement proximal to the wrist (Salada, Vishton, Colgate, & Frankel, 2004). While the information provided by texture from movement across the relaxed hand is useful in the exploration and identification of new objects, TDD is more intrinsically related to active tasks. Knowledge regarding this threshold in an active precision grip is limited. This information is necessary in order to understand TDD in the context of fine motor actions in active, practical tasks desired by prosthetic limb users.

Anisotropic sensitivities of TDD have been observed in numerous studies. Neural activity to static indented bars, psychophysical static groove orientation detection, and static gap detection are all tuned in the distal-proximal directions during scanning studies (Bensmaia, Hsiao, Denchev, Killebrew, & Craig, 2008; Essock, Krebs, & Prather, 1997; Gibson & Craig, 2005). These features passing across dermal ridges can generate more vibrational power, activating FAII mechanoreceptors used in detection (Maeno, Kobayashi, & Yamazaki, 1998). At the tip of the finger, neural encoding of force loading direction is also sensitive to the

distal direction, perpendicular to the papillary ridges (Birznieks et al., 2001). With respect to angular slip direction, slip speed, and slip texture, anisotropic sensitivities in detection thresholds favor the distal-proximal direction as opposed to ulnar-radial. However, direction and speed perception are examined under passive, non-grip tasks (Salada et al., 2004; Wheat & Goodwin, 2000).

In an active grip, heightened direction sensitivities allow for quicker and stronger responses as needed. Jones and Hunter (1992) determined that a reactionary pinch force to a stimulus is increased for distally-travelling stimuli. Hager-Ross (1996) found lower grip force latency and greater grip force safety margin in distal directions and in the direction of gravity, even in an inverted grip. This suggests that grip TDD is biased in certain critically dangerous directions that require prioritized grasp stability, referenced from environmental factors. However, reducing gravity does not affect grip performance or cyclic loading, but does affect force scaling necessary for appropriate safety margins, suggesting internal reference frames (Augurelle, Penta, et al., 2003).

The necessary grip force during normal gravity would, however, apply higher shear forces on the finger pad in the direction of gravity. Since glabrous skin of the finger pad is anisotropic, with stiffness relating to the orientation of the papillary ridges, movements across these ridges would induce more deformation (Wang & Hayward, 2007). Mechanoreceptor sensitivity seems to follow similar patterns of this anisotropy, showing ridge-orthogonal tuning for SA systems and ridge-parallel tuning for FAI (Birznieks et al., 2001). Skin stretch is tied to directional detection, so the axis with more deformation will likely align with the axis of sensitivity (Seizova-Cajic, Karlsson, Bergstrom, McIntyre, & Birznieks, 2014). The orientation of the papillary ridges is not consistent across the finger pad, but the center has ridges primarily orthogonal to the ulnar-radial axis. It is then possible that in Hager-Ross (1996), the

"with gravity" sensitivity is consistently in the axis of decreased stiffness, and information originates from internal properties.

Expectations. Tactile direction sensitivities exist in different directions for multiple contexts, but can be generally reduced to variable and contextual biomechanical loading. Precision grip tends to not rely on scanning across the finger, so the deformation due to shear forces is likely the method of activation. Axes sensitive to tactile direction in precision grip are unclear, but likely will align with the less stiff ulnar-radial axis. Whether those sensitivities are referenced to internal biomechanics or to external effects such as gravity must be jointly determined. An internal reference would provide credence that mechanoreceptor information is the prime source of contextual information for perception, grip structuring, and future planning.

METHODS

Using a precision grip, 14 subjects held a 5 cm cube textured with 60 grit sandpaper that is attached to a six degree of freedom DENSO (Long Beach, CA) VS-G series robotic arm. Based on a two-alternative, forced-choice task, subjects were presented with two 5 mm stimuli, each at 20 mm/s, to the gripped cube and asked to determine whether they were in the "same" or "different" direction. As illustrated in Figure 1, a primary stimulus in the proximal, radial, distal, or ulnar direction was followed by a randomized 300-700 ms interstimuli interval and then a secondary stimulus with a randomized angular difference of ±30° on intervals of 5°. This resulted in 52 permutations, randomly delivered to the subject via a custom LabVIEW (National Instruments, Austin, TX)/Python program. Experimental protocols were reviewed and approved by the Institutional Review Board at Arizona State University.

Each subject performed two types of grip loading: passive and active. For passive, the subject was instructed to let lightly hold onto the object, maintaining contact, but not attempting to stay the object. For active, the subject was instructed to grip onto the cube as if attempting to hold it in place. Force was neither regulated nor observed, but this instruction forced subjects to pay attention to their grip force and attempt to maintain a common force. Trials were blocked into grip loading types to allow the subject to maintain consistent grip for a full set, and rest as desired between blocks. The initial grip loading type was randomized for each subject. Each subject performed two full sets of trials.

In order to explore the reference frame of potential grip sensitivities, two grip orientations were used: horizontal (9 subjects; 5 female, 4 male) and vertical (5 subjects; 3 female, 2 male). The primary stimulus definitions rotated for consistency with the hands' posture. Grip loading and task instructions were identical for each grip orientation.

To avoid unwanted visual and proprioceptive feedback, subjects were blindfolded with their wrist mounted in a cushioned brace attached to a rigid frame. Coordinates from a PhaseSpace motion capture unit (PhaseSpace Inc, San Leandro, CA) were referenced to the robotic arm so that the Y- and Z-axes corresponded with the subject's sagittal plane. Movement of the robotic arm, digits 1 and 2 of the distal phalanxes, digits 1 and 2 of the metacarpophalangeal joints, and the forearm just proximal to the wrist were recorded for each experimental session with timestamps corresponding to individual trials. Motion capture marker distance was defined as the maximum sagittal distance relative to the distance of the robotic arm for each trial.

Sensitivity is defined as the True Positive Rate (TPR) of experimental trials, with correctly identified "Different" trials as True Positives (TP) and correctly identified "Same" trials as True Negatives (TN). As shown in Equation 1, we choose

to define the detection threshold as the angle of change at which the number of TP exceed the number of False Negatives (FN), i.e. when the TPR becomes greater than 50%. This is referred to as the Point of Subjective Verticality (PSV). As the experimental angular steps used are in increments of 5°, the generated sensitivity curves were fit using a fourth order polynomial regression, and solutions for 50% calculated. These solutions were considered the psychophysical limitations and used, alongside response accuracy, to ascribe heightened sensitivities to specific primary stimuli. Accuracy for specific primary stimuli under varied grip conditions is calculated as the total correct responses, TP and TN, for a primary stimulus' total trial permutations (Equation 2). Increased response accuracy and lower psychophysical PSVs indicated existing directional sensitivities.

$$TPR = \frac{TP}{(TP + FN)}, \quad (TPR\ (FN \leq TP) \geq 0.50\ ) = PSV \tag{1}$$

$$Acc_{PP} = \frac{TP + TN}{TP + FP + TN + FN} \tag{2}$$

RESULTS

Motion capture data was used to calculate the absolute maximum distance traveled in the sagittal plane for each trial. Separating the grip loading, grip orientation, and primary stimulus trials, we see that the wrist movement was consistently minimal, but not negligible, as compared to the robot. DP and MCP movement varied with grip loading and primary stimulus. Only in the horizontal grip, active and passive loading show much different changes in the movement of the wrist, DPs, and MCPs. The horizontal grip is of particular interest. In passive loading the DP1 and DP2 are all higher in the Radial-Ulnar axis than in the Distal-Proximal

axis. The vertical grip indicates little change between axes, grip loading, or primary stimulus. In all conditions, DP2 moves slightly more than DP1 (Figure 2).

Psychophysical curves were constructed for the subjects' response "Different," or the True Positive Rate, to each secondary stimulus for each primary stimulus. Initial data was not ideal due to high error in certain subjects. As the task was designed to exceed existing reports of tactile direction discrimination limits and required the subjects' attention, subjects whose TPR was less than 50% for ±30o or 0o trials were excluded. These rules revealed only 2 horizontal grip exclusions and 1 vertical grip exclusion.

To determine the PSV of the psychophysical curves, fourth order polynomial regression was implemented to fit to the data, 95% confidence intervals were calculated, and solutions for 50% TPR calculated (Figure 3). The full results are summarized in Table 1, including accuracy calculations for each primary stimulus under each grip treatment. Determined PSVs occurred within 8.5 to 34.4 degrees, depending on axis and grip conditions. An independent-samples t-test between regression PSVs indicate that PSVs were significantly lower for the Radial-Ulnar axis ($M=15.24$, $SD=5.19$) than the Distal-Proximal axis ($M=26.19$, $SD=4.51$), $t(30)=-6.37$, $p<0.001$, $d=2.25$. Although possibly higher, a separate independent t-test between regression R2 values indicates a close insignificance between the Radial-Ulnar axis ($M=0.846$, $SD=0.78$) and the Distal-Proximal axis ($M=0.739$, $SD=.135$), $t(14)=1.95$, $p=0.072$, $d= 0.975$. While close, the regression fits are not significantly higher for the Radial-Ulnar axis.

These PSVs also imply some asymmetry along certain axes, primarily the Radial-Ulnar axis, where the positive and negative PSVs deviate in magnitude. Due to this axial asymmetry, it is hard to define specific PSVs for the TDD, but the range within the determined PSVs informs us of the windows of direction that would

provide subjective uncertainty. Regardless of grip loading or grip orientation, these "uncertainty window" ranges are narrower for the Radial-Ulnar axes. (Table 1) An independent t-test indicates that the Radial-Ulnar windows (M=30.49, SD=5.03) are less than the Distal-Proximal windows (M=52.39, SD=6.10), $t(14)=7.83$, $p<0.001$, $d=3.91$. In many instances, the Distal-Proximal axes' range limits are only marginally within, or marginally out of, the angular window of the informed experimental design. Coinciding with the narrower uncertainty windows, another independent t-test indicates the Radial-Ulnar axis also has higher accuracy (M=61.80, SD=13.20) than the Distal-Proximal axis (M=37.76, SD=14.28), $t(86)=8.1993$, $p<0.001$, $d=1.74$) (Figure 4).

DISCUSSION

Distal-Proximal points of subjective verticality (PSV) were between 21.6-34.4o, near the literature values, but the Radial-Ulnar axes had PSVs between 8.5-24.4o. The latter were significantly lower in PSV value and uncertainty window range, which addresses concerns over asymmetry of PSVs. Results indicate that a grip sensitivity occurs in the Radial-Ulnar axis, referenced to the orientation of the hand rather than the environment. Passive slip directional sensitivities, although fundamentally different from our experiment, conflict as they are in the Distal-Proximal axis.

Heightened directional sensitivity is clearly referenced to the subjects' hand orientation in ulnar-radial axis during precision grip, but the explanation as to why is not clear. Somatosensory cortex, primarily responsible for the representation of tactile percepts, possesses multimodal representations of passive lateral finger displacement and cutaneous touch (Kim, Gomez-Ramirez, Thakur, & Hsiao, 2015). More specifically, multimodal representations are present for a whole array of contextual components of precision grip: weight, texture, and increased friction

(Salimi et al., 1999a; Salimi, Brochier, & Smith, 1999b, 1999c). While the horizontal grip indicates increased distal phalange movement for the sensitive axis, this trend is not present in the vertical grip. Therefore, the increased sensitivity relationship is unlikely due to the increased digit movement. Further, the increased movement seen in the active loading for horizontal grip does not rectify the distal-proximal and ulnar radial sensitivity discrepancy, but exaggerates the latter. Other passive slip literature indicates that slip texture, speed, and direction sensitivity should exist in the distal-proximal axis, potentially attributed to anisotropic properties of the fingertip surface's dermal ridging (Maeno & Kobayashi, 1998; Maeno et al., 1998).

The likely answer does rely on the anisotropic properties of the finger pads' glabrous skin, but not in terms of scanning. First, the skin is more engaged in precision grip, undergoing large deformations rather than generating vibrational power. Second, papillary ridges at the middle of the finger are orthogonal to the ulnar-radial axis, predicting increased deformation in the respective axis. With increased skin stretch comes increased perception of tactile information (Provancher & Sylvester, 2009; Seizova-Cajic et al., 2014; Wang & Hayward, 2007). During the contradicting passive slip tasks from literature, the glabrous skin is not likely heavily engaged and the tactile stimuli are superficial. Our task, especially under active loading conditions, simulates practical grip activity by engaging more of the inherent biomechanical properties. This increased anisotropic deformation would activate tonic and phasic mechanoreceptor systems. The increased loading condition where subjects are instructed to hold the block in place, would increase deformation in each trial and explain the exaggerated ulnar-radial sensitivity during such conditions. Since fingers' orientations are not controlled to be normal to the manipulandum, this could account for the asymmetrical PSVs seen in the ulnar-radial axis during both orientations. Directional grip detection sensitivity, but not superficial slip sensitivity,

is a function of the amount of potential skin stretch in respective directions, but further investigation focused with such variables quantified is required.

CONCLUSION

Shown in forces, latencies, and orientation sensitivity, precision grip responses are modulated by task context. This chapter looks at the perception of the task, and not the response properties, but shows an internally referenced source of information. While Hager-Ross proposed that reactionary forces are based in external reference frames, tactile direction discrimination is just biomechanically referenced. These are not inherently competing results, but argue the both reactionary responses and perceptual responses stem from directionally dependent activation of the same input. Mechanoreceptor dynamics provide the common source of information due to anisotropic and biphasic activation.

FIGURES

Table 1. Summary of analytical results for each primary stimuli under grip orientations and grip loading conditions. Accuracy: Correct responses over Total trials for each primary stimuli. Detection Thresholds: (+) and (-) indicate the solutions at the PSV for the polynomial fit of the mean subject response, respective to the sign convention indicated in Figure 1. Δ is the range between PSVs R2: Fit Coefficient of Determination.

		Active Loading				Passive Loading			
		Primary Stimulus				Primary Stimulus			
		Proximal	Radial	Distal	Ulnar	Proximal	Radial	Distal	Ulnar
Horizontal Grip	+	34.4	14.3	30.6	10.3	22.9	15	32.1	18.5
	-	22.9	15.1	26.7	9.3	20.8	16.4	22	10.8
PSV	Δ	57.3	29.4	57.3	19.6	43.7	31.4	54.1	29.3
	R^2	0.74	0.9	0.9	0.74	0.91	0.9	0.75	0.83
Accuracy		34.62	62.09	34.62	75.27	47.8	59.34	37.6	61.54
Standard Error (n=7)		1.38	2.11	2.86	2.13	1.73	1.05	2.45	1.05
Vertical Grip	+	32.9	12.8	20.2	18.5	26.9	10.7	27.1	23.8
	-	23.2	23.2	21.6	12.3	27.2	24.4	27.6	8.5
PSV	Δ	56.1	36	41.8	30.8	54.1	35.1	54.7	32.3
	R^2	0.77	0.87	0.74	0.93	0.55	0.84	0.55	0.73
Accuracy		28.85	50.96	42.31	62.5	37.5	54.81	36.5	59.62
Standard Error (n=4)		2.29	2.13	2.72	4.74	4.11	0.92	3.19	4.26

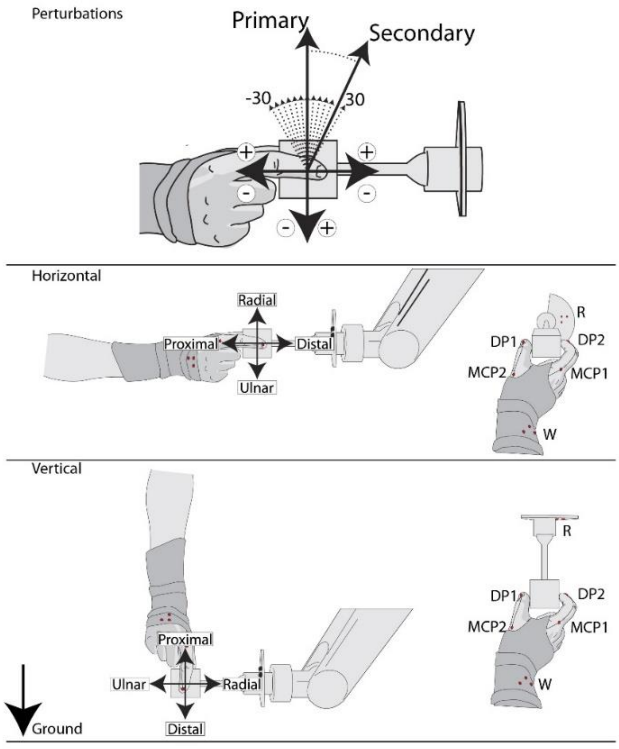

Figure 1. Experimental Setup and Task. Task: The task is a two-alternative, forced-choice paradigm consisting of both a primary and secondary stimulus, with a randomized 300–700 ms interstimuli interval. The primary stimulus is a 5 mm (20 mm/s) center-out-center movement in the proximal, radial, distal, or ulnar direction. The equidistant and equal velocity secondary stimulus differs within ±30° on 5° increments from the primary perturbation, indicated by respective sign conventions. Each subject responds "Same" or "Different" to the stimuli pair. Grip Orientations: Primary stimulus definitions are defined by the rotation of the grip with respect to the ground. PhaseSpace markers on the MCPs, DPs, Wrist, and Robot are also represented as red dots.

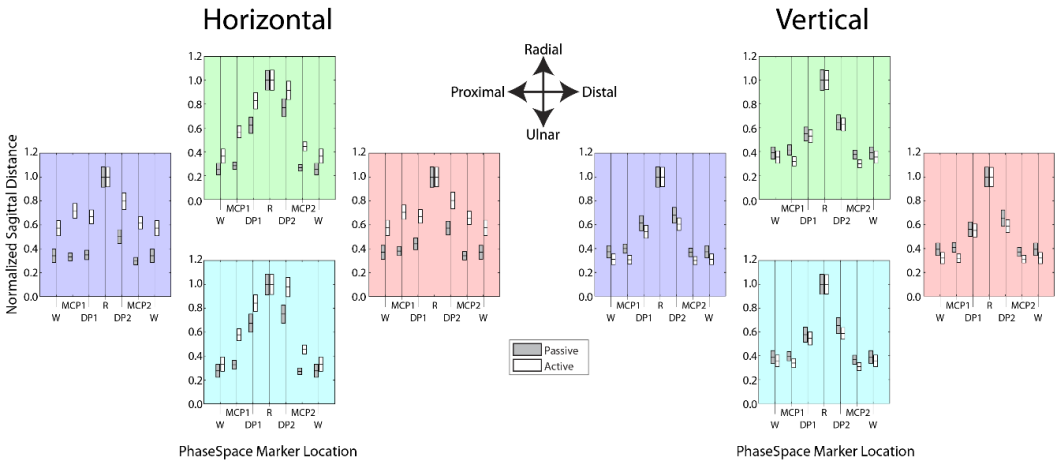

Figure 2. Joint Displacement Due to Task. For each primary stimuli treatment, distances for MCPs, DPs, W, and R is shown relative to R, which represent the robotic arm movement controlling the stimulus magnitude. Plots are the mean movement across subjects for secondary stimuli bounded by the respective positive and negative standard errors.

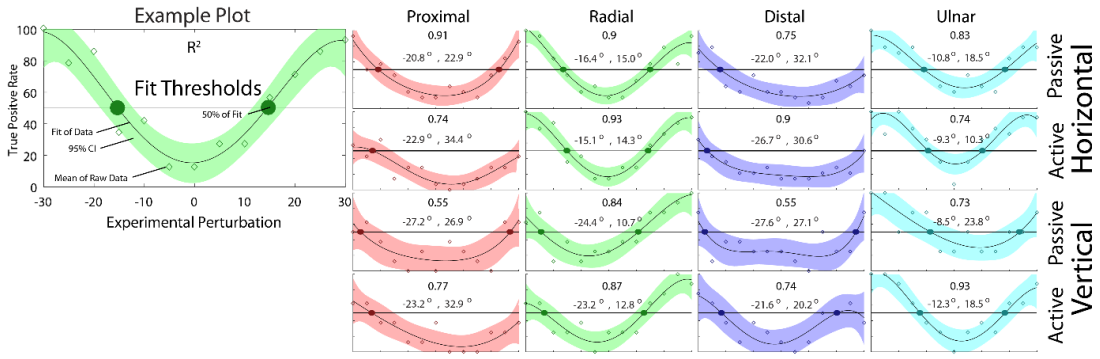

Figure 3. Polynomial Regression Fits of Subject Response Sensitivity. For each primary stimulus in each grip condition, True Positive Rate (TPR) is calculated as a secondary stimuli's True Positives over the sum of respective True Positives (TP) and False Negatives (FN). The PSV mark represents where TP≥FN. Subjects who showed a TPR≤50% for ±30° or 0° secondary stimuli were excluded due to lack of attention or focus during the experiment. The mean TPR is overlaid with a fourth order polynomial regression fit and respective 95% confidence intervals. Solutions for 50%, and R2 are given for each plot.

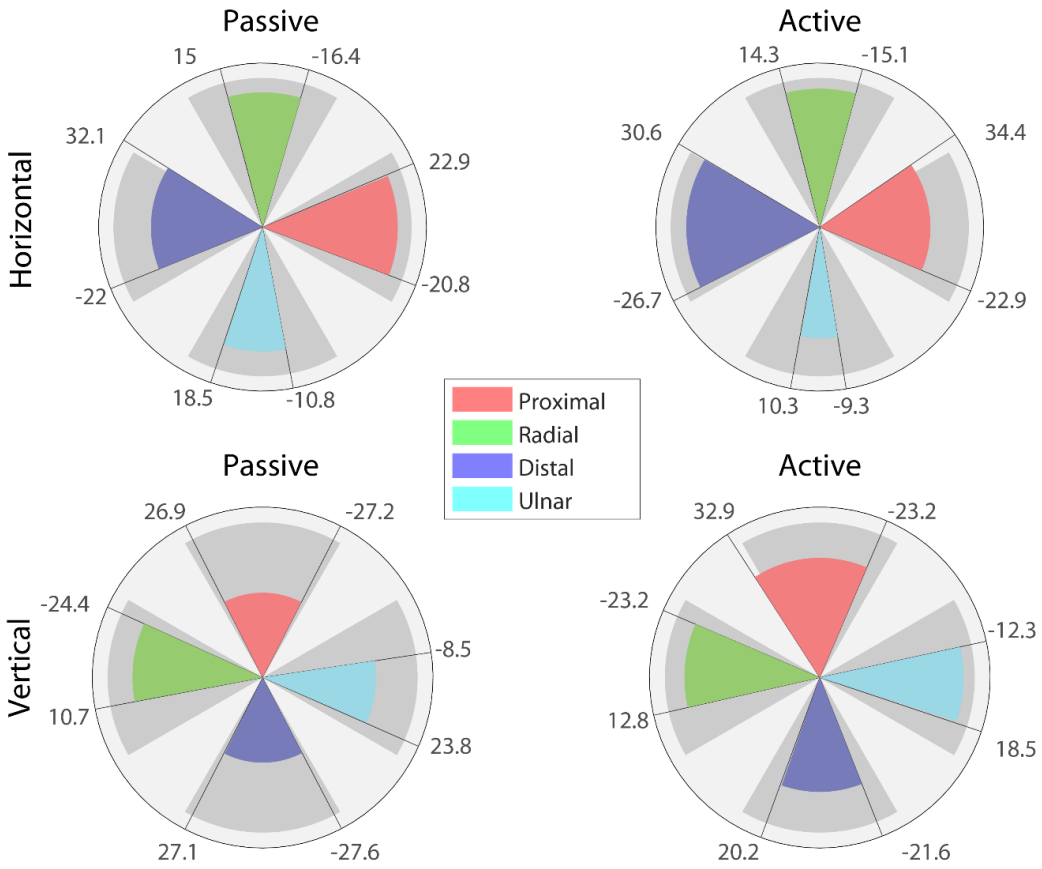

Figure 4. Anisotropic Uncertainty Windows. For each primary stimulus in each grip condition, regression fit solutions as the PSVs. Gray wedges indicate the experimental window of ±30°. Colored wedges indicate the uncertainty range between PSVs for respective directions, where the regression would be less than 50% TPR. Magnitude of the colored wedges is proportional to the respective regression R^2.

Somatosensory Area 1 Multimodal Sensitivity Due to Biomechanical Variations in Precision Grip

Abstract

Multimodal sensitivity is well documented in primate somatosensory cortex during precision grip tasks involving texture, force loading, translational movement, and frictive interaction. Explanations towards multisensory integration are common, as proprioceptive and anticipatory activity are observed in area 1, 2, and 3b of somatosensory cortex. However, many of these multimodal facets can be explained by contextual activation of biomechanical shear loading in the finger pad activating SA and FA mechanoreceptor systems in concert. In this experiment, investigation of the role of rotational perturbations along the distal-proximal grip axes, texture, and orientation supports the notion that cortical perception is mainly modulated by tactile information. In a reach-to-grasp task with a non-human primate, two object orientations and three modes of perturbation were utilized to examine simultaneous neural encoding of hand posture, object movement, and texture. An manipulandum with parallel grip surfaces and force/torque transducers is used to collect data on independent thumb and index finger grip force. The grip surfaces pairs consisted of 60-grade sandpaper and 100% cotton fabric, or 220-grade sandpaper and plexiglass. Sandpapers are used for their quantitative coarseness, plexiglass is used for the smooth machining and temperature normative properties, and cotton is used to incorporate a small amount of softness to compare versus the rigid surfaces. Single unit recordings of cells in somatosensory cortex provide evidence that posture, texture, and perturbation can be jointly neurally encoded. Specific cells produced a more robust response to certain combinations of object orientation, perturbation, and texture while producing diminished responses for other combinations. 47 cells were recorded for the first texture set but are not

appropriately analyzable. In the second texture set of 24 recorded cells, 23 are task related and only 15 do not possess significant normal force variations within conditions. Bimodal cell properties can be explained by biomechanical loading variations. 3 cells sensitive to movement and texture paired the sensitive texture with spatiotemporal texture recognition traits. Cells sensitive to movement are sensitive to plexiglass and cells sensitive to sandpaper are sensitive are diminished in movement. Of the 7 cells sensitive to orientation, all are sensitive to horizontal loading, where tangential shear would be greatest.

INTRODUCTION

Understanding perception during precision grip tasks requires consideration of multiple systems of simultaneous information. Individually perceptible components of information can modulate other components and inform adjustment of the task. However, touch is not a sense that can be wholly described by segregating metrics. Tactile tasks are a conglomeration of complementary aspects informing dynamic self-structuring; the task consequences effect task execution. Contextual perception and responses of precision grip can more easily be described by the associated biomechanical loading than multisensory integration. This is not to say that multisensory integration is absent, nor is it negligible, in motor tasks.

Representation of Texture. Perception of texture depends on the conjoint spatial and temporal properties of the interaction. Coarse textures, textures with high spatial variation, are easily discriminated with static touch and movement does not affect the discrimination (Connor et al., 1990; Lederman, 1974; Lederman & Taylor, 1972; Taylor & Lederman, 1975). With decreasing spatial information, textures began to lose static discriminability around 125 microns between features. In this fine range, discrimination requires temporal information and is associated with the undisturbed vibrational power of the interaction (S. J. BensmaÏa & Hollins, 2003; Hollins & Risner, 2000; Klatzky et al., 2003; LaMotte & Whitehouse, 1986).

Texture information is initially encoded by the relationship of activity between phasic fast adapting (FAII) and tonic slow adapting (SAI) mechanoreceptors. Coarse texture properties of high spatial variation activate the SAI fibers and are unaffected by movement (Connor & Johnson, 1992; K. O. Johnson et al., 2000). Removing these cells via genetic engineering of mice obliterates coarse texture discrimination ability (Maricich et al., 2012). With decreasing spatial variation, the FAII system begins to respond, but only with temporal information

obtained during movement. The vibrational power elicited from fine textures aligns with the FAII system frequency sensitivity range (Bensmaïa & Hollins, 2005; S. BensmaÏa et al., 2005).

Cortical areas 1, 2, and 3b possess representations sensitive to the spatial and temporal components associated with texture perception. Discriminating between temporospatial variation in a passive texture presentation, all areas produce phasic and tonic responses (Tremblay et al., 1996). Responses proportional to coarse groove width and stroke velocity demonstrates both tonic and phasic activity, respectively sensitive to force and velocity. That is, individual representations of tactile information of texture included both spatial and temporally sensitive components (Sinclair & Burton, 1991). In a series of lift and hold tasks, somatosensory cortex shows multimodal sensitivity to texture along with force loading, again showing a spectrum of tonic and phasic activity. While two main systems encode texture in separate spatiotemporal models, the perception of texture is represented by conjoined cortical activity.

Information in Precision Grip. Texture, movement, force loading, and spatial orientation can all feed into the perception and response properties of precision grip. Reactionary force responses in precision grip serve the purpose of maintaining grasp stability. The relationship of loading force to grip force is termed the safety factor and a higher ratio ensures the object will not slip. Movement orthogonal to the precision grip axis induces force responses scaled to the speed of movement and inversely scaled to roughness (Häger-Ross et al., 1996; L. A. Jones & Hunter, 1992) Responses are faster and stronger in the distal direction and with gravity, when gravity is also parallel to the ulnar-radial axis. The perception of weight within precision grip is affected by the surface texture. Weight equivalent objects with finer textures produce a stronger force response and are reported as

heavier than coarse textured objects (Flanagan, Wing, Allison, & Spenceley, 1995). The perception of precision grip information, such as weight or torque, is used in anticipatory loading of future trials (Chouinard, Leonard, & Paus, 2005; Fu et al., 2010; Ohki, Edin, & Johansson, 2002). This is behavior that develops in humans as young as two years old (Forssberg et al., 1992).

Most of these properties can be explained by the frictional force's shear deformation of the anisotropic finger pad, as supported by Chapter 2. Any information used is transmitted from the same variable space: anisotropic mechanoreceptor activation during shear deformation. Peripherally, precision grip activates and utilizes both SA and FA mechanoreceptor systems for grip stability, dynamic grip loading, and directional perception of scanning and loading directions (Birznieks et al., 2001; R. S. Johansson & Westling, 1987; Roland S. Johansson & Vallbo, 1983; Westling & Johansson, 1987).

Common cortical representations of these grip responses manifest across somatosensory cortex in conjoined terms of individual mechanoreceptor systems. Precision grip lift-and-hold tasks show complex multimodal representations of texture, force, and stickiness across somatosensory cortex (Salimi et al., 1999b, 1999c). Individual cells can appear to be sensitive to multiple tactile properties simultaneously, but those properties all relate to the induced deformation. It is argued that these cortical sensitivities are results of the coactive SA and FA systems during shear deformations. Cortical multimodal responses are therefore inherently the result of combining tonic and phasic peripheral signaling. So far, only tangential movements orthogonal to the grip axis are considered. However, rotational perturbations across different axis of precision grip also induce varied response force properties. A present sensitivity to rotations away from the hand on the interdigit

axis promotes the idea of system attention to rotation for grip stability (De Gregorio & Santos, 2013).

Expectations. Multiple lanes of information feed the intrinsic and intentional structuring of precision grip. These response properties exist dynamically, adjusting within the action of the grip due to either reflexive actions or perceptual choices – both of which are initiated by SA and FA mechanoreceptor activation. The interactive relationships of these responses suggest an intimate representation of contextual parameters and sensor input. Perception of texture can be described via temporal and spatial mechanisms of movement generated vibrations and skin displacement models. Texture recognition and perception are not due to the singular presence of vibrational power or skin deformation, but the relationship of activation between the SA and FA systems. Tactile force loading, orientation context, and spatiotemporal texture estimation schemes are intimately associated with the execution of complex tactile tasks such as precision grip maintenance. Tangential action of the finger pad during precision grip can account for most of this information. It is unclear if these bimodal sensitivities are present during rotational perturbations, but are expected in cortical representations specific to the thumb and index finger in area 1 and 3b of primary somatosensory cortex.

METHODS

One *Macaca mulatta*, herein referred to as NHP-K, was trained on a reach to passive precision grip task with his left hand. Passive grip indicates the primate must maintain the hold of the object as it moves and not release force on the object. A six degree of freedom DENSO (Long Beach, CA) VS-G series robotic arm precisely presented a textured manipulandum to the NHP at different grip postures. This manipulandum was designed to possess parallel and opposing Nano-17 force torque sensors from ATI Industrial Automation (Apex, NC) with an appropriate width for

NHP grip aperture. During grip, the manipulandum was perturbed rotationally in the proximal-distal axis. During the grip, recordings from somatosensory cortex were performed via single-unit electrodes. Analysis of Variance (ANOVA) was performed for cellular firing rate and normal loading force across all factors. The Arizona State University Institutional Animal Care and Use Committee approve experimental protocols. (APPENDIX A) The Arizona State University Department of Animal Care and Technologies provide veterinary supervision and care for all surgeries.

Implantation. Area 3b is in the postcentral gyrus below area 1, both components of the primary somatosensory cortex. The hand representation of area 1 and 3b occurs at just medial to the terminus of the intraparietal sulcus. Coordinates for these cortical structures were obtained via an overall of CT and MRI data for NHP-K. A custom polyether ether ketone (PEEK) chamber implant was designed for NHP-K using a combination of stereotactic electrode placement software Monkey Cicerone, 3D medical imaging software Mimics, and 3D design software SolidWorks. To ensure chamber implantation was over the chosen location, the design used the surface shape of the skull for the 3D interface mesh (McAndrew, VanGilder, Naufel, & Tillery, 2012). This allowed a secure fit to the organic shape of the skull and little to no deviation of the intended coordinates. Under isoflurane anesthesia, a 2 cm diameter craniotomy was opened over the specific coordinates with dura mater remaining intact, the chamber was secured over the craniotomy via bone screws, and the chamber was sealed with a plexiglass lid. The chamber design successfully contoured on the cranium, required no acrylic adhesion, was centered over the exact stereotactic placement coordinates. Using the PEEK material and avoiding acrylic adhesion resulted in a biocompatible implant with minimal complications for NHP-K. (Figure 1)

Behavioral Paradigm. All task behavior was controlled via custom LabView programs. The task followed a rigid structure with a series of conditional events. (Figure 1) Before blocks of trials, the robotic arm would attach a manipulandum with a specific texture. Trial initiation depend on NHP-K maintaining contact with a holdpad for five seconds. Upon initialization, the robotic arm would present the textured manipulandum at 0o horizontal or at 30o pronated. After a short random wait of 0.5-1.5 seconds, reach was cued via an auditory tone. Once thumb (D1) and index (D2) sensors indicated simultaneous 1N load for 1 second, the perturbation began. Maintained force was required from grip onset to the end of the perturbation. Perturbations included 30o supination, 30o pronation, and no rotation. After a brief random interval between 0.5 and 1.5 seconds, perturbations consisted of one second of rotation, one second of hold, and one second to return to the initial orientation. Trial failure could occur due to leaving the holdpad before the auditory cue, failing to initiate precision grip, failing to maintain precision grip through perturbation, or violent action on the manipulandum determined by a torque sensor on the robotic arm. Trial success occurred if NHP-K did not violate any of the previous rules. Separate auditory cues indicated failure and success, while successful trials also elicited a juice reward. An important note to reiterate is that the grip is passive, not possessing control of the manipulandum movement, but must maintain force due to unexpected and unpredictable rotations.

Complete data sets were defined as five repeats for two textures and each perturbation and posture treatment. This results in 60 trials, which were randomly presented and experimentally blocked by texture. Blocking was necessary as switching textures required large robotic arm movements that tended to agitate NHP-K. Sessions were kept to two textures at a time: cotton (soft) versus coarse sandpaper and plexiglass (smooth) vs fine sandpaper.

In order to align behavioral data with neurophysiological data for appropriate and precise analysis, behavioral timing and conditional events were recorded for each trial. Events included trial parameters such as texture or presentation angle, holdpad release, individual force sensor contact onset and offset, perturbation start and end, and trial success. Kinetic data of the force sensors was recorded at 200Hz through a PXI real-time chassis in order to determine onset of grip and analyze variation in normal grip loading under the different treatments.

Neurophysiology Recording. The implant design included an interface for mounting a Global Biotech NaN-XY electrode drive system. Using this system, up to four tungsten Harvard electrodes and guide tubes were mounted onto independent electrode drives with precision motors. Electrode coordinates on this system were limited to a circular grid of 1mm x 1mm resolution; the x-axis consisting of –caudal to +rostral and the y-axis consisting of –lateral to +medial. As the dura mater literally means the "tough mother" and would damage the electrodes, the platform was manually lowered until the guide tube tips were adequately penetrated enough to allow unimpeded electrode travel. As NHP-K performed the behavioral paradigm, electrodes were slowly driven into cortex until a cell could be identified.

Amplification, neural recording, and event handling was performed using a PLEXON MAP Data Acquisition system. Neural data was recorded at 40 kHz, and cells were identified and sorted with PLEXON software SortClient. Once a cell was localized and waveforms sorted, the electrode depth was recorded, the behavioral paradigm reset to start randomization and record a complete data set. Once NHP-K completed the trial set, receptive fields were obtained with a fine brush.

Analysis. If a cell maintained activity and NHP-K completed a full trial set, the waveforms of the associated trials were resorted and refined in OfflineSorter. With refined spike times, firing rate was calculated for each trial using a 25ms wide

triangular kernel iterated each 1 ms (Nawrot et al, 1999). To alleviate concerns of timing due to LabView event generation that arose mid experiment, digit contact events were refined by comparing the recorded kinetic data and the stored event times. Precise alignment of the neural and kinetic data was achieved via manual correction of the contact events, but only for cells recorded during the latter portion of the experiment. These trials were limited to the fine sandpaper and smooth plexiglass textures. Due to this, the information from the coarse sandpaper and soft cotton trials is informative, but not definitive. The exploration of the neural space during this allowed for much more precise coordinate choices during the latter experiments; locations that elicited small D1 and D2 receptive fields were well documented.

With precise and complete events, mean firing rate and mean normal load force for each digit was calculate for trial epochs of pre-grip, grip, and post grip. ANOVA tests for mean firing rate and mean normal loading force were performed across factors of epoch, texture, grip posture, and perturbation type. Experimental blocking by texture types was considered by implementing nesting to the texture effect in the ANOVA. Significant effects seen in mean firing rate factors were only considered truly significant if the associated effect of mean normal loading force was not significant. For example, significantly different cellular activity between texture types was only considered true if the force between the two conditions was not significantly different.

RESULTS

For the former portion of the experiment, considering soft cotton and coarse sandpaper, 42 cells were recorded with complete trial sets and receptive fields on D1 or D2. Of these 42 cells, 37 were task related by showing significant activity of firing rate during grip, 22 showed a significant effect to texture, 16 showed a significant

effect to grip posture, and 10 showed a significant interaction effect of texture and posture. Unfortunately, timing issues prevent us from appropriately analyzing the kinetic data associated with these datasets. Without this ability, definitively concluding sensitivities to these factors would be irresponsible. In addition, many of these cells demonstrated pre-contact firing, which caused the reevaluation of the timing scheme. Moving forward with the second set of textures, the timing issues were alieved and precise contact events allow for association of kinetic data and definitive observations of any pre-contact firing activity.

For the latter portion of the experiment, considering fine sandpaper and smooth plexiglass, 24 cells were recorded with complete trial sets and receptive fields on D1 or D2. (Table 2) Of these 24 cells, 23 were task related by showing significant activity of firing rate during grip, but only 15 did not show associated significance to force. Ensuring no significant normal loading force effects, 11 cells were sensitive to texture, 7 to posture, 7 to perturbation type, 4 to posture and texture interaction, 2 to posture and perturbation interaction, and 3 to perturbation and texture interaction. No cells found exhibited significant activity to the interaction of all three effects. (Figure 3)

The response properties of these cells were varied. (Figure 4) Cells possessed static activity which often slightly decreased during the trial along with normal loading force. Dynamic responses of cells varied from onset activity, onset and offset activity, to one cell – without a discernable receptive field –that suppressed activity during the grip epoch. Most cells had a combination of dynamic onset activity with lower static activity, maintained over the grip epoch. In a very interesting result, most of the cells recorded in this portion of the experiment demonstrate some, if not robust, activity between 0 and 1000ms preceding contact. In some instances, this activity even precedes the holdpad release event.

DISCUSSION

Data Considerations. The limited cell count of this paper is due to many physiological, equipment, and behavioral factors. Not all cells discovered in recording sessions were recorded to completion. NHP-K often became agitated due to robot movement or environmental conditions, and cells were lost before complete trial sets could be competed. In effort to limit time and potential for agitation, priority fell on cells with small single digit receptive fields with obvious task related activity.

Unfortunately, the 48 cells recorded with the first two textures are not able to support any definitive conclusions. The inaccurate timing events allow best guesses at trial segmentation and provide no ability to account for normal loading magnitude effect on activity. However, the receptive fields were similarly small and located on D1 and D2. This allowed for refined exploration in the second set of textures, and supports the presence of localized single digit responses at the stereotactic coordinates. In addition, the aim was to observe activity in both area 1 and 3b, but the sub 3mm depths reported in the second texture set cells indicate that 3b was not penetrated. While similar receptive fields and pre-grip firing are seen in histologically confirmed area 3b, all conclusions made are done so with the assumption that cells recorded are only in area 1 of somatosensory cortex.

Orientation Sensitivity. All cells sensitive to orientation exhibited higher activity to the horizontal initial posture than the pronated. Two cells were sensitive to both orientation and perturbation, exhibiting higher activity during supination perturbations. While present, this data indicates either proprioceptive input to the representation or change in tangential force. Since only the normal force data was ensured to be significantly the same across treatments, neither conclusion can be made. While the likely explanation is shear force increase due to the angle of grip being parallel to gravity, proprioception information projections from area 3a to area

1 are also well documented in passive limb and digit movements (Kim et al., 2015; London & Miller, 2013).

Simultaneous SA and FA Response Presence. Results indicate complex input to area 1 from multiple mechanoreceptor systems and an unidentified anticipatory information source. Cells possess contradicting information with regards to texture responsivity and receptive field size. Response dynamics of single cells can be comprised of a distinct or blended tonic and phasic components. Effects of rotational movement on firing rate could be explained by gleaning temporal information about the object.

To begin understanding the multiple inputs suggested, consider the receptive field sizes of the SAI and FAII systems. Only cells with small single digit receptive fields associated with SAI were recorded, but PC receptive fields are large. The latter encodes the vibrational power of fine texture receptive fields and responsible for fine texture discrimination. Both textures in the latter portion of the experiment, smooth plexiglass and 220 grit sandpaper, have spatial surface geometrical features less than 100 um. As discussed, texture sensitivity in this range is due to temporal information from the FAII system. Therefore, eight of the eleven texture responsive cells exhibiting smooth plexiglass sensitivity receive contrary receptive field and vibrational power information, implying simultaneous mechanoreceptor input.

In addition, the response dynamics of cells with texture sensitivity possess tonic SAI and phasic FAII properties; three showing dynamic activity such as onset bursts, 4 showing static consistent responses, and 4 showing hybrid responses. Since the task is passive, with NHP-K maintaining grip but not exploring the manipulandum, the necessary temporal information likely comes from a brief window during onset of precision grip. Understandably, higher activity at the onset of grip is seen in six of the eight cells sensitive to the smooth texture. The three cells sensitive

to the sandpaper show some dynamic activity combined with mostly tonic activity. The tonic versus phasic firing activity, and the contradiction of fine texture detection and small receptive fields show traits from both systems actively represented.

Considering the role of perturbation, it is known that whole arm movement can modulate single cell activity. With small, rotational perturbations, it is suggested that bimodal sensitivity to smooth texture and movement perturbation conditions are additionally due to increased activation of the temporal tactile system. While only three cells demonstrated a bimodal sensitivity to texture and perturbation, the significant conditions of these cells support this suggestion. Two bimodal cells sensitive to the smooth texture were also sensitive to movement perturbations, where the temporal loading variations might provide appropriate vibrational power or FAII activation. The one bimodal cell sensitive to the coarser texture exhibited the opposite: temporal information from rotational movement reduced activity. While no scanning motions are known to be produced, torque within the grip axes induces a catch-up reactionary response. Synchronous change in force load and associated skin deformations produces temporal variation at the edges of the finger pad. The mechanistic question arises. Do intragrip torque loading or cyclic loading of glabrous tissue provide the temporal activation necessary for texture discriminability, or is the informative vibrational power only generated from lateral frictive interactions? With regards to single unit neurons in area 1, the increased deformations due to grip rotation appears to support finer texture detection.

Anticipatory Firing Activity. before contact is abundant across the primary somatosensory cortex areas 1, 2, 3a, and 3b. Pre-grip activity may come from numerous potential sources: proprioceptive information from area 3a which is intimately connected to motor area 4, motor planning, or skin stretch during grasp posturing. Interestingly, the Ruffini SAII mechanoreceptors responsive to skin

stretch in the human hand are not observed in neurophysiological monkey studies. However, SAI Merkel cells appear to be responsible for transducing this information in non-human primates (Kenneth O Johnson, 2001; Paré, Smith, & Rice, 2002).

Since SAI activity can be inferred via texture sensitivity and dynamics, then it is possible – but not concluded – that the anticipatory firing partially arises from the same system. However, activity in some cells starts before NHP-K leaves the hold pad – when the grasp is only an idea. At this point, NHP-K is stationary observing the robot present, reducing the possibility that this activity is solely due to motor action or proprioception.

Preparing for expected sensations associated to motor tasks is vital to proper control. Behaviorally, tactile memory is employed from previous actions to estimate initial grip force and torque, followed by adaptive loading schemes (Fu et al., 2010; Ohki et al., 2002). EEG studies indicate that, sans movement, tactile expectation modulates beta band suppression of sensorimotor cortex – increasingly with enhanced attention to the expected stimuli (van Ede, Szebényi, & Maris, 2014). Specific encoding of tactile experience for subsequent grips execution occurs in primary motor cortex area 4 as activity scaling to previous trials' loading (Chouinard et al., 2005; R. S. Johansson & Westling, 1987). Architectonic connections between area 1 and 4 may provide mutually beneficial information of tactile experience and consequence expectation. Encoding of previous experience in area 4 could result in the observed area 1 anticipatory activation.

CONCLUSION

Area 1 of the primary somatosensory cortex in *Macaca mulatta* provides information of multiple aspects of precision grip. Statistical sensitivity of single cells to texture, initial hand orientation, and passive grip rotation can largely be described

by texture information and their varied activation. Texture is encoded by the activation of separate mechanoreceptor systems in temporal and spatial dimensions – sometimes temporally supplemented by intragrip rotational movement. Proprioceptive information is present in area 1 and 3b of the somatosensory cortex, which could explain orientation sensitivity and potentially the presence of pre-contact firing. However, pre-contact firing can onset before hold pad release, indicating some tactile or motor ideation received from encoded tactile experience in area 4. Overall, area 1 seems to have biphasic contributions from cutaneous area 3b texture and loading information, motor planning due to tactile memory seen in pre-event firing, and either area 3a proprioceptive information or increased shear induced information due to orientation. The latter two conclusions are the weakest in terms of mechanism, but the precontract firing firmly indicates integration of more than mechanoreceptor systems. Importantly the relationship between orientation loading and shear force will be explored further in the data.

FIGURES

Table 1. Response characteristics of the four mechanoreceptor populations. (Wolfe et al., 2008)

	Size of Receptive Field	
Adaptation Rate	Small	Large
Slow	Slow-Adapting type I (SAI) (Merkel)	Slow-Adapting type II (SAII) (Ruffini)
Fast	Fast -Adapting type I (FAI) (Meissner)	Fast -Adapting type II (FAII) (Pacinian)

Table 2. Recorded Cell Response Properties. Recorded cells of the second set of textures: fine 220 grit sandpaper and smooth plexiglass.

				Independent of Normal Loading								
				Dynamics			Texture		Perturbation		Orientation	
	Total	Task	Pre-Grip	Phasic	Tonic	Combined	Fine	Smooth	Movement	Stationary	Horizontal	Pronated
Area 1 Cells	24	23	16	10	9	4	3	8	6	1	7	0

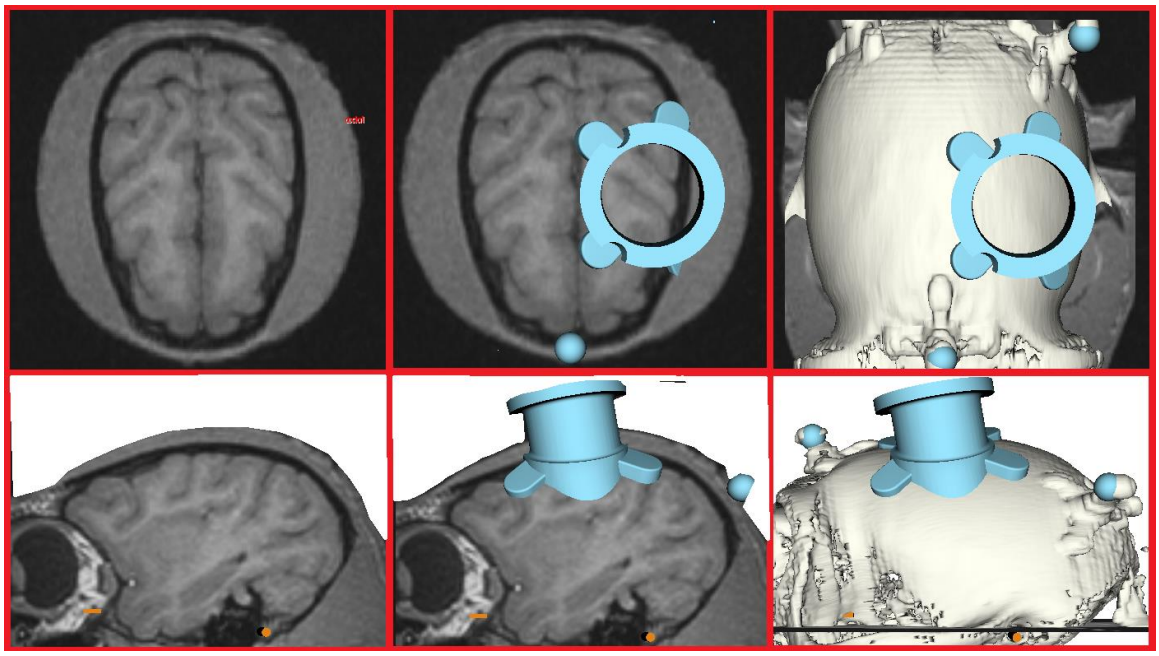

Figure 1: Targeted Implant. A custom chamber constructed from biocompatible polyether ether ketone and designed to contour NHP-K skull over the precise stereotactic coordinates confirmed via CT and MRI scan overlay.

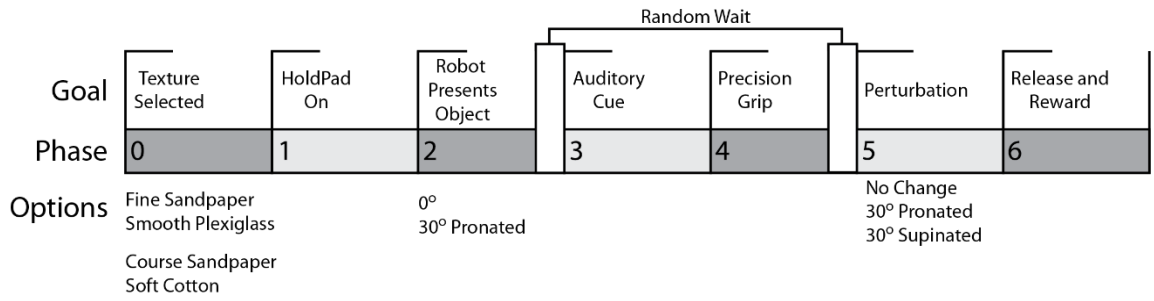

Figure 2: Behavioral Paradigm Structure. The task's specific phases and associated goals required execution in the specific order. Only after consecutive completion of each goal under the trials specific parameters was the trial considered successful and the NHP-K rewarded. If a phase condition was not met or NHP-K failed to maintain grip, the trial was considered a failure. Failed trials re-entered into the potential trial pool and a new trial was randomly selected.

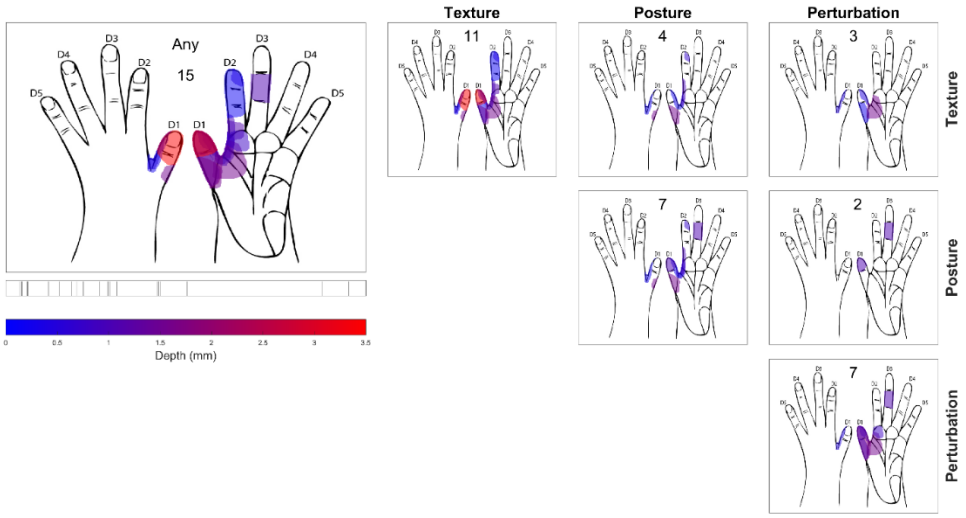

Figure 3: Task Related Receptive Fields. Receptive fields for cells with significant effects of firing rate to trial parameters and no significant effects to associated normal loading forces. Depth of recorded cell is coded to color and sites indicated along the legend. All receptive fields reported are cutaneous and any associated with the volar thumb wrapped around and possessed components on the palmar side.

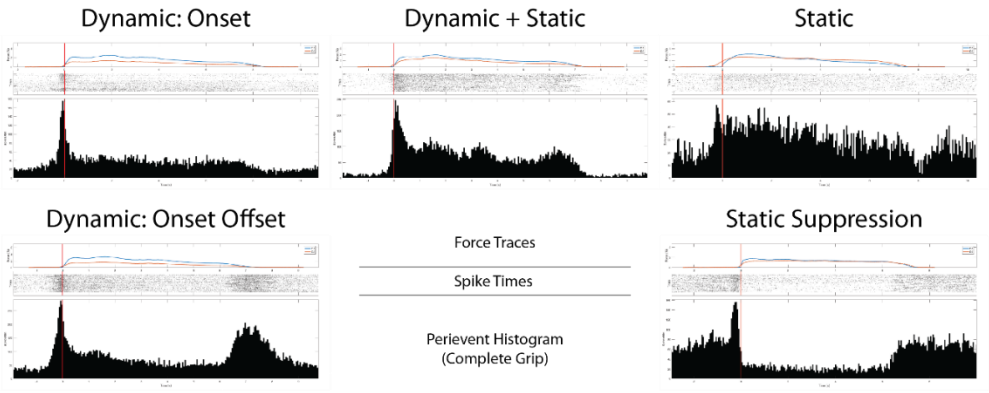

Figure 4: Example Observed Response Dynamics. Response dynamics of recorded cells aligned on the completion of precision grip. D1 and D2 force traces show normal force load averaged across all conditions, with the completed grip indicated by a red line where both digits achieve simultaneous contact. Cell activity varied in both its dynamic and static states. All included cells possessed some level of pre-contact firing, preceding complete grip and incomplete grip where only a single digit achieves contact.

Comparison of gamma phase locking properties between time variant Peripheral Nerve Stimulation and mechanical stimulation.

Abstract

Precision grip activation of multiple mechanoreceptor systems induces a biphasic response of SAI and FA mechanoreceptors that inform adjustment and perception of the task. These conjunctive temporal dynamics are present in somatosensory representations of active grip tasks as well. Employing time variant dynamics in stimulation schemes for sensory feedback has produced interesting results, but without a physiologically sound rationale. A composite stimulation consisting of onset-release pulses and sustained stochastic stimulations internally mimics natural time variant properties, but may not have a congruous external effect. Using well documented cortical sensory dynamics in the gamma band oscillations as a platform for natural perception, specific metrics are identified as Perceptually Typical gamma (PTγ). PTγ consists of bottom up early phase locked activity within 100 ms of the event and latent P300 associated non-phase locked activity, argued as top down recognition of the stimuli. Median nerve induced pain sensations violate these conditions by extending phase locking into the top down perceptual recognition range. Using PTγ as a platform for the ideal sensation properties, responses to mechanical, vibrotactile, and varied peripheral nerve stimulation is explored. Arrays precisely implanted into cortical somatosensory representation of the hand recorded LFP responses to FAST-LIFE median nerve stimulation. Strategies consisted of constant current varied frequency (CCVF), varied current constant frequency (VCCF), suprathreshold constant current varied stochasticity (CCVS), constant current varied biomimetically (CCVB –onset-release burst patterns), and a combination of the previous two termed Bimodal Biomimetic (BB) that mimics cortical and peripheral dynamics. Punctate stimulation followed PTγ

trends while vibrotactile stimulation produced latent phase locked gamma. CCVF and VCCF stimulations induced high amounts of latent phase locked activity. CCVS simultaneously diminished all phase locking and the onset-release gamma magnitude. CCVB stimulation elicited distinct phase locked gamma peaks separated by gamma attenuation. Finally, BB stimulation closely mimicked PTγ properties of low latency phase locking and latent non-phase locking gamma augmentation.

INTRODUCTION

Appropriate Somatosensory Feedback. In a case study of a subject with complete somatosensory deafferentation and intact motor control, the lack of somatosensation created difficulty in most aspects of daily life. While larger motor could eventually be overcome with visual cues and refined motor strategies, fine motor tasks chronically suffered in impairment and the ability to learn new motor tasks was significantly hindered (Marsden 1984). Visual feedback may provide opportunities for error correction but fine digit tasks often obscure the interaction of interest from sight and obliges feedback to somatosensation. Realistically, vision is only used in tactile tasks when learning or failing – often the same. In bimodal visual-tactile task, there is evidence of neural summation when working together but tactile information disrupts and supersedes visual information when competing (Forster et al., 2002; Miller, 1993).

Prosthetic users exhibit similar difficulty in the lack of somatosensation. Over the last few decades, a generous estimation of abandonment rate for prosthetic users averages at about one in every five patients. Despite advancements in degrees of freedom and myoelectric control, the lack of comfort in usage and the lack of practical feedback prevent appropriate adjustment and error correction in daily tasks. The frustration that arises from task failure discourages patients and creates an arduous situation out of a potentially beneficial one. User desire for graded and

visually independent feedback is paramount (Biddiss & Chau, 2007; Peerdeman et al., 2011).

Basic tactile feedback in prostheses are possible, but the acuity and localization of sensations is still difficult and impractical. Vibrotactile stimulation can benefit proprioceptive estimation, but psychophysical sensitivity to intensity or frequency is low (Mann, 1973). Punctate force feedback on the residual limb provides improvement in performance, but not to natural levels. Even peripheral nerve stimulation with localized and graded percepts produces less than ideal performance results. The percepts induced are typically not congruous with normal sensations; vibration, tingling, pulsing are commonly reported but not present in most active tactile tasks (Dhillon & Horch, 2005; Gasson et al., 2005). Only recently have graded precise activation been achieved with natural sensation using time variant stimulation properties. In bidirectional prosthetic tasks, varying current as a function of sensor activation or varying pulse width in a defined sinusoidal fashion provides high tactile gradation success, with the latter specifically reported "as natural as could be" (Raspopovic et al., 2014; D. Tan et al., 2014). Both patterns are effectively delivering temporal variance of charge delivery in two modes: onset – offset force ramping and temporally independent sustained time variance.

To overcome the feedback limitations of prosthetics, stimulation needs to produce sensations induced from natural tasks, but which metrics are necessary for practical stimulation remains unclear. Physiologically, reactions and perceptions of weight, texture, and movement in precision grip tasks are based on the context-variable shear force distribution on the finger pads (Häger-Ross et al., 1996; Seizova-Cajic et al., 2014; Wang & Hayward, 2007; Westling & Johansson, 1984). Perception of these conditions are used to intentionally adjust and plan anticipatory force loadings for new grips (Chang, Flanagan, & Goodale, 2008; Forssberg et al.,

1992; Fu et al., 2010). These perceptions are corrected by initial encoding in SAI and FA mechanoreceptor activity, (R. S. Johansson & Westling, 1987; Westling & Johansson, 1987) similar to and preceding the biphasic response common in the somatosensory cortex (Salimi et al., 1999a, 1999b, 1999c).

Cortical Metrics of Perception. Cortical power dynamics are generally segregated into three bands of frequencies: alpha at 8-12 Hz, beta at 14-28 Hz, and gamma at 30 to 100 Hz. The first signals to onset are gamma within 20ms of stimulation events, followed by decreasing frequency bands. With regards to attended sensory stimuli, gamma augmentation scales with stimuli intensity at about ~250 ms (Fukuda et al., 2008; Gross et al., 2007; Jokeit & Makeig, 1994; Rossiter, Worthen, Witton, Hall, & Furlong, 2013; Tallon-Baudry & Bertrand, 1999; Zhang et al., 2012). In an active task with vision occluded that prioritizes tactile information, the low frequency gamma is also present in somatosensory cortex (Murthy & Fetz, 1992). Frequency dynamics can be evaluated in terms of phase locking between trials or between channels. Modulation of between channel phase locking is dubbed synchronization, and can indicate simultaneous activations of different cortical structures as a fundamental process in cortical computation (Fries, 2009). Phase locking between trials is just referred to by a band's phase locking state, i.e. phase-locked gamma (PLγ) or non-phase locked gamma (NPLγ). Phase locking in this meaning indicates stimuli responses with little trial to trial variance in the latency of activity (Lachaux et al., 1999; Roach & Mathalon, 2008).

Subject naivety to auditory, visual, or tactile stimuli produces distinct augmentations in the NPLγ and PLγ between 30 and 65 Hz. In tasks where subjects received an untrained stimulus, low latency PLγ is present. Only when the subject is trained to respond to a certain input does NPLγ appear at approximately 250 ms. In similar tasks with a distraction component, the subject must make a perceived

choice based on the inputs and NPLγ is present for all trials but enhanced for the target stimulus, whether vision, auditory, or tactil (Bauer, Oostenveld, Peeters, & Fries, 2006; Goffaux et al., 2004; Gurtubay, Alegre, Labarga, Malanda, & Artieda, 2004b; Tallon-Baudry et al., 1996; Yordanova, Kolev, & Tamer, 1997).

Painful stimuli induced by lasers provides similar augmentation of NPLγ that scales with the pain rating, with no increase of latent PL. In contrast, painful stimulations induced via median nerve stimulation or electrotactile stimulation produce PLγ at time points that were NPLγ during non-painful stimuli (Babiloni et al., 2001, 2002; Rossiter et al., 2013; Tecchio et al., 2008). These are the only observed modes of stimulation that would invoke this latent phase locking. There is weak evidence for latent phase locked evoked potentials due to vibration, but no strong conclusions are made as the reports were of visible alpha waves (D. Johnson et al., 1980b).

The top-down cortical processing seen at P300 due to abstract tasks (Duncan-Johnson & Donchin, 1982; Gray et al., 2004; Wood, Allison, Goff, Williamson, & Spencer, 1980; Yang & Zhang, 2009) and tactile recognition (Yamaguchi & Knight, 1991) aligns with the perceptually related 250ms NPLγ activity across multiple sensory systems. This pattern of onset PLγ presence and latent PLγ absence is herein referred to Perceptually Typical Gamma (PTγ). Conversely, the latent presence of PLγ will herein be referred to as Perceptually Atypical Gamma (PAγ). Using the properties of bottom up low latency PLγ versus top down P300 NPLγ, evaluation of the differences between punctate, vibrotactile, and peripheral nerve stimulation strategies with time variant properties is possible.

Composite Stimulation Strategy. Defining the cortical differences between stimulation modes will allow for the evaluation of different peripheral nerve schemes. Mechanical punctate stimulation can be used to represent a practical contact percept

and vibrotactile stimulation can provide a baseline of the impractical vibration percept commonly observed from constant frequency stimulation patterns. Utilizing onset-release patterns and stochasticity, a composite stimulation pattern can be constructed that mimics the peripheral and cortical activity seen during active grip. Although termed static, neither the peripheral nor the cortical responses of the response is perfectly constant in timing or magnitude. Integrating noise into the primary stimulus may increase resemblance to physiological representations, but the external effect is unclear in terms of detectability and phase locking. Some level of noise is present in all cortical signals as the brain is not deterministic. Deterministic neuron models demonstrate phase locking to input, while models that include noise are more accurate predictors of cell sensitivity and activity (Bulsara, Jacobs, Zhou, Moss, & Kiss, 1991; Longtin, 1993). The addition of stochastic properties to a stimuli are well investigated in terms of stochastic facilitation, where a subthreshold noise signal can randomly push a primary signal over some detection criterion (Benzi et al., 1981). In the tactile system, stochastic noise as vibration can increase detection of small physical geometries, and aligns with increased gamma synchronization. However, suprathreshold noise can mask these previously detectable percepts (Collins et al., 1997; Ward et al., 2006). In subjects with pathological neural noise, the onset of phase-locked gamma is significantly reduced in auditory detection tasks (Roach & Mathalon, 2008; Winterer et al., 2000). A balance of stochasticity is necessary then, to both reduce the undesired latent phase locking without masking a primary signal but also sustaining gamma activity.

Expectations. Punctate stimulation is expected to follow PTγ, while vibrotactile and standard stimulation trains of CCVF or VCCF will likely follow PAγ. Stochastically time variant patterns will likely follow PTγ, but act as a negative mask by diminishing onset phase locking that represents sensory input (Collins 2006).

Onset-offset bursts at the separated ends of stimulation will likely each follow distinct PTγ activation, potentially perceived as entirely separate sensations. If assumptions hold, combining the latent CCVS PTγ and onset CCVB PTγ constructs a time variant stimulation strategy that mimics the peripheral and cortical biphasic representations of tactile tasks. The gamma patterns observed in passive punctate stimulation are expected to closely match the gamma patterns in the culminating BB stimulation strategy.

METHODS

A single *Macaca mulatta* is involved in this experiment, herein referred to as NHP-R. Cortical arrays are implanted into somatosensory cortex of the left hemisphere and peripheral nerve arrays are implanted in the contralateral median nerve. Mechanical and peripheral stimulation is passive, without the need for NHP-R feedback. Arizona State University Institutional Animal Care and Use Committee approve experimental protocols. (APPENDIX A) The Arizona State University Department of Animal Care and Technologies provide veterinary supervision and care for all surgeries.

Experimental Paradigm. Punctate, vibrotactile, and all peripheral nerve stimulation are delivered in similar experimental paradigms. A single location, either a fingertip or a stimulation electrode, is chosen. For peripheral nerve stimulation, the appropriate current amplitude is calculated from the determined activity thresholds, discussed later under stimulation. Each level of associated stimulation is repeated five times and the overall set delivered in randomized order. For peripheral nerve stimulation, this is repeated ten times resulting in 50 trials (n=50). For mechanical stimulation, there are 9 punctate sessions (n=45), 10 wide range frequency vibrotactile sessions (n=50), 5 low range frequency vibrotactile sessions (n=25). Recording of all stimulation patterns involves a one second pre-stimulus window, a

half second of stimulation, and a half second post-stimulus window. For the task, NHP-R is restrained and stimulation passively applied. Each trial resulted in a juice reward, and any trials where NHP-R is agitated are immediately discarded.

Implantation. Somatosensory areas 1 and 3b in the right hemisphere of NHP-R are targeted for electrode implantation using stereotactic atlas coordinates. Following a craniotomy performed under isoflurane anesthesia, topographic features of cortex are used to refine the location of the hand representation. Two 32 channel N-Form Modular Bionic (Santa Clara, CA) arrays were implanted subdurally in the right post central gyrus, medial to the terminus of the intraparietal sulcus. The arrays consists of a 2x2 arrangement of probes, with 7 electrode sites per probe ranging from 2 to 3.5 mm in depth. Each probe also had a shallow electrode site 1 mm into the cortex used as a reference for recording equipment. (Figure 1) The depth of these probes indicates likely area 1 placement, with potential area 3b at the deepest sites.

Designed by Nerves Incorporated (Dallas, TX), a set of novel fascicle specific targeted longitudinal intrafascicular electrode (FAST-LIFE) arrays with integrated cuff electrodes are used for peripheral stimulation. Each array has 9 intrafascicular sites and 6 cuff sites composed of laser cut platinum suspended in a silicon mesh. Intrafascicular electrodes allow for precise recruitment and the cuff electrodes provides the opportunity to stimulate larger populations. Targeted microsurgical dissection of peripheral nerve fascicles ensures the intraneural electrodes penetrate fascicles with desired sensory and/or motor functions.

In NHP-R's left arm, arrays are first implanted into the sensory and motor distributions of the ulnar and median nerves at the wrist, but deteriorate due to manufacture error. After explanting and recovery, implantation is successful with a second set of arrays into the medial and lateral components of the median nerve

corresponding to the distal anterior interosseous and terminal median distributions. Peripheral implantation and execution of the fascicle specific targeting (FAST) is performed by Jonathan Cheng of Nerves Incorporated, who developed the method.

Connecting to the subcutaneous arrays requires the manufacturing of a custom transcutaneous housing. (APPENDIX B) To ensure stability, the housing mounts onto an osteo-integrated bone plate on the left humerus of NHP-R. ProtoLabs (Maple Plain, MN) manufactures the bone plate and the housing components via laser-sintered titanium with high resolution and acceptable biocompatibility. This provided easy access and secure chronic housing for the connectors. To reduce the opportunities for damaging the device and the implantation site, NHP-R wore a fitted custom jacket from Lomir Biomedical (Québec, Canada).

Neurophysiological Interface. Recordings and stimulations are performed with a Grapevine Neural Interface Processor from Ripple Neuro (Salt Lake City, UT) and custom software developed in MATLAB (Natick, MA). Cortical electrodes are recorded at 30k Hz through Ripple Micro+Stim front ends, with no filters applied. Peripheral electrodes are stimulated via Ripple Nano2 front ends, which allow in-vivo impedance measurements and varied stimulation current resolution. Impedance values were stored at the beginning of stimulation sessions.

Stimulation. Two modes of mechanical stimulation are delivered to the fingertips of NHP-R's left hand: vibrotactile and punctate. Force equivalent vibratory stimulation is delivered via a translating probe attached to a speaker mounted cable. Vibration frequencies occur in two subsets: a narrow range from 10 Hz to 35 Hz on 5 Hz intervals and a wide range from 10 Hz to 110 Hz on 20 Hz intervals. Frequency signals are generated in MATLAB and delivered through a translating probe attached to a vibration generator (3B Scientific). Amplitude of the signal is calibrated to ensure equivalent average force of the probe across frequencies. Punctate

stimulation consisted of 0.1 to 1 mm, on intervals of 0.15 mm. Stimulation is delivered via a servo-mounted cable in a custom housing, with translation distance calibrated to the servo rotation. In both cases, the fingertip rests against the device actuation point and stimulation lasts for a 0.5 second window of each trial. Both modes also had "No Stimulation" and "No Contact" control conditions.

There is an inherent risk to this passive task that the cortex will not respond while a percept is active. These percepts can be potentially nociceptive or unpleasant. In order to avoid the risk of causing distress and to avoid NHP-R becoming agitated, stimulation should be limited to lower frequencies and lower amplitudes. After initial testing of variant responses and NHP-R sensitivity, stimulation is kept below 250uA and consistently performed for 0.5 seconds at 40 Hz frequency and 500 μs wide anodal leading charge balanced pulses.

As the participation of NHP-R is passive, detection thresholds are not obtained. Instead, cortical responses to varied current amplitude are determined using the Parameter Estimation by Sequential Trial (PEST) method. This method sequentially narrows in on the parameter of choice using the "positive" or "negative" detection results of a previous trial. In this task, "positive" responses occurred when multiple cortical channels demonstrated 100% RMS increase of the stimulation window to the baseline, determined online after each trial. These current amplitude levels for each channel are dubbed Activity Thresholds (AT) and used to choose appropriate values for stimulation schemes.

Five different timing schemes are considered, based on existing stimulation paradigms and biomimetic patterns. Basic stimulation patterns are used to investigate the commonly induced percepts. First, Constant Current Varied Frequency (CCVF) stimulation is delivered at 10 to 35 Hz on intervals of 5 Hz. Amplitude is chosen to be 100% of the respective channel's determined activity

threshold (120%AT). Second, Varied Current Constant Frequency (VCCF) stimulation is delivered at 40 Hz from 0 to 120%AT on intervals of 20%AT. (Figure 2)

In the second set of stimulation schemes, more complex timing is introduced. In these, the 40 Hz frequency of stimulation is redefined as the average number of pulses per second. Four levels of Constant Amplitude Varied Biomimetic (CAVB) stimulation are performed at 120%AT. CAVB stimulation consists of increased clustering of onset-offset bursts at the start and end of the stimulation train, biased towards onset using a combination of exponential functions. Next, six levels of Constant Amplitude Varied Stochasticity (CAVS) stimulation are delivered at 100%AT in order observe any masking effect. Stochasticity here is defined as increased randomization of interpulse timing. In culmination, combination of four levels of CAVB and a consistent CAVS pattern is created and delivered. This combinatory scheme is referred to as Bimodal Biomimetic (BB) stimulation. It consists of the varied onset offset clustering of CAVB at 120%AT combined with a consistent level 5 pattern of high CAVS at 100%AT.

For each stimulation session, it is important to keep train patterns consistent between all trials. While timing variation is sometimes involved in the construction of the train, there is no inter-trial variation. This allows us to infer responses as results of timing principles and not inter-trial temporal variation of the pulse timing.

Analysis. Analysis focuses on the local field potential recordings from the cortical arrays. The planned analysis revolves heavily around time-frequency transformations of continuous traces, but the absence of spiking information is unexpected. Recordings of neural information are performed at 30k Hz in 1.5-second-long trials. Offline, the data is filtered through an 8 order 1000 Hz low pass bidirectional filter, and down sampled to 3000 Hz.

Using the FieldTrip Toolbox in MATLAB, filtered trials of each stimulation condition are linearly detrended and transformed into a complex time-frequency representation. To achieve adequate spectral estimates in both frequency and time resolution, a multitaper transform with a fixed 200 ms window and 12 Hz bandwidth is used. Multitaper spectral estimation uses pair-wise orthogonal tapers to obtain independent estimates from the same sample, providing more reliable estimations of a single trials spectral power without losing inter-trial variability. This yields a complex time-frequency spectral estimate for each point of the trial time course and from 0-100 Hz. The measure used to evaluate event related power, ERP%(t,f), is determined by the percent change of the power, P(t,f), corrected by the baseline window from -0.5 second to -0.1 seconds. This scales the each frequency's power to its respective baseline, providing meaningful comparisons across the spectrum. Equation 2.

A point by point one way ANOVA across stimulation levels determines significant time-frequency clusters for each stimulation location and modality (Maris & Oostenveld, 2007). The ANOVA produces a time-frequency representation of the F-statistic across a respective stimulation levels. A nonparametric distribution for statistical comparison is constructed by 2000 random permutations of the trials. Using alpha<0.05, a critical value is determined for each time-frequency point, resulting in masks of time-frequency significance: $ERP\%_{sig}(t,f)$. This provides the ability to investigate time-frequency clusters that are significantly responsive to stimuli. Only significant points of ERP% within the gamma band of 30-65 Hz are considered.

$$P(t_{\gamma Sig}, f) = ERP\%(t_{\gamma Sig}, f) = \left[P(t_{\gamma Sig}, f) - P(t_{base,f})\right]/P(t_{base,f}) \times 100 \quad (2)$$

In addition, the phase synchrony of each stimulation condition is measured by calculating the Phase Lock Value (PLV) across all relevant trials (LaChaux 1999,

roach 2009). Using the average magnitude of the normalized complex spectral density F(t,f), PLV is estimation of the consistency of phase. Equation 3. Using PLV, components of the time-frequency representation significant to simulation are classified as phase locked or non-phase locked to stimulation. Significant phase locking is determined by PLV measures that exceed a 95% confidence interval PLVCI, calculated by repeating the PLV calculation using trials of all conditions and permuted 5000 times across cortical electrodes. After averaging across gamma frequencies, the maximum value represents PLVCI. In other words, the maximum PLV of sufficiently random trials represents the minimum level that trials could be significantly locked.

$$PLV(\mathrm{t}, f) = \left|\frac{1}{N}\sum_{n=1}^{N}\frac{F_n(\mathrm{t},f)}{|F_n(\mathrm{t},f)|}\right| \quad (3)$$

In order to dissect the phase-locked and NPLγ, the time domain significance of PLV is used to create a second time-frequency mask. Since the PLV confidence interval is calculated as the average across all gamma frequencies, this mask applies to time points across all frequencies. To alleviate comparative issues between these, power is averaged across the frequency domain and integrated across the time domain. Respectively, this assigns equivalence for magnitude of power anywhere in the gamma range and accounts for varied activity within time domain. In the time domain, significant ERP% with PLV above the confidence interval are considered phase-locked. Equation 4. Conversely, the NPLγ is the frequency averaged and time integrated gamma where the time-frequency ANOVA is significant and the time domain PLV is not significant.

$$\int PL\gamma = ER\%(t,f) * \Delta t, t \in \left\{\left[\left(\frac{1}{N_f}\sum_{f=\gamma} PLV(t,f)\right) > PLV_{CI}\right] \cap \left[ER\%_{sig}(t,f)\right]\right\} \quad (4)$$

$$\int NPL\gamma = ER\%(t,f) * \Delta t, t \in \left\{\left[\left(\frac{1}{N_f}\sum_{f=\gamma} PLV(t,f)\right) \leq PLV_{CI}\right] \cap \left[ER\%_{sig}(t,f)\right]\right\} \quad (5)$$

Proper magnitude estimation of separate PLγ and NPLγ in the time domain allows for the investigation of inter-trial variance. Across multiple sensory systems, the immediate onset of gamma is phase locked to stimuli. For this reason, analysis is broken into onset and latent time domains. Due to the windowed nature of time-frequency analysis, onset time includes data bounding the stimulus by -50 ms to 150 ms. The latent time domain, from 200 ms to 400 ms, is designed to bound the existing representation of cortical perception seen in an abundance of perception dependent NPLγ literature

To clarify the process:

I. Transform local field potentials to event related power, corrected by the baseline power of each frequency, ERP%(t,f)

II. Use non-parametric analysis to determine significant time frequency points across stimulation conditions, ERP%sig(t,f).

III. Determine time points of significant phase locking by calculating PLV(t,f) and PLVCI.

IV. Separate data into onset and latent time distinctions.

V. Calculate the PLγ by integrating the ERP%(t, γ) that is stimulation significant and PLV significant.

VI. Calculate the NPLγ by integrating the ERP%(t,γ) that is stimulation significant and not PLV significant.

VII. Integrate significant gamma states within onset and latent time domains to compare to the perceptually appropriate standard.

RESULTS

Mechanical Stimulation Responses to mechanical stimulation did not produce highly localized responses to each of the digits. As local field potentials represent larger populations of neurons, and the somatosensory representations of the digits are within 1mm of each other, the cortical arrays demonstrated broad activity for multiple digits. Punctate stimulation was the most localized, with strongest responses on D2 through D4. The most lateral probes on the array are G1 and A1 (refer to Figure 1) with I1 and E1 approximately 0.8mm medial. Individual digits were represented across the entire first array, but G1 and A1 had strongest response to digit 2 while I1 and E1 preferred both digit3 and digit 4. The second array, implanted more medially, consistently had limited, if not absent, responses.

Shown averaged across probe G1, punctate stimulation produces strong evoked P125 potentials followed by N175, similar to literature reports of unattended mechanical stimulation. There is a slight P250 inflection at high magnitudes of punctate stimulation, but dwarfed by the initial P125. Upon retraction of the punctate effector, the evoked response repeats as if to a distinct stimulation. Any presence of P250 in the initial evoked response is not present in the post-stimuli evoked response. (Figure 3)

Vibrotactile stimulation at low frequency consistently demonstrates P125 and N175 potentials as well. At lower frequencies of 10 to 30 Hz, initial response precedes repeated evoked peaks concurrent with stimulation frequency. Presence of this repetition diminishes greatly above 35 Hz, but obvious frequency dependent activity is present by visual inspection. Higher frequencies demonstrate slight increases in the latent portion of stimulation, but this is not obviously apparent, especially in the low frequency stimulations. In raw data, prevalent offset responses are not present. This is not shown in the averaged trials, as data processing required

the late samples to be removed. The stimulator had a direct event of stimulation sent to the recording processor, but had frequency dependent latency of stimuli deliver. This resulted in a reduced time window for comprehensive analysis, and the post-stimulation epoch is not statistically accessible.

Using nonparametric statistical method, a point-by-point ANOVA determines cortical channels with significant gamma response to specific fingertip stimulation. No channels indicated significant activity on the physical control condition. Digits with prominent evoked potentials, D2 through D4, have 14, 10, and 2 respective channels with time-frequency points significant to punctate stimulation. Activity spreads to D1 and D5 with vibrotactile stimulation showing 28, 26, 28, 30, and 6 significant channels. Significant time frequency gamma clusters varied in size, with some including almost the entire 30 through 65 Hz range and others with only a few frequency or time points. (Figure 4)

Momentarily ignoring the significance of phase-locking, the overall evoked gamma and the phase lock value trends can be observed. Punctate stimulation increases in overall magnitude with indentation level, with activity starting at 0.1 mm. A P200 inflection is increasingly prominent, overcoming the P125 onset response at some level between 0.4 mm and 0.55 mm. Vibrotactile stimulation levels do not vary in force so the P200 potential seen in large indentations is seen in all conditions, peaking at 50Hz stimulation and attenuates at higher vibrotactile frequencies. Consistently for punctate, the average power across significant gamma exceeds the average power of all gamma. This demonstrates the purpose of the time-frequency statistics in isolating the more powerful responses of stimulation. Vibrotactile stimulation demonstrates a close equivalency between the two, due to less discriminating significance masks. Punctate stimulation provides more selective

time and frequency significance than the vibrotactile masks, which show include most of the stimulation window and gamma frequencies.

Phase Locking Value calculations cross the 95% confidence interval near the onset and offset of all punctate stimulation, with proportional magnitude. Vibrotactile gamma exhibits phase locking significance at onset, at P200, and occasionally sustained throughout stimulation. This is especially noticeable at 35 Hz stimulation, with the entire stimulation window demonstrating significant phase locking. (Figure 5)

Dissecting the proportions of gamma between phase locking states creates temporally variable representations. Only the event related power of interest is selected by the application of the time-frequency significance mask and the significant or non-significant PLV mask: $ANOVA_{sig}(t,f)$ and PLV(t)>CI or $ANOVA_{sig}(t,f)$ and PLV(t,f)<=CI. Averaging across the gamma band within these masks results in separate non-continuous time series. The midpoint estimation integral of these time series within defined onset and latent time windows dictates the presence of PTγ or perceptually atypical gamma, primarily differentiated by the presence of latent gamma phase locking. The observation of this is explained in Figure 6, with the onset and latent window outlined in the evoked traces, comparison of phase locked gamma and non-phase locked gamma in magnitude, and the comparison of phase locked gamma and non-phase locked gamma in ratio. The latter provides the easiest visualization of the activity, providing a ratio of zero when phase locked activity is absent – ideally in the latent window.

In the onset time window of mechanical stimulation, significant channels of each digit indicate positive trends in PLγ for both punctate and vibrotactile stimulations. (Figure 7) Vibrotactile NPLγ keeps constant across frequencies, but grades with magnitude of punctate stimulation. In almost all mechanical stimulation

conditions, both states of gamma appear, with the overall gamma and the NPLγ generally greater than the PLγ. The two ranges of vibrotactile stimulation demonstrate different levels of activity at the same frequency. The narrow range, 0 through 35 Hz, produces a dramatically high PLγ presence while the similar values in the wider range do not. This could likely be due to the lower number of samples affecting the time-frequency or PLV significance calculations. While differences exist between stimulation modes, the non-phase lock gamma power presents across all digits for all mechanical stimulation. In the latent time window, significant channels of each digit indicate an almost complete absence of PLγ during punctate stimulation. Therefore punctate stimulation is consistent with the PTγ trends described previously. At larger indentations on digit 2, the NPLγ even exceeds overall gamma. For all vibrotactile stimulations except high frequency vibrations, NPLγ appears and can exceed PLγ. This is indicative of the perceptually atypical gamma seen with median nerve and painful electrotactile stimuli. Observing the ratio of PLγ to NPLγ paints a clearer portrait of this activity. (Figure 8) Ratios close to zero indicate a larger presence of NPLγ than PLγ, and ratios of zero indicate a complete lack of PLγ. This is seen across the latent window of punctate stimulation, but not vibrotactile stimulation.

Peripheral Nerve Stimulation. Peripheral electrode impedance over the course of two months is relatively stable. Determining the activity threshold via the PEST method determined appropriate levels of stimulation for 7 intrafascicular and 4 cuff electrodes in the terminal distribution and 8 intrafascicular and 3 cuff electrodes in the anterior interosseous distribution. This data is present in Appendix B. Terminal distribution implant stability is high, with some variation, but the anterior interosseous distribution implant shows a decay in active channels after about a month of implantation. This coincides with a broad increase in impedance for that

array. In result, complete data sets for 8 (5 intrafascicular, 3 cuff) terminal distribution channels and a single anterior interosseous distribution intrafascicular channel are included in analysis. Incomplete data sets for 3 more anterior interosseous channels (2 intrafascicular, 1 cuff) have partial data sets of only VCCF and CCVS.

The evoked potentials across all stimulation electrode followed similar patterns, with varied magnitudes of responses. Evoked potentials and evoked gamma for all stimulation electrodes are in Appendix C. The second terminal branch intrafascicular electrode highlights these patterns. (Figure 9) All stimulations, except VCCF at low levels, demonstrated a strong positive potential at 75ms, earlier than the unattended mechanical stimuli, consistently followed by a negative inflection. While CCVF and VCCF have increased activity at 250ms, there is no peak and is visually identifiable entrainment of the stimulus. A 250ms potential, within the P300 definition range, is clear for time variant patterns CCVS, CCVB, and BB. The only demonstration of offset evoked potentials occurs in CCVB and BB around P50 after stimulation. BB also demonstrates a higher P250 response than CCVB or CCVS. In terms of evoked potentials, the stimulation pattern with the most similarity to punctate stimulation is the composite biomodal biphasic scheme.

Using the same statistical methods as mechanical stimulation, a point-by-point ANOVA determines cortical channels with significant gamma response to each stimulation channel. (Figure 10) Significance masks resulting from the VCCF stimulation provide the time-frequency response of interest for all stimulation patterns, except CCVF. This allows comparison between standard patterns and time variant patterns with a focus on the change in phase locking significance. All peripheral channels with complete data sets demonstrated significant cortical activity. The only anterior interosseous branch channel with a complete data set

produced significant activity only on one channel. The terminal branch channels produced 19 significantly active channels on average, with broad time-frequency significance. Cortical channels significant to the peripheral nerve stimulation largely overlap with the cortical channels significant to mechanical stimulation, except in the case of the anterior interosseous nerve channel.

As before, ignoring the significance of phase-locking briefly allows investigation of the evoked gamma and the phase lock value trends. Ideally, similarities between PTγ seen in punctate stimulation can be identified within the peripheral stimulation results. Again, this included latent evoked gamma, onset and offset phase locking, and prominence around P200. (Figure 11) The early evoked potentials of P75 are also seen in the evoked gamma across all stimulation modes. Peaks close to P200 are present for higher levels of VCCF and CCVF, and low levels of CCVS before the pattern becomes increasingly time variant. CCVB and BB stimulations demonstrate slight P200 inflections, but to a much smaller degree. With increasing time variance of CCVS, the evoked gamma at 200ms actually becomes a negative inflection. This trend is seen in the BB stimulation pattern as well, but partially balances with the combined CCVB P200 potential.

Low frequencies of CCVF and high levels of VCCF demonstrate persistent phase locking across a majority of the stimulation window. On the contrary, the CCVS stimulations demonstrate clear diminishment of phase locking as time variance increased. CCVB stimulation demonstrated a loss in both latent phase locking and latent evoked gamma. However, a benefit is increased onset-offset phase locking and gamma.

Standard stimulations schemes demonstrate constant phase locking over the latent portions of stimulation, violating PTγ conditions. The evoked gamma is maintained in the CCVS scheme without latent phase locking, However, there is

variably present onset phase locking, and absent offset phase locking. Latent evoked gamma of CCVS and the onset-offset gamma of CCVB unified into and evoked gamma response with increased similarity to the PTγ traits.

Dissecting the phase-locking states provides the trends of these significant responses for each peripheral stimulation channel. First, the single anterior interosseous channel is addressed because of its unique responses. This stimulation channel demonstrated almost no phase locking in the onset nor the latent window, even to high levels of VCCF or CCVF. In fact, the composite BB stimulation is the only stimulation modes to induce phase locked gamma and it also largely followed PTγ trends.

For all terminal branch stimulation channels, the onset window is dominated by PLγ, with positive linear trends in CCVF and VCCF for all sites. (Figure 12a, 13a) Increasing the three modes of time variant stimulation decreases onset PLγ across all stimulation sites. In comparison, NPLγ in this window is generally dwarfed, but exhibits positive trends in the time variant stimulations. Onset PLγ is never completely absent in the terminal branch stimulation sites.

In the latent window, similar positive trends in onset PLγ are observed for VCCF and CCVF. PLγ responses to time variant stimulations generally trend negative, with maximum conditions of most stimulation trends eliminating it entirely. However, the CCVS and CCVB stimulations also reduce the NPLγ. The BB stimulations provided the ideal response of increasing non-phase locked trends with decreasing phase locked trends. Only one terminal branch electrode exhibited phase locked gamma at the highest level of BB stimulation. (Figure 12a, 13b)

These trends are reinforced looking at the ratio between PLγ and NPLγ of the cuff electrodes and the intrafascicular electrodes. (Figure 12b, 13c, 13d) In the

onset window, this ratio high across all terminal branch stimulation electrodes and stimulation schemes, except low levels of VCCF and higher levels of CCVS. In the latent window, the ratio is much lower, and generally less than one, indicating a stronger NPLγ presence than PLγ. However, in the higher levels of the time variant stimulation strategies, the ratio is diminished or absent. From the aforementioned evoked traces however, the lack of onset and offset activity of CCVS and CCVB indicate that these stimulation patterns do not wholly mimic punctate stimulation. Combining the evoked patterns of the BB stimulation and the diminished latent PLγ indicate a more complete mimicry of the punctate responses.

Discussion

Perceptually Typical Gamma Definition. In this discussion, it is primarily important to distinguish two assumptions. One, the violation of typical gamma only occurs in terms of latent phase locking gamma presence. Literature suggests a defined and supported timing structure of typical PL and NPLγ in multiple modes of sensory perception. The vision, auditory, tactile, and pain systems exhibit this pattern in remarkably similar manners. PTγ manifests as onset PLγ and increased latent NPLγ at approximately 250ms. Attention to and perception of a stimulus enhances the latent NPLγ. For this reason, a strong inattention or weak perception would produce no increase in latent NPLγ. This does not indicate an atypical sensation as this attention-associated decrease does no incur an increased PLγ, and therefore the only violation in typicality would be the presence of significant latent phase locking. In terms of latent gamma, only pain responses elicited from peripheral nerve stimulation and from electrotactile violate the proposed structure (Babiloni et al., 2002; Rossiter et al., 2013).

Second, the attention to stimuli is not important to demonstrate the traits of practical and impractical stimuli. This study successfully investigates the deviation

between the typical gamma pattern of normal somatosensory activation and the observed violation from atypical non-painful mechanical stimuli. Then, the resulting deviation is applied to the results of varied patterns of median nerve stimulation. The goal is to identify stimulation parameters that modulate the violation of PTγ. All stimulations in this experiment are passive and require no perceptual response from NHP-R, as the goal is the cortical difference between stimuli not the perceptual difference. The passivity indicates any latent NPLγ responses within the time window of perceptual recognition are potentially a result of the primate paying sudden attention to an unexpected stimulus. This is primarily seen in higher levels of current intensity, frequency, or time variant stimulations with biomimetic components. However, this puts the term "perceptually typical gamma" into question. The non-attended task, presence of early evoked potentials and gamma, and the general lack of P300 evoked gamma indicate that the cortical representations observed are not likely representing attended stimuli or perceptual decisions. However, the comparison between responses is valid in terms of bottom up input to the somatosensory system. The definition of PTγ still applies, as the onset phase locking is only appropriately present in onset of perceived/attended and unperceived stimuli. The lack of latent phase locking is also a key component of difference to this definition. Therefore, this study is a strong investigation into the stimulation parameters, as the violation of appropriate input provides a predictive estimate of imminent perception. The manipulation of this early cortical processing can contribute to the construction of desired percepts.

Peripheral Electrode Considerations. Cortical recruitment of peripheral stimulation is larger than expected with wider sets of significantly active channels present than in mechanical actuation. The intrafascicular stimulation was expected to provide smaller recruitments of neuronal populations, but seemed to perform

contrarily. This could be a result of stimulation parameters chosen. The 500 μsec pulse width is large, but the time required to sweep through all stimulation parameters sets was not available with this experiment. Once a set of parameters demonstrated little agitation on NHP-R, the more pressing experiments were performed.

The first set of electrodes implanted failed due to manufacture error, setting the experiment back four months. Once NHP-R recovered, the experimental timeline was reduced to two months. In the appendices, the impedances over this experimental window show a sharp increase one month post implant for many channels across both arrays. This coincides with sharp change or loss in channels with determined activity thresholds. Upon explanation of these arrays, it was discovered that similar deterioration of the first set occurred for all of the anterior interosseous implant and most of the terminal median implant. This explains the limited number of complete data sets obtained.

Successful Modulation of Gamma Phase Locking. Overall, the punctate stimulation demonstrates the predicted pattern of gamma phase locking activity. As the indentation magnitude increases, so does the latent non-phase locked response and a P300 peak eventually does manifest. Other traits observed supplement the perceptually typical definition by incorporating: (1) the presence of early onset-offset evoked potentials, (2) the presence of significant onset-offset phase locking, and (3) the sustained evoked gamma with no phase locking between the prominent onset and offset patterns. Vibrotactile stimulation violated the PTγ definition in almost all cases by demonstrating sustained or latent phase locking and no offset response in terms of evoked potential, evoked gamma, or phase locking. Due to this, the violations of the defined rules does not necessarily indicate a painful response, but an atypical sensation of repeated bottom up activity. Static tactile activation and

highly dynamic tactile activation provide highly different cortical representations that provide necessary comparisons to peripheral nerve stimulation.

Peripheral nerve stimulation behaved largely as expected, with standard stimulation patterns violating the PTγ responses. Consistent timing of pulses within the CCVF and VCCF show persistent phase locking throughout the stimulation window. This is similar to the vibrotactile stimulation PTγ violations and provides evidence that the two modes activate the sensory system in similar methods. Hence, this is comparable to one of the most common elicited percepts in somatosensory stimulation: vibration and pulsing. If the cortical input representation can be modulated away from this similarity and maintain the effects of punctate stimulation, the perception of the stimuli would likely move away from these impractical sensations.

The different stimulation patterns with time variant properties modulate in manners consistent with this goal. Increasing interpulse variability significantly decreases the sustained phase locking, but loses the large onset and offset responses associated with punctate stimulation. However the opposite is seen using onset-offset burst patterns. Creating a composite stimulation paradigm by combining the masking and sustained properties of the CCVS and the phase locking onset-offset dynamics from the CCVB, cortical representations can be modulated into the conditions that satisfy perpetually typical gamma. However, the balance between this onset-offset stimulation and the sustained stochasticity can likely be optimized.

This raises many questions about stimulation parameters that should be asked for natural sensations. Exploration of this stimulation mode's efficacy can be broken into each contributing component with many opportunities for refinement. What properties of the onset-offset bursts modulate the phase locked response most effectively? At present, the onset offset bursts differ in magnitude than the stochastic

stimulations, and are precisely timed with low interpulse variability. Initial investigations should involve the effect of this magnitude ratio to determine what properties are necessary to achieve the onset-offset phase locking in the presence of noise. In the responses shown, the CCVB stimulation produced very large peaks of phase locking, while punctate stimulation produced barely significant peaks. It is likely that low magnitude CCVB can contribute the desired effect on a modulated scale. This would be analogous to the human touch, and how the rate of tactile sensation is not differentially perceived, but an important component of proper reactions. This would need to be carefully balanced with the noise from the stochastic signal.

Stochastic noise can mask a signal at high levels, or boost a signal at optimal levels. At optimal levels, the stochastic signal is randomly pushing the primary signal past some criterion of detection, providing the basic mechanism of stochastic facilitation. Results indicate that phase locking is reduced by neural noise, but non-phase locked data is also reduced. The N300 inflection at higher CCVS is consistent with high noise in a sensory system masking the primary signal – suggesting that if a P300 inflection were to be achieved, it would have to overcome this artificial negative baseline. With optimization, the stochastic component needs diminish phase locking but not incur this negative inflection that would likely mask any primary signals. Inclusion of optimized stochastic variance and the balanced current intensity ratio could work as an "on-demand" stochastic facilitation model. A primary signal consisting of the minimized onset-offset phase locking represents rate of contact while the stochastic stimulation provides sustained gamma presence and increases sensitivity to tactile properties. Conceptually, this model would be a great benefit to active tasks in prosthetic users in just providing increased sensitivity only while

contacting an object. If the actual percepts of the sensation manifest in more typical and practical tactile sensations, the result is profound.

As a final note, the curious case of the anterior interosseous stimulation channel needs to be discussed. Implantation in a nerve that primary innervates forearm muscles is not expected to produce robust activity in the hand area of somatosensory cortex. Therefore, response to stimulation on only a single cortical channel is mundane. However, if we maintain the definition of PLγ as sensory input, the results of this stimulation channel are particularly interesting. The only time significant PLγ activity is present in somatosensory cortex due to anterior interosseous stimulation is as result of the Bimodal Biomimetic stimulation composited herein this study. That is, a nerve innervating muscles associated with finger movements demonstrates input to somatosensory cortex only when the stimulation is designed to mimic normal physiological dynamics. This provides an exciting exploration of what filters are placed on afferent information from grip tasks to somatosensory cortex. However, a single channel of stimulation providing a single channel of activity is not enough for a concrete conclusion, especially with degradation of peripheral implants in vivo.

CONCLUSION

It is shown that punctate stimulation follows the same rules of other sensory systems with regards to the presence and timing of phase locked and non-phase locked. These rules are violated by vibrotactile stimulation, confirming that the deviation from these typical traits does not solely induce pain. Standard constant frequency stimulation patterns violate PTγ conditions, explaining the common pulsing, vibration, and pain percepts elicited in sensory feedback. Composition of a stimulation pattern based on neurophysiological tactile information is performed by combining tonic and phasic dynamics with stochastic noise. Using this pattern in

median nerve stimulation achieves modulation from atypical responses into appropriate cortical representations. These lack latent PLγ, but maintain NPLγ and biomimetic onset-offset evoked potentials. The variables of the biphasic stimulation model are not well investigated herein, but provide a strong groundwork for future stimulation schemes in terms of practical sensation or practical benefit to tactile sensitivity.

FIGURES

Figure 1. Cortical Array Structure and Representation. The N-Form cortical arrays

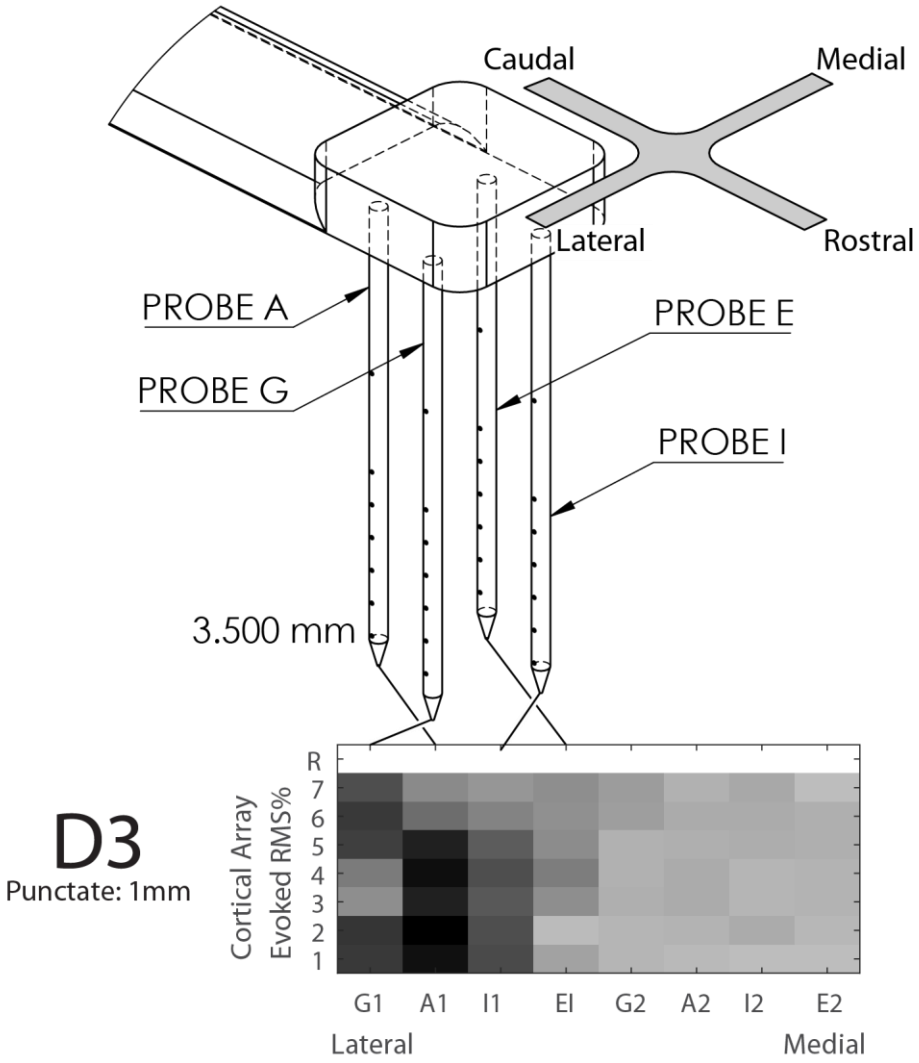

consist of a 2x2 arrangement of probes, with 7 recordings sites and a single shallow reference. Two arrays are implanted into somatosensory cortex, with direction defined in the figure. Below is an example response of the array to illustrate the medial-lateral and depth arrangement of the figure.

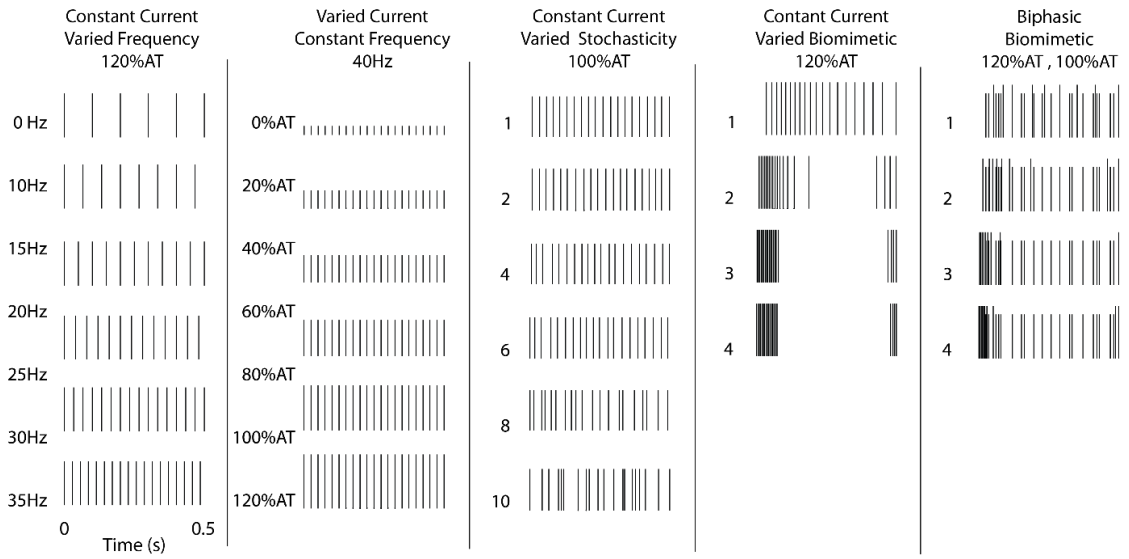

Figure 2. Stimulation Patterns. Illustrated are the timing patterns associated with stimulation. CCVF and VCCF are obvious. The BB stimulation uses the 8th level of CCVS across the 4 levels of CCVB.

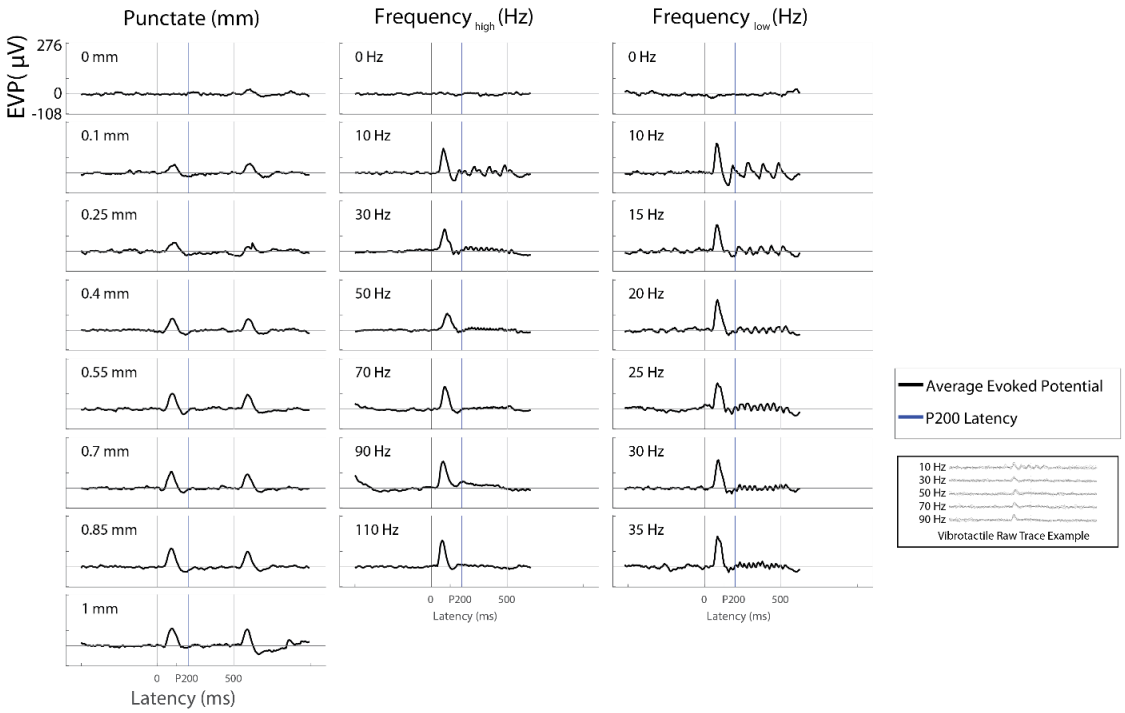

Figure 3. Evoked Potentials to Mechanical Stimulation. Trial averaged responses of each stimulation level for each stimulation mode make the variation in response immediately apparent. The repeated stimuli of the low frequency vibrotactile stimulation creates a visually obvious entrainment of repeated evoked potentials. This is mostly eliminated by 40 Hz. Due to equipment latency, truncation of the the latter portions of trials is necessary. Therefore the offset response absence is not obvious, but the inset of raw data demonstrates the lack of any large magnitude offset response across multiple frequencies.

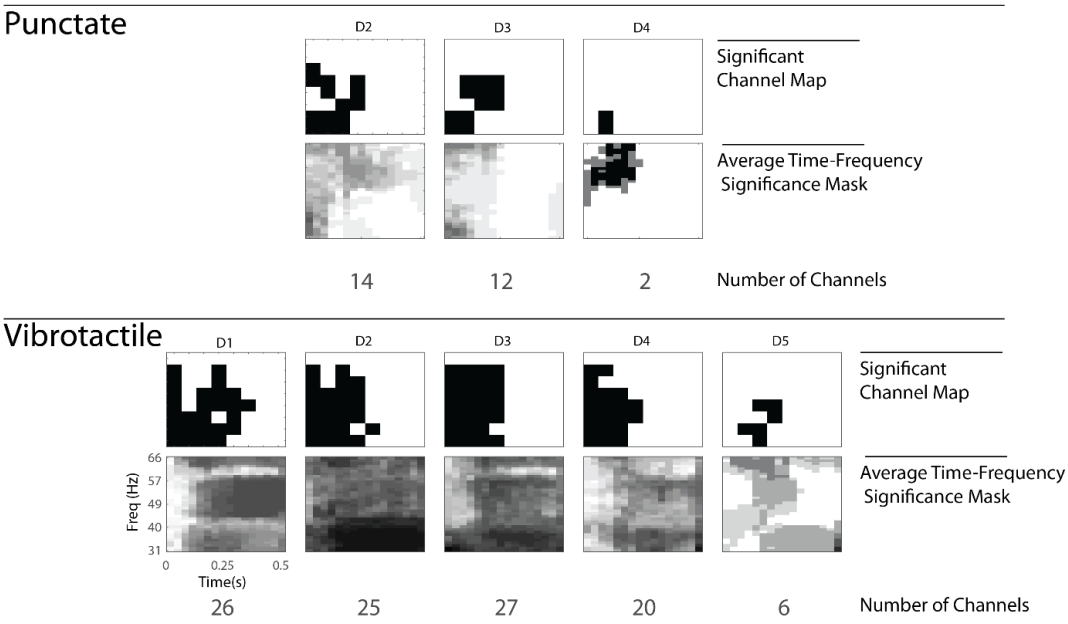

Figure 4. Cortical Significance to Mechanical Stimulation. For the significance channel map, refer to Figure 1 to understand the physical arrangement of this illustration. Typically, only channels on the most medial array significantly respond over stimulation levels. The average time-frequency significance mask is constructed by averaging the Boolean mask for each significant channel to show common points of response.

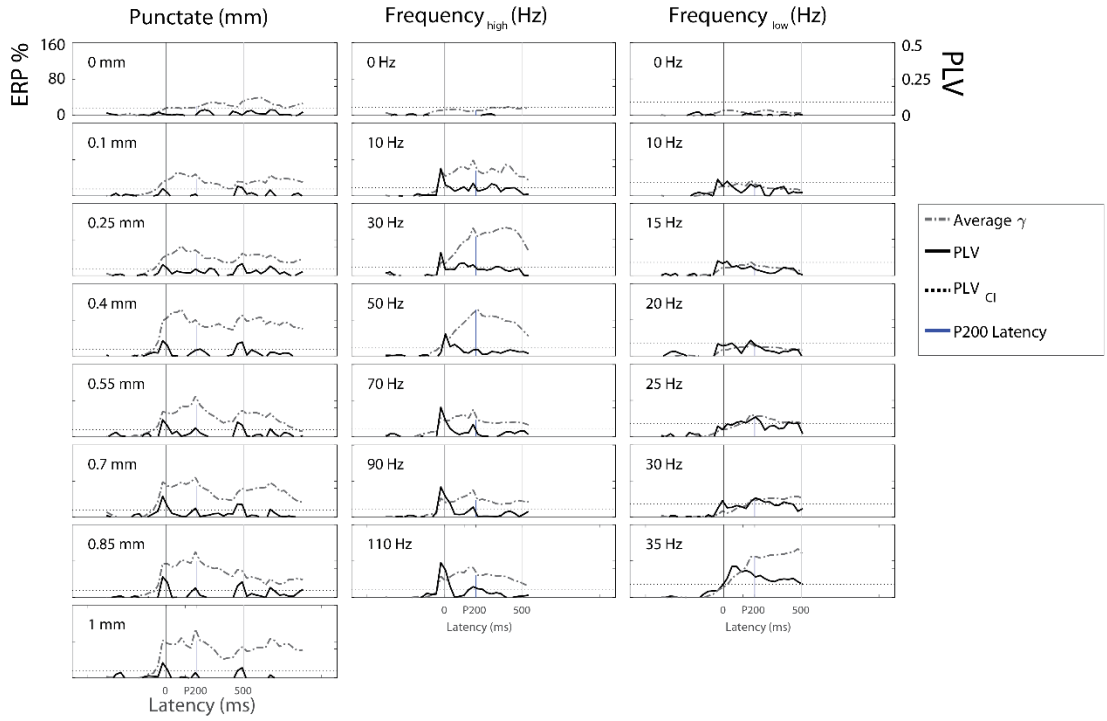

Figure 5. Evoked Gamma to Mechanical Stimulation. For the 7 cortical channels on the G1 probe, the average evoked gamma activity is plotted against the phase locking value. Where PLV crosses the horizontal dotted line, the PLV confidence interval, the gamma is considered phase locked.

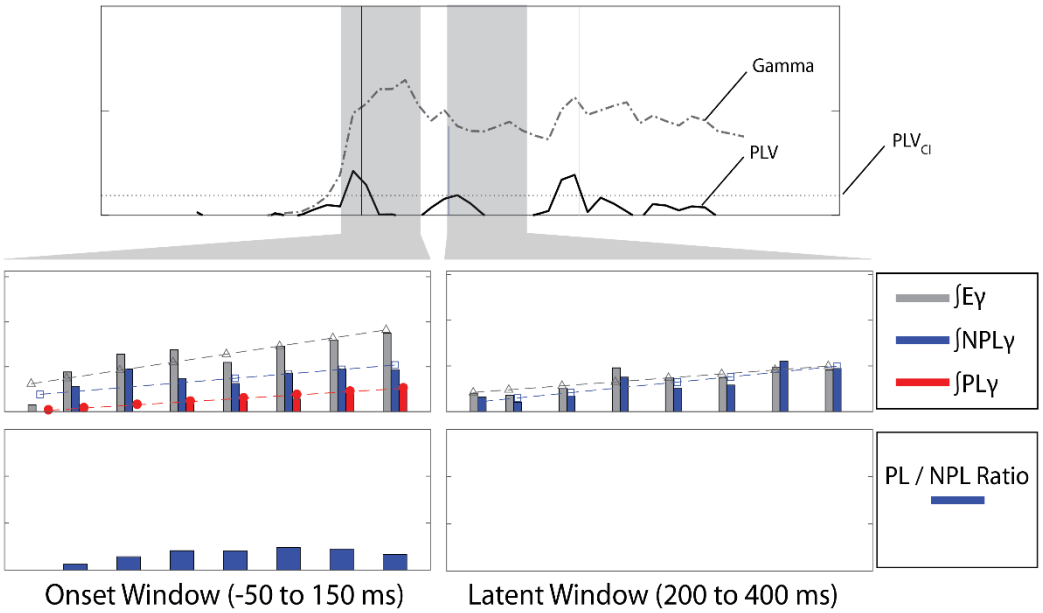

Figure 6. Onset and Latent Window Segregation. The gamma can be examined in two windows, the onset, between -50 and 150 ms of the stimulus, and the latent window, between 200 and 400 ms. The segregated phase locked and non-phase locked gamma can be compared between the two windows, as seen in the second row. Phase locked gamma should only be present in the onset window, while absent in the latent window. Due to this ideal of latent absence, the ratio of phase locked gamma to non-phase locked gamma should be low or zero in the latent window, shown in the final row.

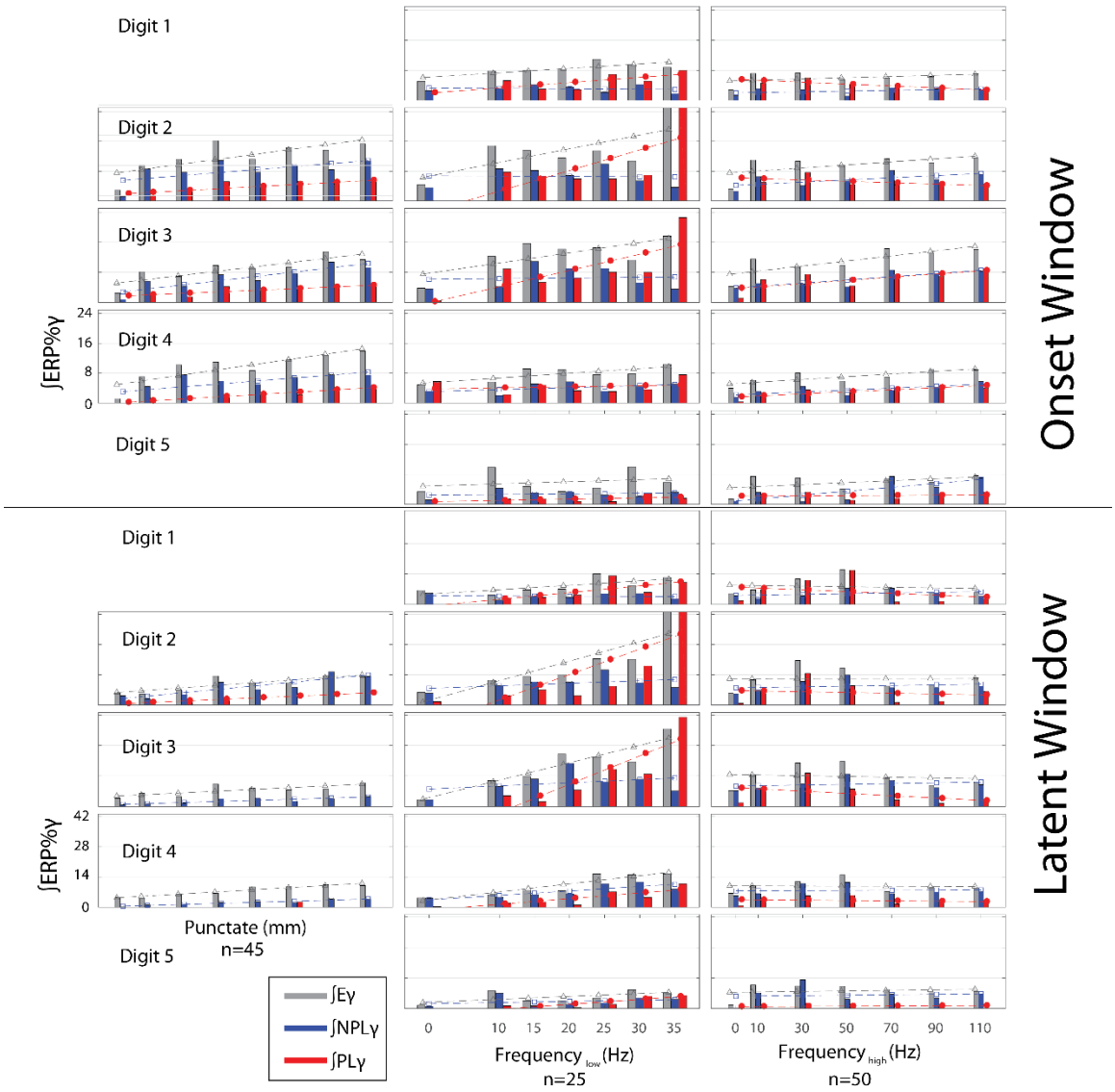

Figure 7. Trends in Gamma Power Over Mechanical Stimulation for both Onset and Latent Time Windows. Punctate stimulation follows PTγ with little to no latent phase locked gamma. Vibrotactile violates the typicality with considerable phase locked gamma in the latent window.

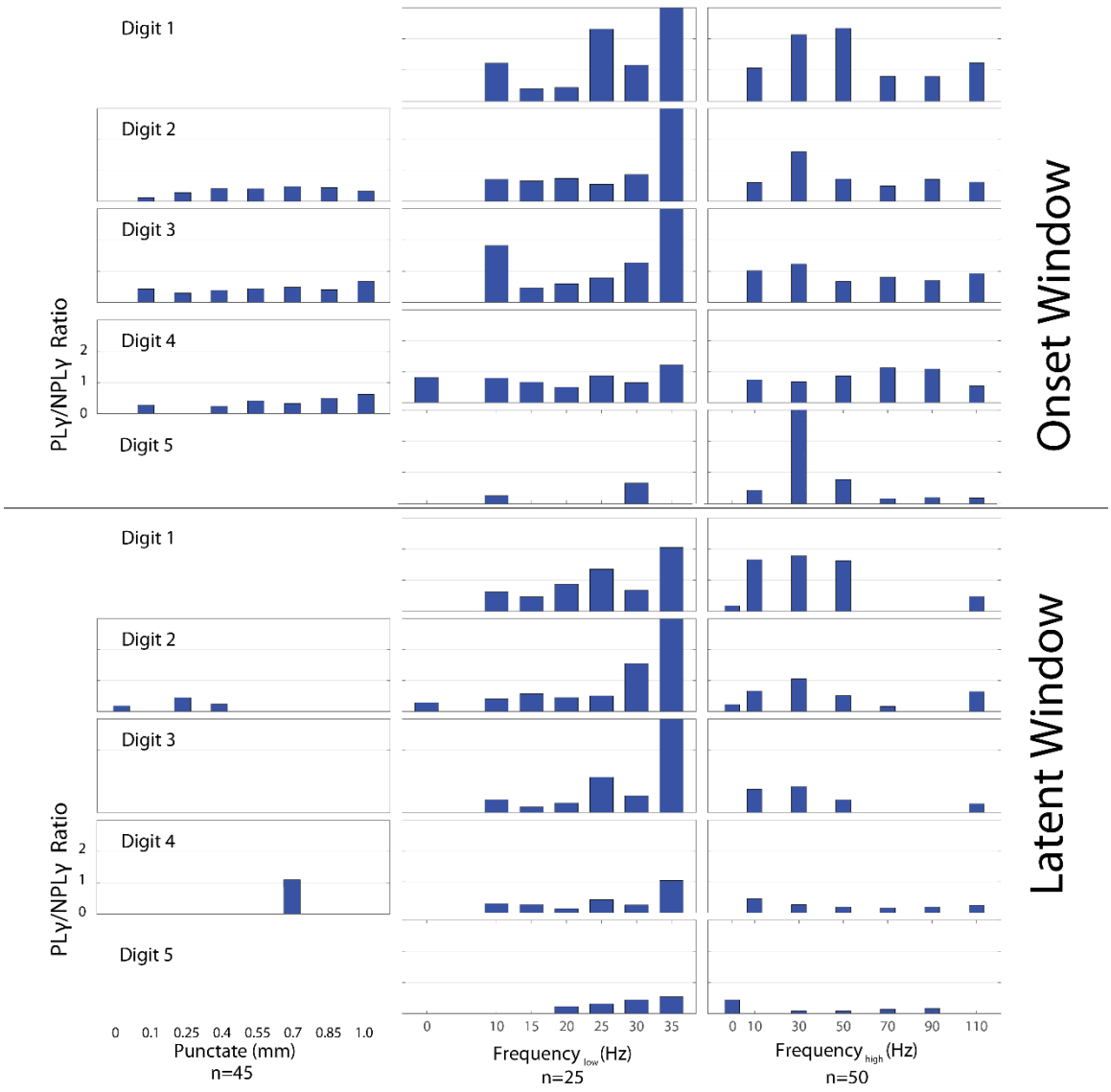

Figure 8. Trends in Gamma Power Ratio Over Mechanical Stimulation for both Onset and Latent Time Windows. In these figures, the appropriate trends in gamma are much easier to observe. The magnitude of phase locked gamma to non-phase locked gamma allows for a simple observation of their relation. In the latent window, the punctate stimulation shows ratios of zero for most conditions, while the vibrotactile stimulation has ratios greater than zero for most a high majority of stimulation conditions.

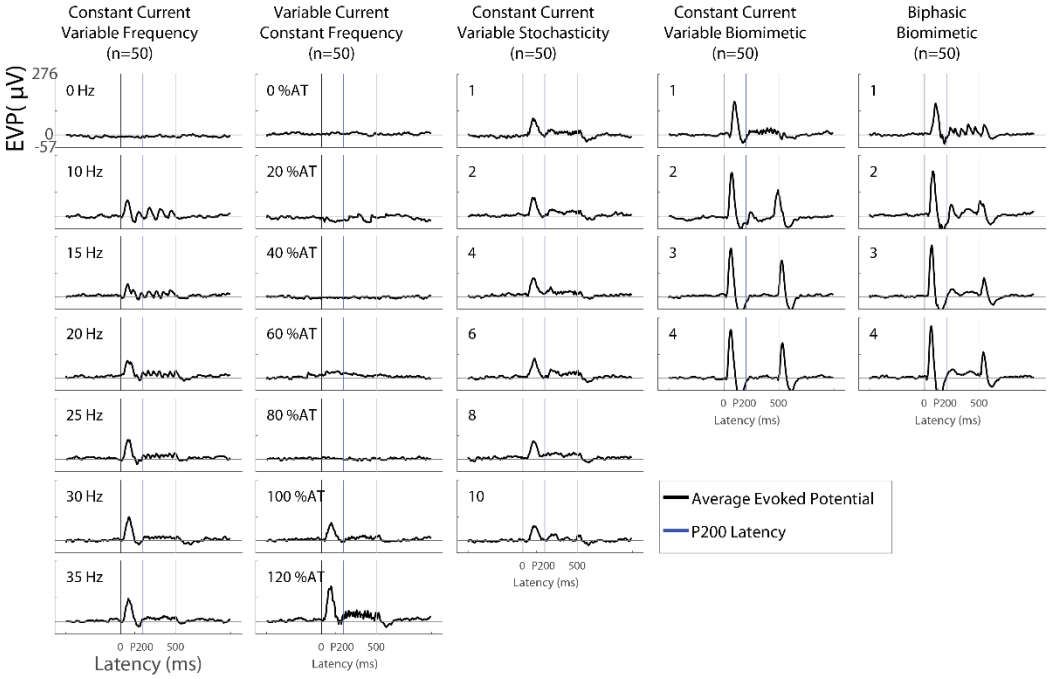

Figure 9. Evoked Potentials to Peripheral Nerve Stimulation. Similar to Figure 3. Note the entrained responses to variable frequency, the diminished response of CCVS, the onset-offset potentials of CCVB and BB, with the latter also indicating a P250 peak, often associated with perceptual recognition of a stimulation.

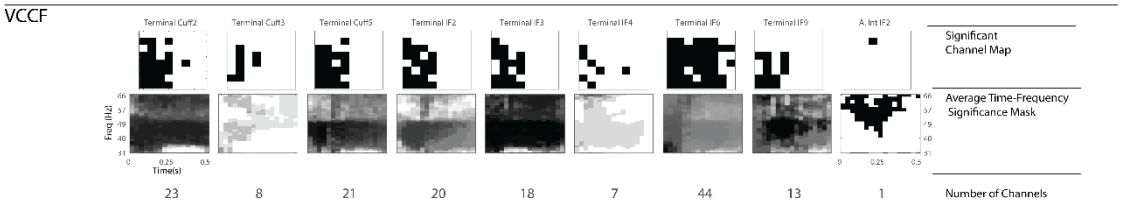

Figure 10. Similar to Figure 4, the channels significant to peripheral nerve stimulation channels. The effect is broad and typically encompassing more channels than the mechanical stimulation. However, the anterior interosseous nerve stimulation channel only showed significance on a single cortical channel. The time frequency significance is also highly inclusive, with most channels representing the entire set of domains.

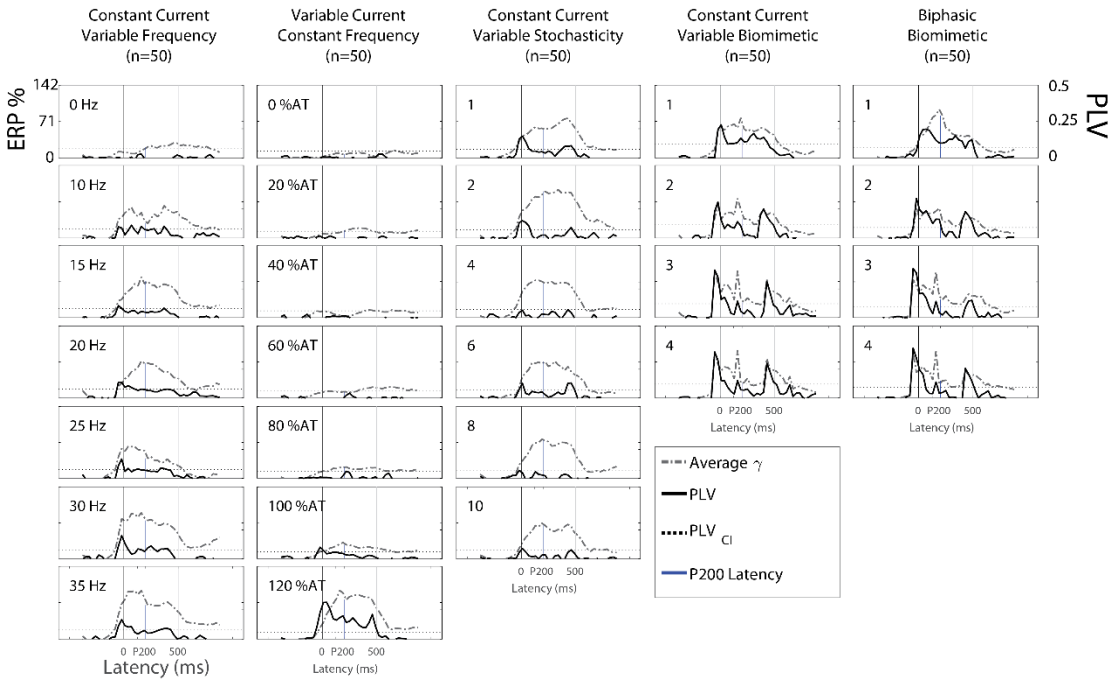

Figure 11. Evoked Gamma to Peripheral Nerve Stimulation. For the 7 cortical channels on the G1 probe, the average evoked gamma activity is plotted against the phase lock value. The presence of phase locking in CCVF and VCCF is abundantly clear. This is diminished if not absent in time variant stimulations. The BB stimulation possesses the desired traits of onset-offset phase locking, sustained gamma, and little to no latent phase locking.

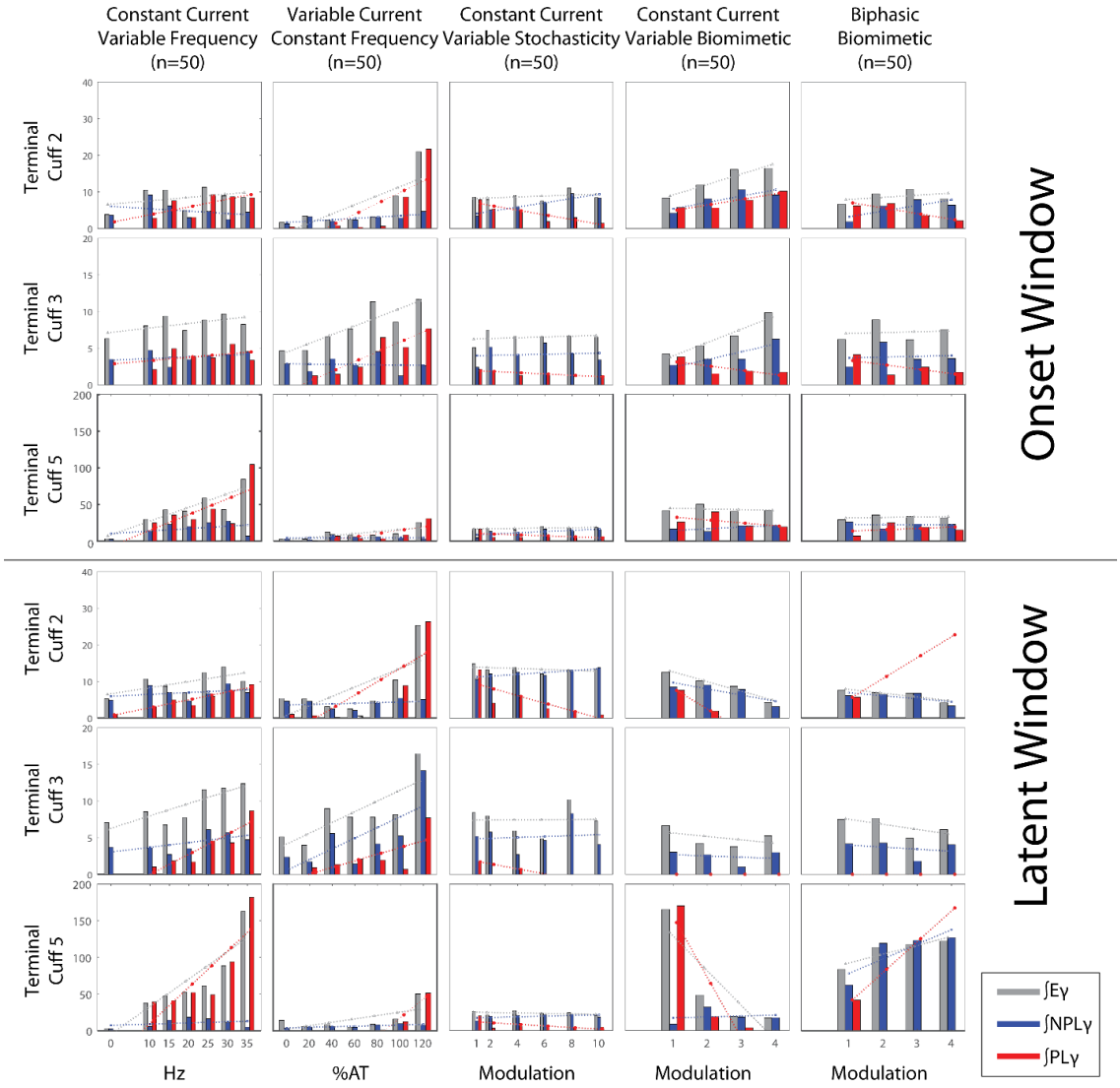

Figure 12a. Trends in Gamma Power Over Cuff Electrode Stimulation for both Onset and Latent Time Windows. Refer to Figure 6 for explanation of arrangement.

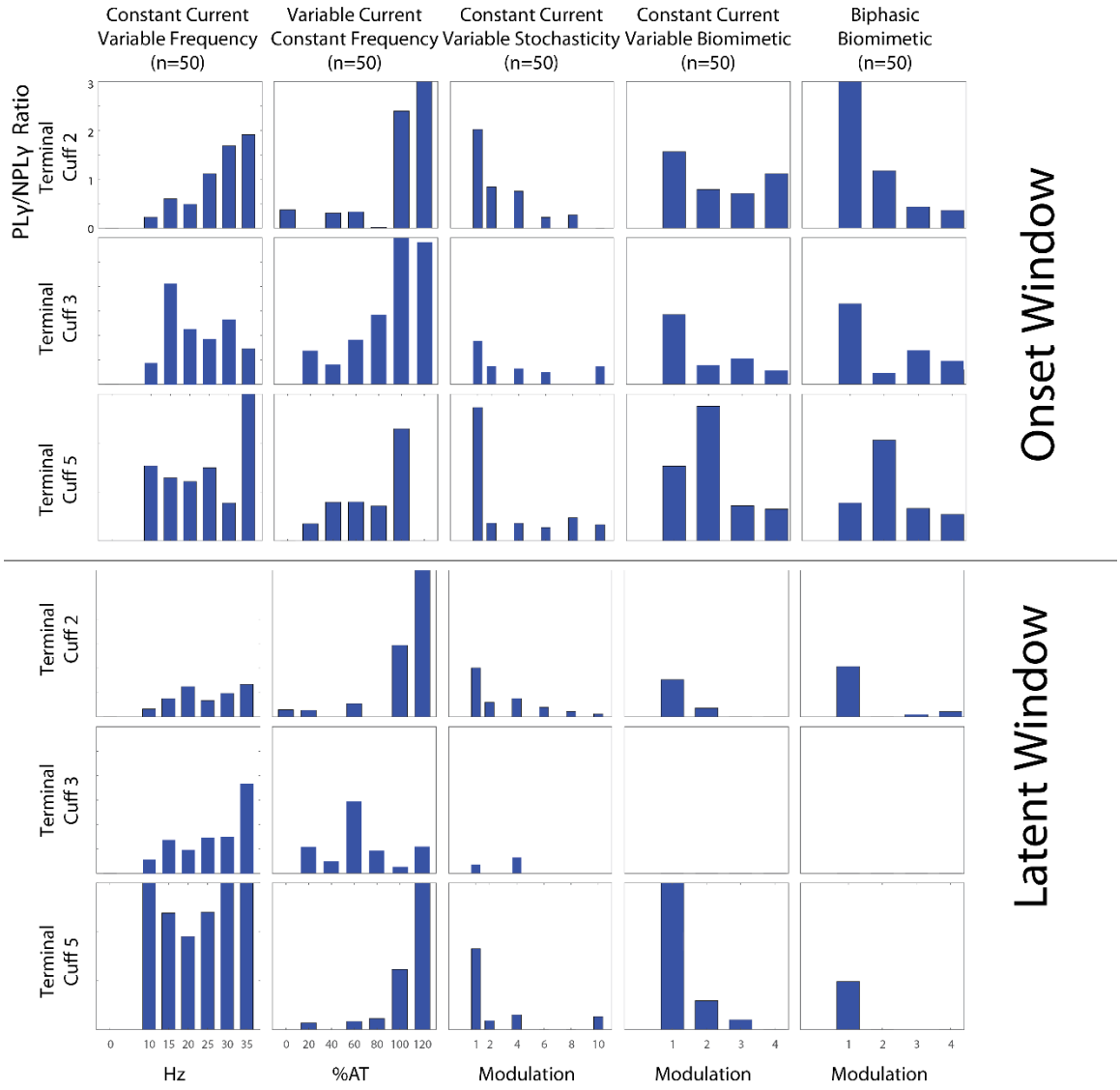

Figure 12b. Trends in Gamma Power Ratio Over Cuff Electrode Stimulation for both Onset and Latent Time Windows. Refer to Figure 6 for explanation of arrangement. Time Variant stimulation patterns are closer to the gamma typicality.

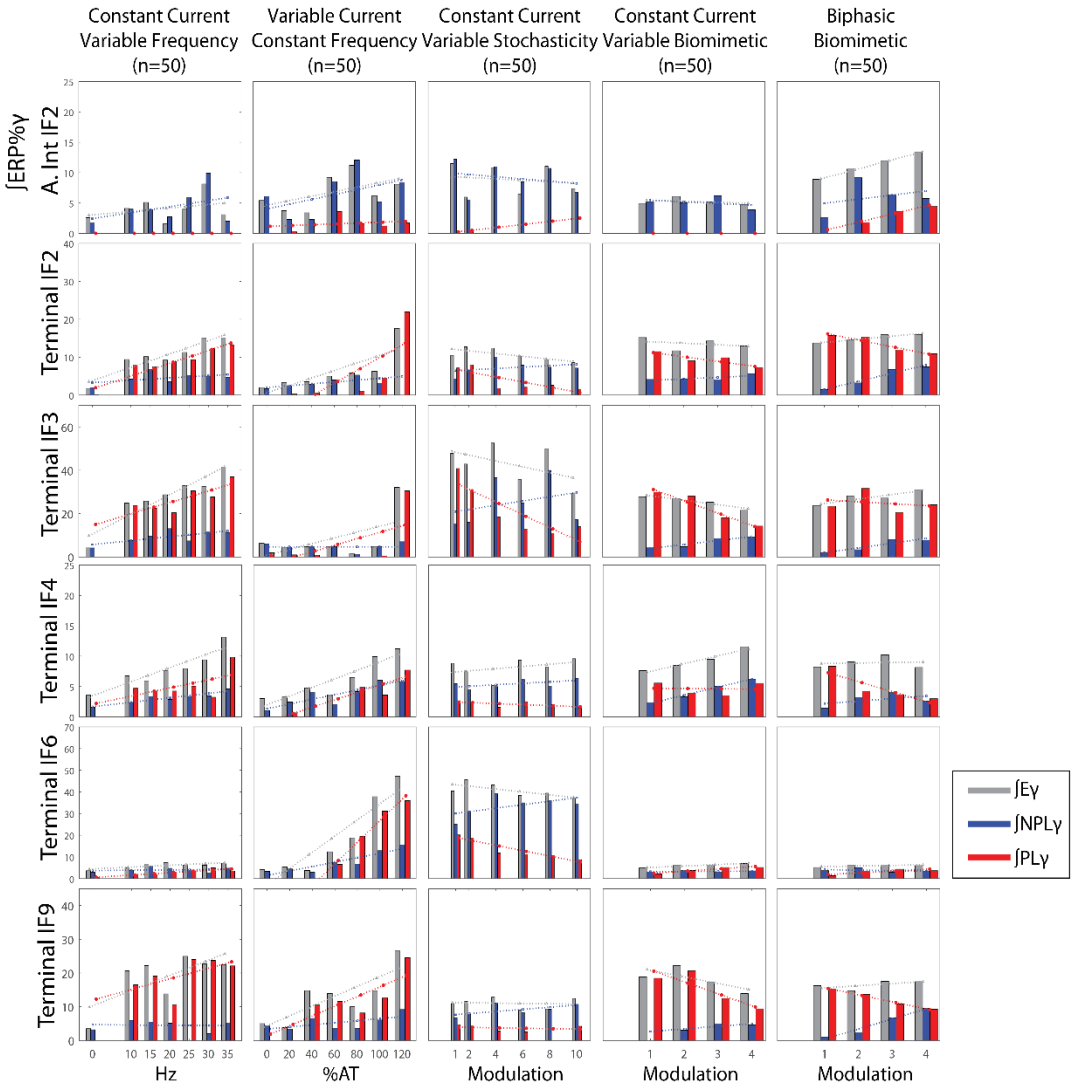

Figure 13a. Trends in Gamma Power Over Intrafascicular Electrode Stimulation for the Onset Time Window. Refer to Figure 6 for explanation of arrangement. . Refer to Figure 6 for explanation of arrangement.

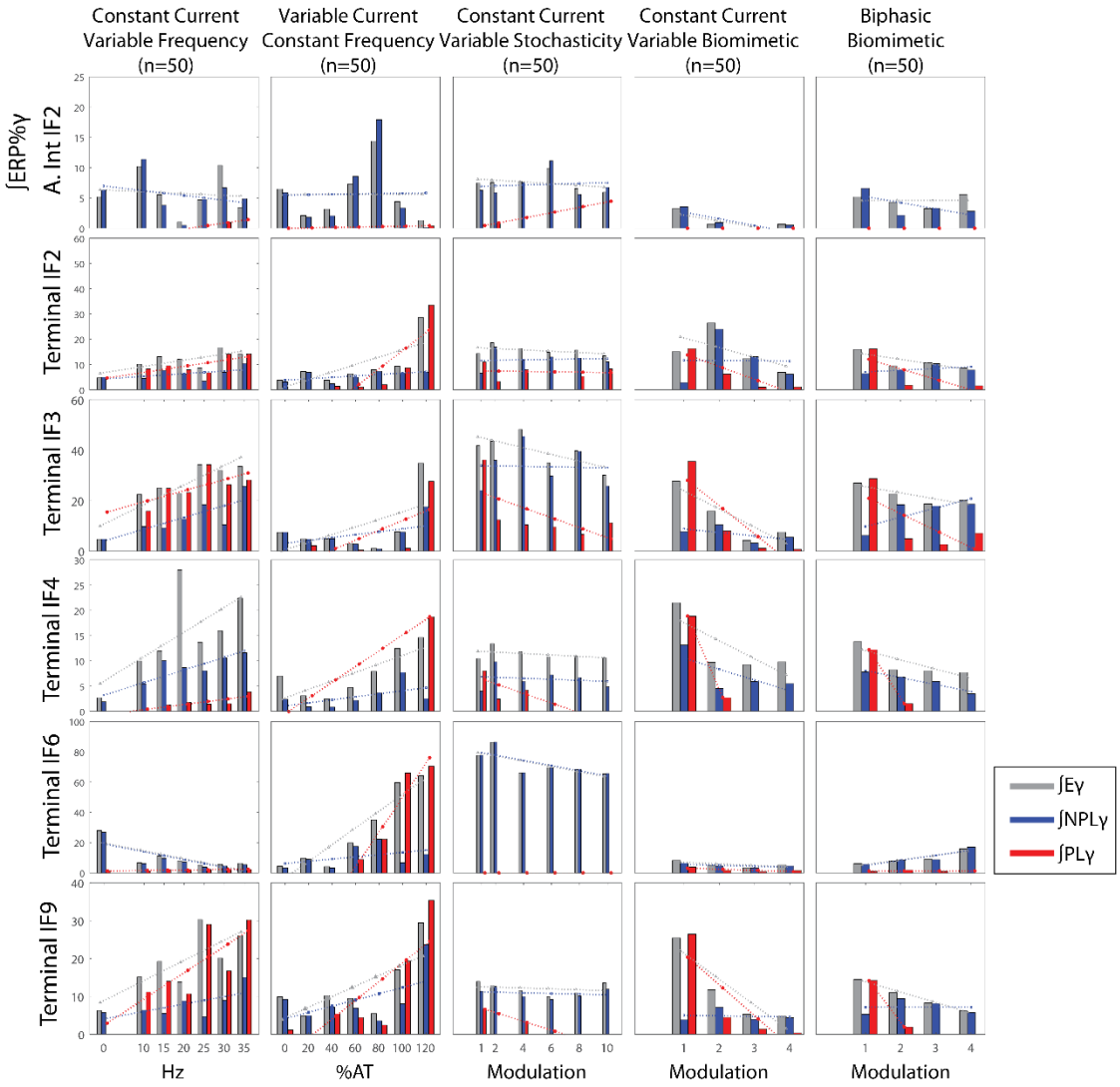

Figure 13b. Trends in Gamma Power Over Intrafascicular Electrode Stimulation for Latent Time Window. Refer to Figure 6 for explanation of arrangement.

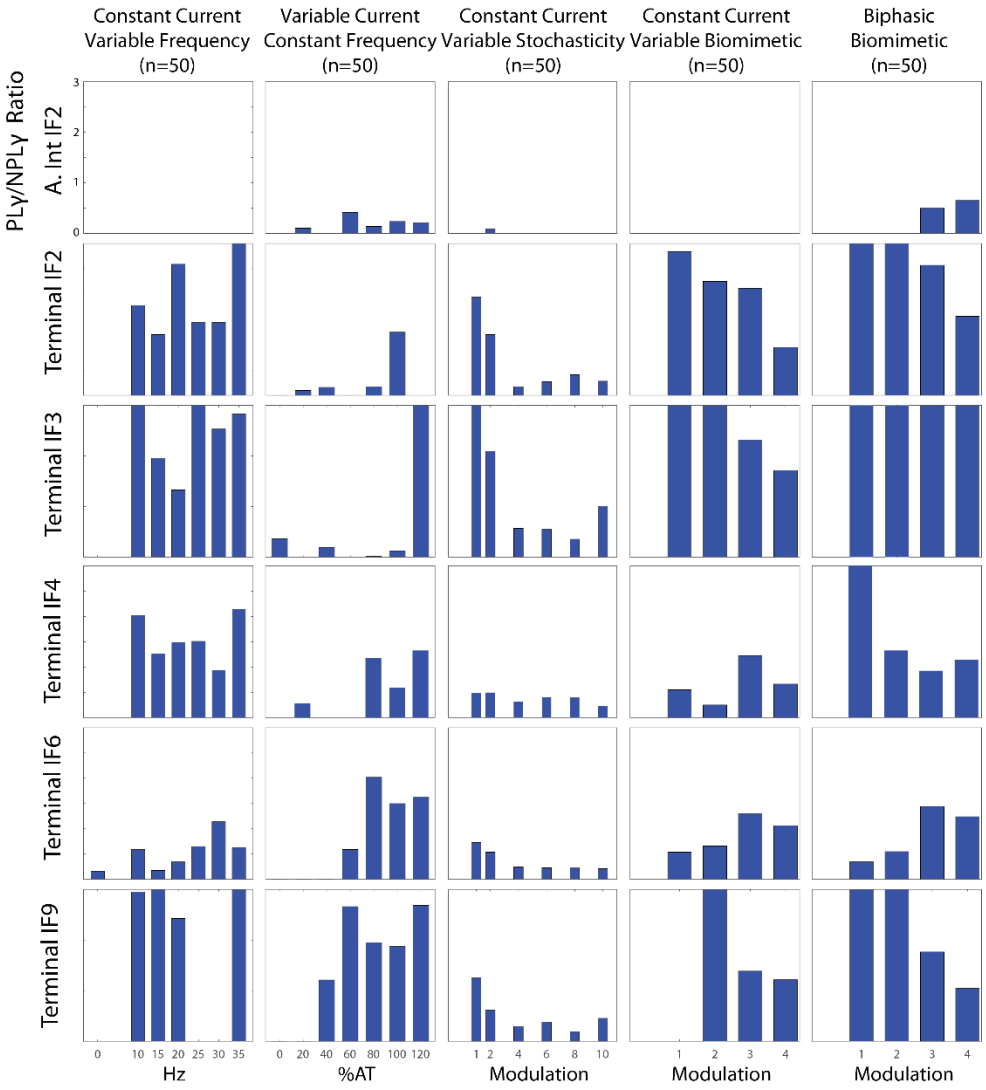

Figure 13c. Trends in Gamma Power Ratio Over Intrafascicular Electrode Stimulation for Onset Time Window. Refer to Figure 6 for explanation of arrangement.

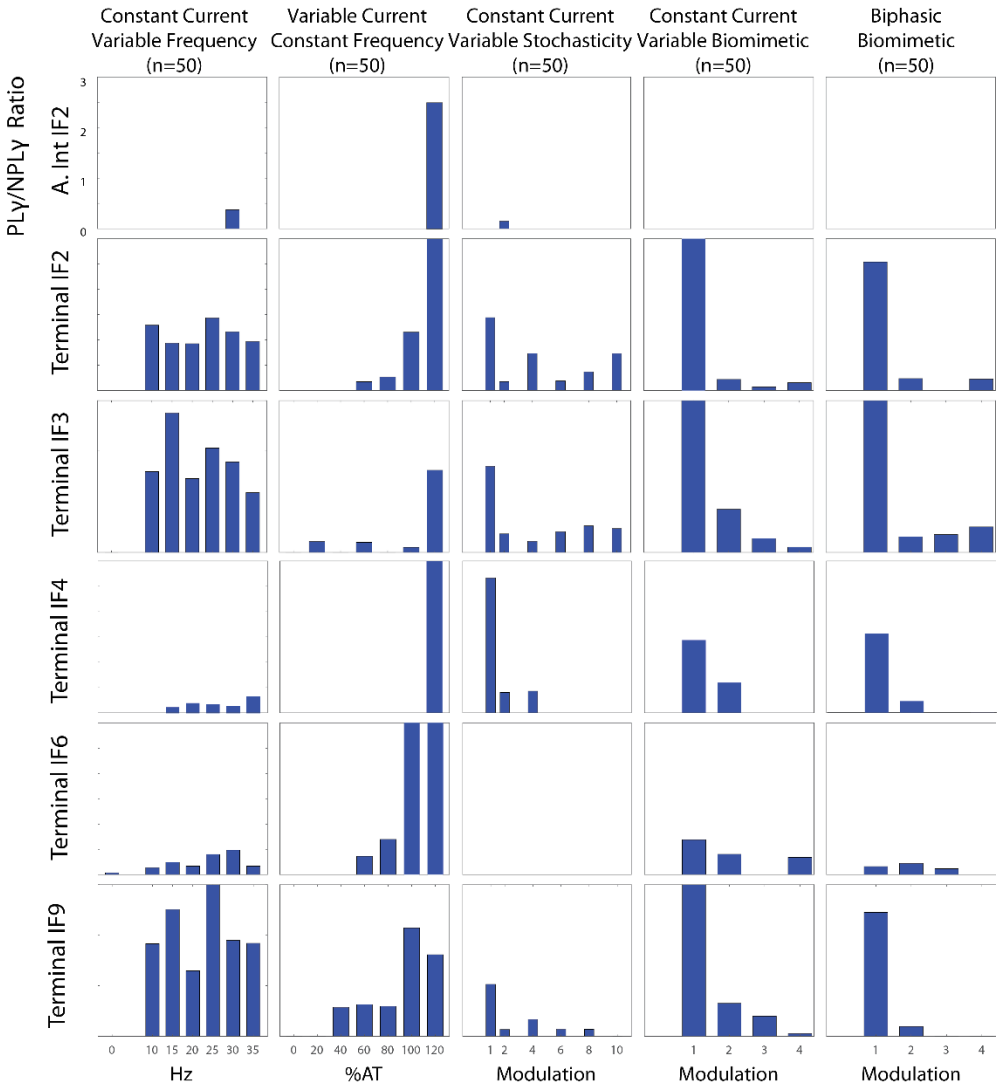

Figure 13d. Trends in Gamma Power Ratio Over Intrafascicular Electrode Stimulation for Latent Time Window. Refer to Figure 6 for explanation of arrangement.

CONCLUSIONS

The focus of this dissertation is to argue that complex contextual somatosensory feedback may be delivered in a reduced variable space by mimicking the parallel tonic and phasic physiological inputs. The proposition of designing time variant stimulation strategies is based on the argument that contextual perception within tactile tasks primarily depends on the variant shear forces applied to the nonlinearly deformable primate finger pad and the induced tactile neural responses. An initial investigation into using a physiologically mimicking Bimodal Biomimetic stimulation reveals cortical activity closer to punctate pressure, which is more practical for use in somatosensory feedback. In the future, investigations should be into this paradigm's ability to create actual percepts, modulate those percepts, and provide contextual information based on the modulation of internal stimulus parameters.

SENSORY INPUT MODULATION

Hager-Ross 1996 argues that the sensitivities to grip reaction are externally referenced, but the inverted grip does not control against lateral finger pad deformation. In addition, the study is intrinsically different from a perceptual study, as the latencies demonstrate evidence that subspinal circuitry is necessary to the response. In Chapter 1, "Anisotropic Psychophysical Sensitivities in the Perception of Tactile Direction in a Precision Grip," the discriminability of tactile direction is shown to be sensitive across the finger pad. This is controlled against gravity by a vertical oriented grip, and confidently determined that the reference frame is due to internal biomechanics rather than external contexts. Deformation of the finger pad in contact and directionally dependent axes seems to inform perception, utilizing the anisotropic activation of the mechanoreceptor systems.

Many papers report multimodal activity of cells within somatosensory cortex, but modes investigated can all be mechanically related. Changes in weight and frictional coefficients require varied grip forces to maintain an appropriate safety margin, which in turn is affecting the finger pad deformation in contextually anisotropic manners. The primary mechanoreceptors responsible for this sensory input are coactivated in complex grips. This is reinforced by Chapter 2, "Somatosensory Area 1 Multimodal Sensitivity Due to Biomechanical Variations in Precision Grip." Limited recording from area 1 demonstrates sensitivities to multiple modes of a precision grip task. The orientation, texture, and a rotational perturbation of grip are examined. It is well established that the SAI and FAII mechanoreceptors encoding for static and phasic activity are respectively responsible for coarse and fine texture discrimination. For perturbation-texture bimodal cells, the increased movement of the grip increased activity on cells reactive to fine texture and static trials increased activity on cells reactive to coarse textures. All cells, including bimodal, sensitive to orientation of grip are sensitive to the horizontal grip, which mechanically induces the strongest shear forces. The shear force of the grips will be investigated in future work.

These bimodal cells reported and observed typically consist of an onset-offset component combined with a sustained activity. This pattern is likely due to the conjoined temporal activation of these SAI and FA, with a strong FA response indicating onset of activity and the SAI sustained response provides maintenance and sensitivity to any fine FA deviations. Therefore, the ideal artificial feedback for proper sensation should mimic this biphasic input.

The presence and response of sensory input is thoroughly investigated across sensory systems using the 30 to 60 Hz gamma range. Upon sensory stimulation, there is a fast onset of PLγ followed by augmentation of NPLγ around 250ms. Using punctate

and vibrotactile stimulation as models of typical and atypical sensations, the efficacy of various peripheral nerve stimulations is examined. In Chapter 3, "Comparison of Gamma Phase Locking Properties Between Time Variant Peripheral Nerve Stimulation and Mechanical Stimulation," it is shown it is shown that punctate stimulation response aligns with the literature of other sensory systems. As vibrotactile stimulation violates the rule of absent latent phase locking, punctate response defines the desired traits of peripheral stimulation response for this chapter. This stimulation produces onset-offset slight phase locking with sustained gamma throughout, and some augmentation to particularly large punctate indentations. Using time variant properties, these responses can be modulated. Clustering stimulation pulses to the edges of the stimulation window results in strong onset and offset evoked potentials and gamma, but loses sustained gamma. Stochastic signals produce sustained NPLγ, but have little to no onset-offset phase locking. Combining the two stimulation patterns produces responses similar to punctate stimulation. This provides a platform of investigation in the properties of this bimodal biomimetic stimulation.

FUTURE WORK

It is paramount to quantify the perceptual and cortical difference in responses to variations of the individual components in this composite strategy. The combination of time, or force if in an active task, dynamic stimulation paired with on-demand stochastic activity provides many mathematical and behavioral avenues of exploration.

Touching on a few examples of work that have provided participation opportunities already can illustrate the interesting paths to pursue. Working the Nerves Incorporated, there is opportunity to work with partial hand amputees with implanted electrodes similar to the ones in Chapter 3. The obvious experiment is having a human subject judge the perception of these composite stimulation trains while the magnitude

ratio and stochastic noise are balanced. If we can employ tactilely practical sensations, two experiments have preliminary data that will hopefully be explored.

First, the sensitivity to stimulation on an intrafascicular electrode seems to increase when minute amount of current is applied through a cuff electrode on the same nerve. In a similar manner to stochastic facilitation, the secondary signal masks the primary signal if it gets too high. However, in some cases the large effect of increased sensitivity is seen with cuff stimulation as low as 1 μA. If a significant increase in sensitivity can be made across multiple stimulations sites by providing very finite energy to the system, the benefits for chronic stimulation are immense in terms of battery life, stimulator requirements, and reduced electrical injection to the nerve. Neural responses have been recorded with NHP-R at low levels of cuff stimulation in an attempt to look at the change in latent NPLγ. However, since NHP-R is not attending to the tasks there is not a pronounced response. Investigations into the increases of sensory input PLγ at onset of stimulation are underway. Potentially, this will indicate a stronger input signal due to cuff facilitation. Ideally, the results would exhibit a response greater than the sum of its parts. Utilizing this with the composite strategy will be interesting, as it could potentially provide stochastic sustained component separately rather than on the same channel, but at reduced magnitudes necessary.

Second, experiments are underway to recreate a study of tactile input's effect on proprioceptive estimation (Rincon-Gonzalez et al., 2011). The experiment has subjects passively receive an arm movement to varied locations over a flat surface and report where the tip of the arm was located. For non-affected subjects, the error estimation decreases significantly when the tip of the finger is placed on the surface. In partial hand amputees, an instrumented prosthetic is used to cue peripheral nerve stimulation upon the touch of the finger to the surface. This results in the investigation of four modes by iterating Hovering over the target, Contacting the target, and

receiving FeedBack stimulation: H-FB, C-FB, H+FB, C+FB. Feedback stimulation consists of constant frequency and produces common vibration percepts.

Compared to the H-FB, the error of estimation increases greatly with prosthetic C-FB. H+FB demonstrates less error than the C-FB, but not comparable to H-FB. The interesting condition arises in C+FB, as the subject receives two competing strategies of estimation: (1) learned estimation based on years of the error prone limb-prosthetic interaction and (2) novel estimation based on the error reducing stimulation percept. Both are similar in mechanisms in which the user "feels it and then estimates where the fingertip would be compared to the feeling." It would be interesting to explore the effect of typical versus atypical stimulation strategies in these conditions. It is not impractical to predict a more natural sensation would help overwrite the limb-prosthetic estimation strategy and provide inherent or subconscious user credence to the new stimulation, thus allowing for more reduction in error.

WORK CITED

Atkins, D., Heard, D., Donovan, W., Atkins, D. J., Donovan, W. H., Heard, D. C., … Heard, C. (1996). Epidemiologic overview of individuals with upper-limb loss and their reported research priorities. https://doi.org/10.1097/00008526-199600810-00003

Augurelle, A.-S., Penta, M., White, O., & Thonnard, J.-L. (2003). The effects of a change in gravity on the dynamics of prehension. *Experimental Brain Research*, *148*(4), 533–540. https://doi.org/10.1007/s00221-002-1322-3

Augurelle, A.-S., Smith, A. M., Lejeune, T., & Thonnard, J.-L. (2003). Importance of Cutaneous Feedback in Maintaining a Secure Grip During Manipulation of Hand-Held Objects. *Journal of Neurophysiology*, *89*(2), 665–671. https://doi.org/10.1152/jn.00249.2002

Babiloni, C., Babiloni, F., Carducci, F., Cincotti, F., Rosciarelli, F., Arendt-Nielsen, L., … Rossini, P. M. (2002). Human brain oscillatory activity phase-locked to painful electrical stimulations: A multi-channel EEG study. *Human Brain Mapping*, *15*(2), 112–123. https://doi.org/10.1002/hbm.10013

Babiloni, C., Babiloni, F., Carducci, F., Cincotti, F., Rosciarelli, F., Rossini, P. M., … Chen, A. C. N. (2001). Mapping of early and late human somatosensory evoked brain potentials to phasic galvanic painful stimulation. *Human Brain Mapping*, *12*(3), 168–179. https://doi.org/10.1002/1097-0193(200103)12:3<168::AID-HBM1013>3.0.CO;2-O

Bauer, M., Oostenveld, R., Peeters, M., & Fries, P. (2006). Tactile Spatial Attention Enhances Gamma-Band Activity in Somatosensory Cortex and Reduces Low-Frequency Activity in Parieto-Occipital Areas. *Journal of Neuroscience*, *26*(2), 490–501. https://doi.org/10.1523/JNEUROSCI.5228-04.2006

Bensmaïa, S., & Hollins, M. (2005). Pacinian representations of fine surface texture. *Perception & Psychophysics*, *67*(5), 842–854. https://doi.org/10.3758/BF03193537

BensmaÏa, S., Hollins, M., & Yau, J. (2005). Vibrotactile intensity and frequency information in the Pacinian system: A psychophysical model. *Perception & Psychophysics*, *67*(5), 828–841. https://doi.org/10.3758/BF03193536

BensmaÏa, S. J., & Hollins, M. (2003). The vibrations of texture. *Somatosensory & Motor Research*, *20*(1), 33–43. https://doi.org/10.1080/0899022031000083825

Bensmaia, S. J., Hsiao, S. S., Denchev, P. V., Killebrew, J. H., & Craig, J. C. (2008). The tactile perception of stimulus orientation. *Somatosensory & Motor Research*, *25*(1), 49–59. https://doi.org/10.1080/08990220701830662

Benzi, R., Sutera, A., & Vulpiani, A. (1981). The mechanism of stochastic resonance. *Journal of Physics A: Mathematical and General*, *14*(11), L453. https://doi.org/10.1088/0305-4470/14/11/006

Biddiss, E. A., & Chau, T. T. (2007). Upper limb prosthesis use and abandonment: A survey of the last 25 years. *Prosthetics and Orthotics International*, *31*(3), 236–257. https://doi.org/10.1080/03093640600994581

Birznieks, I., Jenmalm, P., Goodwin, A. W., & Johansson, R. S. (2001). Encoding of Direction of Fingertip Forces by Human Tactile Afferents. *Journal of Neuroscience*, *21*(20), 8222–8237.

Brochier, T., Boudreau, M. J., Paré, M., & Smith, A. M. (1999). The effects of muscimol inactivation of small regions of motor and somatosensory cortex on independent finger movements and force control in the precision grip. *Experimental Brain Research*, *128*(1–2), 31–40.

Bulsara, A., Jacobs, E. W., Zhou, T., Moss, F., & Kiss, L. (1991). Stochastic resonance in a single neuron model: theory and analog simulation. *Journal of Theoretical Biology*, *152*(4), 531–555.

Chang, E. C., Flanagan, J. R., & Goodale, M. A. (2008). The intermanual transfer of anticipatory force control in precision grip lifting is not influenced by the perception of weight. *Experimental Brain Research*, *185*(2), 319–329. https://doi.org/10.1007/s00221-007-1156-0

Chouinard, P. A., Leonard, G., & Paus, T. (2005). Role of the Primary Motor and Dorsal Premotor Cortices in the Anticipation of Forces during Object Lifting. *Journal of Neuroscience*, *25*(9), 2277–2284. https://doi.org/10.1523/JNEUROSCI.4649-04.2005

Clippinger, F. W., Avery, R., & Titus, B. R. (1974). A sensory feedback system for an upper-limb amputation prosthesis. *Bulletin of Prosthetics Research*, 247–258.

Collins, J. J., Imhoff, T. T., & Grigg, P. (1997). Noise-mediated enhancements and decrements in human tactile sensation. *Physical Review E*, *56*(1), 923–926. https://doi.org/10.1103/PhysRevE.56.923

Connor, C. E., Hsiao, S. S., Phillips, J. R., & Johnson, K. O. (1990). Tactile roughness: neural codes that account for psychophysical magnitude estimates. *Journal of Neuroscience*, *10*(12), 3823–3836.

Connor, C. E., & Johnson, K. O. (1992). Neural coding of tactile texture: comparison of spatial and temporal mechanisms for roughness perception. *Journal of Neuroscience*, *12*(9), 3414–3426.

Curio, G., Mackert, B. M., Burghoff, M., Neumann, J., Nolte, G., Scherg, M., & Marx, P. (1997). Somatotopic source arrangement of 600 Hz oscillatory magnetic fields at the human primary somatosensory hand cortex. *Neuroscience Letters*, *234*(2–3), 131–134.

Dadarlat, M. C., O'Doherty, J. E., & Sabes, P. N. (2015). A learning-based approach to artificial sensory feedback leads to optimal integration. *Nature Neuroscience*, *18*(1), 138–144. https://doi.org/10.1038/nn.3883

De Gregorio, M., & Santos, V. J. (2013). Precision grip responses to unexpected rotational perturbations scale with axis of rotation. *Journal of Biomechanics*, *46*(6), 1098–1103. https://doi.org/10.1016/j.jbiomech.2013.01.017

Delgado-Martínez, I., Badia, J., Pascual-Font, A., Rodríguez-Baeza, A., & Navarro, X. (2016). Fascicular Topography of the Human Median Nerve for Neuroprosthetic Surgery. *Frontiers in Neuroscience*, *10*. https://doi.org/10.3389/fnins.2016.00286

Dhillon, G. S., & Horch, K. W. (2005). Direct neural sensory feedback and control of a prosthetic arm. *IEEE Transactions on Neural Systems and Rehabilitation Engineering*, *13*(4), 468–472. https://doi.org/10.1109/TNSRE.2005.856072

DiCarlo, J. J., & Johnson, K. O. (2000). Spatial and Temporal Structure of Receptive Fields in Primate Somatosensory Area 3b: Effects of Stimulus Scanning Direction and Orientation. *The Journal of Neuroscience*, *20*(1), 495–510.

DiCarlo, J. J., Johnson, K. O., & Hsiao, S. S. (1998). Structure of receptive fields in area 3b of primary somatosensory cortex in the alert monkey. *The Journal of Neuroscience*, *18*(7), 2626–2645.

Donchin, E., Kubovy, M., Kutas, M., Johnson, R., & Tterning, R. I. (1973). Graded changes in evoked response (P300) amplitude as a function of cognitive activity. *Perception & Psychophysics*, *14*(2), 319–324. https://doi.org/10.3758/BF03212398

Duncan-Johnson, C. C., & Donchin, E. (1982). The P300 component of the event-related brain potential as an index of information processing. *Biological Psychology*, *14*(1), 1–52. https://doi.org/10.1016/0301-0511(82)90016-3

Engel, A. K., Moll, C. K. E., Fried, I., & Ojemann, G. A. (2005). Invasive recordings from the human brain: clinical insights and beyond. *Nature Reviews. Neuroscience*, *6*(1), 35–47. https://doi.org/10.1038/nrn1585

Essock, E. A., Krebs, W. K., & Prather, J. R. (1997). Superior sensitivity for tactile stimuli oriented proximally-distally on the finger: Implications for mixed class 1 and class 2 anisotropies. *Journal of Experimental Psychology: Human Perception and Performance*, *23*(2), 515–527. https://doi.org/http://dx.doi.org.ezproxy1.lib.asu.edu/10.1037/0096-1523.23.2.515

Flanagan, J. R., Wing, A. M., Allison, S., & Spenceley, A. (1995). Effects of surface texture on weight perception when lifting objects with a precision grip. *Perception & Psychophysics*, *57*(3), 282–290. https://doi.org/10.3758/BF03213054

Forssberg, H., Kinoshita, H., Eliasson, A. C., Johansson, R. S., Westling, G., & Gordon, A. M. (1992). Development of human precision grip. II. Anticipatory control of isometric forces targeted for object's weight. *Experimental Brain Research*, *90*(2), 393–398.

Forster, B., Cavina-Pratesi, C., Aglioti, S. M., & Berlucchi, G. (2002). Redundant target effect and intersensory facilitation from visual-tactile interactions in simple reaction time. *Experimental Brain Research*, *143*(4), 480–487. https://doi.org/10.1007/s00221-002-1017-9

Friedman, D. P., Murray, E. A., O'Neill, J. B., & Mishkin, M. (1986). Cortical connections of the somatosensory fields of the lateral sulcus of macaques: evidence for a corticolimbic pathway for touch. *The Journal of Comparative Neurology*, *252*(3), 323–347. https://doi.org/10.1002/cne.902520304

Fries, P. (2009). Neuronal Gamma-Band Synchronization as a Fundamental Process in Cortical Computation. *Annual Review of Neuroscience*, *32*(1), 209–224. https://doi.org/10.1146/annurev.neuro.051508.135603

Fu, Q., Zhang, W., & Santello, M. (2010). Anticipatory Planning and Control of Grasp Positions and Forces for Dexterous Two-Digit Manipulation. *Journal of Neuroscience*, *30*(27), 9117–9126. https://doi.org/10.1523/JNEUROSCI.4159-09.2010

Fukuda, M., Nishida, M., Juhász, C., Muzik, O., Sood, S., Chugani, H. T., & Asano, E. (2008). Short-latency median-nerve somatosensory-evoked potentials and induced gamma-oscillations in humans. *Brain*, *131*(7), 1793–1805.

Garraghty, P. E., Florence, S. L., & Kaas, J. H. (1990). Ablations of areas 3a and 3b of monkey somatosensory cortex abolish cutaneous responsivity in area 1. *Brain Research*, *528*(1), 165–169. https://doi.org/10.1016/0006-8993(90)90213-U

Gasson, M., Hutt, B., Goodhew, I., Kyberd, P., & Warwick, K. (2005). Invasive neural prosthesis for neural signal detection and nerve stimulation. *International Journal of Adaptive Control and Signal Processing*, *19*(5), 365–375. https://doi.org/10.1002/acs.854

Geyer, S., Schleicher, A., & Zilles, K. (1999). Areas 3a, 3b, and 1 of Human Primary Somatosensory Cortex. *NeuroImage*, *10*(1), 63–83. https://doi.org/10.1006/nimg.1999.0440

Gibson, G. O., & Craig, J. C. (2005). Tactile spatial sensitivity and anisotropy. *Perception & Psychophysics*, *67*(6), 1061–1079. https://doi.org/10.3758/BF03193632

Goffaux, V., Mouraux, A., Desmet, S., & Rossion, B. (2004). Human non-phase-locked gamma oscillations in experience-based perception of visual scenes. *Neuroscience Letters*, *354*(1), 14–17. https://doi.org/10.1016/j.neulet.2003.09.029

Gong, Y., Matthews, N., & Qian, N. (2002). Model for stochastic-resonance-type behavior in sensory perception. *Physical Review E*, *65*(3), 031904. https://doi.org/10.1103/PhysRevE.65.031904

Gray, H. M., Ambady, N., Lowenthal, W. T., & Deldin, P. (2004). P300 as an index of attention to self-relevant stimuli. *Journal of Experimental Social Psychology*, *40*(2), 216–224. https://doi.org/10.1016/S0022-1031(03)00092-1

Gross, J., Schnitzler, A., Timmermann, L., & Ploner, M. (2007). Gamma Oscillations in Human Primary Somatosensory Cortex Reflect Pain Perception. *PLoS Biology*, *5*(5). https://doi.org/10.1371/journal.pbio.0050133

Gurtubay, I. G., Alegre, M., Labarga, A., Malanda, A., & Artieda, J. (2004a). Gamma band responses to target and non-target auditory stimuli in humans. *Neuroscience Letters*, *367*(1), 6–9. https://doi.org/10.1016/j.neulet.2004.05.104

Gurtubay, I. G., Alegre, M., Labarga, A., Malanda, A., & Artieda, J. (2004b). Gamma band responses to target and non-target auditory stimuli in humans. *Neuroscience Letters*, *367*(1), 6–9. https://doi.org/10.1016/j.neulet.2004.05.104

Häger-Ross, C., Cole, K. J., & Johansson, R. S. (1996). Grip-force responses to unanticipated object loading: load direction reveals body- and gravity-referenced intrinsic task variables. *Experimental Brain Research*, *110*(1), 142–150. https://doi.org/10.1007/BF00241383

Hashimoto, I., Mashiko, T., & Imada, T. (1996). Somatic evoked high-frequency magnetic oscillations reflect activity of inhibitory interneurons in the human somatosensory cortex. *Electroencephalography and Clinical Neurophysiology/Evoked Potentials Section*, *100*(3), 189–203. https://doi.org/10.1016/0168-5597(95)00244-8

Hollins, M., & Risner, S. R. (2000). Evidence for the duplex theory of tactile texture perception. *Perception & Psychophysics*, *62*(4), 695–705. https://doi.org/10.3758/BF03206916

Ide, M., & Hidaka, S. (2013). Tactile stimulation can suppress visual perception. *Scientific Reports*, *3*. https://doi.org/10.1038/srep03453

J, Y., V, K., & T, D. (1997). The phase-locking of auditory gamma band responses in humans is sensitive to task processing. *Neuroreport*, *8*(18), 3999–4004.

Johansson, R. S., & Westling, G. (1984). Roles of glabrous skin receptors and sensorimotor memory in automatic control of precision grip when lifting rougher or more slippery objects. *Experimental Brain Research*, *56*(3), 550–564. https://doi.org/10.1007/BF00237997

Johansson, R. S., & Westling, G. (1987). Signals in tactile afferents from the fingers eliciting adaptive motor responses during precision grip. *Experimental Brain Research*, *66*(1), 141–154. https://doi.org/10.1007/BF00236210

Johansson, R. S., & Westling, G. (1988). Coordinated isometric muscle commands adequately and erroneously programmed for the weight during lifting task with precision grip. *Experimental Brain Research*, *71*(1), 59–71. https://doi.org/10.1007/BF00247522

Johansson, Roland S., & Vallbo, Å. B. (1983). Tactile sensory coding in the glabrous skin of the human hand. *Trends in Neurosciences*, *6*, 27–32. https://doi.org/10.1016/0166-2236(83)90011-5

Johnson, D., Jürgens, R., Kongehl, G., & Kornhuber, H. H. (1975). Somatosensory evoked potentials and magnitude of perception. *Experimental Brain Research*, *22*(3), 331–334. https://doi.org/10.1007/BF00234774

Johnson, D., Jürgens, R., & Kornhuber, H. H. (1980a). Somatosensory-evoked potentials and perception of skin velocity. *Archiv Für Psychiatrie Und Nervenkrankheiten*, *228*(2), 95–100. https://doi.org/10.1007/BF00365597

Johnson, D., Jürgens, R., & Kornhuber, H. H. (1980b). Somatosensory-evoked potentials and vibration. *Archiv Für Psychiatrie Und Nervenkrankheiten*, *228*(2), 101–107. https://doi.org/10.1007/BF00365598

Johnson, K. O., Yoshioka, T., & Vega-Bermudez, F. (2000). Tactile functions of mechanoreceptive afferents innervating the hand. *Journal of Clinical Neurophysiology: Official Publication of the American Electroencephalographic Society*, *17*(6), 539–558.

Johnson, Kenneth O. (2001). The roles and functions of cutaneous mechanoreceptors. *Current Opinion in Neurobiology*, *11*(4), 455–461. https://doi.org/10.1016/S0959-4388(00)00234-8

Jokeit, H., & Makeig, S. (1994). Different event-related patterns of gamma-band power in brain waves of fast- and slow-reacting subjects. *Proceedings of the National Academy of Sciences*, *91*(14), 6339–6343.

Jones, E. G., Coulter, J. D., & Hendry, S. H. (1978). Intracortical connectivity of architectonic fields in the somatic sensory, motor and parietal cortex of monkeys. *The Journal of Comparative Neurology*, *181*(2), 291–347. https://doi.org/10.1002/cne.901810206

Jones, L. A., & Hunter, I. W. (1992). Changes in Pinch Force with Bidirectional Load Forces. *Journal of Motor Behavior*, *24*(2), 157–164. https://doi.org/10.1080/00222895.1992.9941611

Kim, S. S., Gomez-Ramirez, M., Thakur, P. H., & Hsiao, S. S. (2015). Multimodal Interactions between Proprioceptive and Cutaneous Signals in Primary Somatosensory Cortex. *Neuron*, *86*(2), 555–566. https://doi.org/10.1016/j.neuron.2015.03.020

Klatzky, R. L., Lederman, S. J., Hamilton, C., Grindley, M., & Swendsen, R. H. (2003). Feeling textures through a probe: Effects of probe and surface geometry and exploratory factors. *Perception & Psychophysics*, *65*(4), 613–631. https://doi.org/10.3758/BF03194587

Lachaux, J. P., Rodriguez, E., Martinerie, J., & Varela, F. J. (1999). Measuring phase synchrony in brain signals. *Human Brain Mapping*, *8*(4), 194–208.

LaMotte, R. H., & Whitehouse, J. (1986). Tactile detection of a dot on a smooth surface: peripheral neural events. *Journal of Neurophysiology*, *56*(4), 1109–1128.

Lederman, S. J. (1974). Tactile roughness of grooved surfaces: The touching process and effects of macro- and microsurface structure. *Perception & Psychophysics*, *16*(2), 385–395. https://doi.org/10.3758/BF03203958

Lederman, S. J., Loomis, J. M., & Williams, D. A. (1982). The role of vibration in the tactual perception of roughness. *Perception & Psychophysics*, *32*(2), 109–116. https://doi.org/10.3758/BF03204270

Lederman, S. J., & Taylor, M. M. (1972). Fingertip force, surface geometry, and the perception of roughness by active touch. *Perception & Psychophysics*, *12*(5), 401–408. https://doi.org/10.3758/BF03205850

London, B. M., & Miller, L. E. (2013). Responses of somatosensory area 2 neurons to actively and passively generated limb movements. *Journal of Neurophysiology*, *109*(6), 1505–1513. https://doi.org/10.1152/jn.00372.2012

Longtin, A. (1993). Stochastic resonance in neuron models. *Journal of Statistical Physics*, *70*(1–2), 309–327. https://doi.org/10.1007/BF01053970

Macefield, V. G., Häger-Ross, C., & Johansson, R. S. (1996). Control of grip force during restraint of an object held between finger and thumb: responses of cutaneous afferents from the digits. *Experimental Brain Research*, *108*(1), 155–171. https://doi.org/10.1007/BF00242913

Maeno, T., & Kobayashi, K. (1998). American Society of Mechanical Engineers, Dynamic Systems and Control Division (Publication) DSC. Presented at the Proceedings of the 1998 ASME International Mechanical Engineering Congress

and Exposition. Retrieved from https://keio.pure.elsevier.com/en/publications/fe-analysis-of-the-dynamic-characteristics-of-the-human-finger-pa

Maeno, T., Kobayashi, K., & Yamazaki, N. (1998). Relationship between the Structure of Human Finger Tissue and the Location of Tactile Receptors. *JSME International Journal Series C*, *41*(1), 94–100. https://doi.org/10.1299/jsmec.41.94

Mann, R. W. (1973). Prostheses control and feedback via noninvasive skin and invasive peripheral nerve techniques. *Neural Organization and Its Relevance to Prosthetics*, 177–195.

Maricich, S. M., Morrison, K. M., Mathes, E. L., & Brewer, B. M. (2012). Rodents Rely on Merkel Cells for Texture Discrimination Tasks. *Journal of Neuroscience*, *32*(10), 3296–3300. https://doi.org/10.1523/JNEUROSCI.5307-11.2012

Maris, E., & Oostenveld, R. (2007). Nonparametric statistical testing of EEG- and MEG-data. *Journal of Neuroscience Methods*, *164*(1), 177–190. https://doi.org/10.1016/j.jneumeth.2007.03.024

Marsden, C. D., Rothwell, J. C., & Day, B. L. (1984). The use of peripheral feedback in the control of movement. *Trends in Neurosciences*, *7*(7), 253–257. https://doi.org/10.1016/S0166-2236(84)80218-0

Matsuo, T., Kawasaki, K., Osada, T., Sawahata, H., Suzuki, T., Shibata, M., … Hasegawa, I. (2011). Intrasulcal Electrocorticography in Macaque Monkeys with Minimally Invasive Neurosurgical Protocols. *Frontiers in Systems Neuroscience*, *5*. https://doi.org/10.3389/fnsys.2011.00034

McAndrew, R. M., VanGilder, J. L., Naufel, S. N., & Tillery, S. H. (2012). Individualized recording chambers for non-human primate neurophysiology. *Journal of Neuroscience Methods*, *207*(1), 86–90.

Meek, S. G., Jacobsen, S. C., & Goulding, P. P. (1989). Extended physiologic taction: design and evaluation of a proportional force feedback system. *Journal of Rehabilitation Research and Development*, *26*(3), 53–62.

Miller, S. C. (1993). *The Effects of Redundant Visual, Auditory, and Tactile Stimuli on a Minimum Information Tracking Task*. S.l.: Distributed by ERIC Clearinghouse.

Murthy, V. N., & Fetz, E. E. (1992). Coherent 25-to 35-Hz oscillations in the sensorimotor cortex of awake behaving monkeys. *Proceedings of the National Academy of Sciences*, *89*(12), 5670–5674.

Neumann, C., Evett, I. W., Skerrett, J. E., & Mateos-Garcia, I. (2012). Quantitative assessment of evidential weight for a fingerprint comparison. Part II: A generalisation to take account of the general pattern. *Forensic Science International*, *214*(1), 195–199. https://doi.org/10.1016/j.forsciint.2011.08.008

Nicolelis, M. A. L., Ghazanfar, A. A., Stambaugh, C. R., Oliveira, L. M. O., Laubach, M., Chapin, J. K., … Kaas, J. H. (1998). Simultaneous encoding of tactile information by three primate cortical areas. *Nature Neuroscience*, *1*(7), 621–630. https://doi.org/10.1038/2855

Nowak, D. A., & Hermsdörfer, J. (2003). Selective deficits of grip force control during object manipulation in patients with reduced sensibility of the grasping digits. *Neuroscience Research*, *47*(1), 65–72. https://doi.org/10.1016/S0168-0102(03)00182-2

O'Doherty, J. E., Lebedev, M. A., Hanson, T. L., Fitzsimmons, N. A., & Nicolelis, M. A. L. (2009). A Brain-Machine Interface Instructed by Direct Intracortical Microstimulation. *Frontiers in Integrative Neuroscience*, *3*. https://doi.org/10.3389/neuro.07.020.2009

O'Doherty, J. E., Lebedev, M. A., Ifft, P. J., Zhuang, K. Z., Shokur, S., Bleuler, H., & Nicolelis, M. A. L. (2011). Active tactile exploration using a brain-machine-brain interface. *Nature*, *479*(7372), 228–231. https://doi.org/10.1038/nature10489

Ohki, Y., Edin, B. B., & Johansson, R. S. (2002). Predictions Specify Reactive Control of Individual Digits in Manipulation. *Journal of Neuroscience*, *22*(2), 600–610.

Paré, M., Smith, A. M., & Rice, F. L. (2002). Distribution and terminal arborizations of cutaneous mechanoreceptors in the glabrous finger pads of the monkey. *The Journal of Comparative Neurology*, *445*(4), 347–359. https://doi.org/10.1002/cne.10196

Peerdeman, B., Boere, D., Witteveen, H., Huis in 't Veld, R., Hermens, H., Stramigioli, S., … Misra, S. (2011). Myoelectric forearm prostheses: State of the art from a user-centered perspective. *Journal of Rehabilitation Research & Development*, *48*(6), 719–737.

Polich, J. (2007). Updating P300: An Integrative Theory of P3a and P3b. *Clinical Neurophysiology : Official Journal of the International Federation of Clinical Neurophysiology*, *118*(10), 2128–2148. https://doi.org/10.1016/j.clinph.2007.04.019

Pons, T. P., Garraghty, P. E., Cusick, C. G., & Kaas, J. H. (1985). The somatotopic organization of area 2 in macaque monkeys. *The Journal of Comparative Neurology*, *241*(4), 445–466. https://doi.org/10.1002/cne.902410405

Pons, T. P., Garraghty, P. E., & Mishkin, M. (1988). Lesion-induced plasticity in the second somatosensory cortex of adult macaques. *Proceedings of the National Academy of Sciences of the United States of America*, *85*(14), 5279–5281.

Pons, T. P., Wall, J. T., Garraghty, P. E., Cusick, C. G., & Kaas, J. H. (1987). Consistent features of the representation of the hand in area 3b of macaque monkeys. *Somatosensory Research*, *4*(4), 309–331.

Provancher, W. R., & Sylvester, N. D. (2009). Fingerpad Skin Stretch Increases the Perception of Virtual Friction. *IEEE Transactions on Haptics*, *2*(4), 212–223. https://doi.org/10.1109/TOH.2009.34

Randolph, M., & Semmes, J. (1974). Behavioral consequences of selective subtotal ablations in the postcentral gyrus ofMacaca mulatta. *Brain Research*, *70*(1), 55–70. https://doi.org/10.1016/0006-8993(74)90211-X

Raspopovic, S., Capogrosso, M., Petrini, F. M., Bonizzato, M., Rigosa, J., Di Pino, G., … Micera, S. (2014). Restoring Natural Sensory Feedback in Real-Time Bidirectional Hand Prostheses. *Science Translational Medicine*, *6*(222), 222ra19-222ra19. https://doi.org/10.1126/scitranslmed.3006820

Rearick, M. P., & Santello, M. (2002). Force synergies for multifingered grasping: effect of predictability in object center of mass and handedness. *Experimental Brain Research*, *144*(1), 38–49.

Rincon-Gonzalez, L., Buneo, C. A., & Tillery, S. I. H. (2011). The Proprioceptive Map of the Arm Is Systematic and Stable, but Idiosyncratic. *PLOS ONE*, *6*(11), e25214. https://doi.org/10.1371/journal.pone.0025214

Roach, B. J., & Mathalon, D. H. (2008). Event-Related EEG Time-Frequency Analysis: An Overview of Measures and An Analysis of Early Gamma Band Phase Locking in Schizophrenia. *Schizophrenia Bulletin*, *34*(5), 907–926. https://doi.org/10.1093/schbul/sbn093

Rodriguez, E., George, N., Lachaux, J. P., Martinerie, J., Renault, B., & Varela, F. J. (1999). Perception's shadow: long-distance synchronization of human brain activity. *Nature*, *397*(6718), 430–433. https://doi.org/10.1038/17120

Rossiter, H. E., Worthen, S. F., Witton, C., Hall, S. D., & Furlong, P. L. (2013). Gamma oscillatory amplitude encodes stimulus intensity in primary somatosensory cortex. *Frontiers in Human Neuroscience*, *7*. https://doi.org/10.3389/fnhum.2013.00362

Salada, M., Vishton, P., Colgate, J. E., & Frankel, E. (2004). Two experiments on the perception of slip at the fingertip. In *12th International Symposium on Haptic Interfaces for Virtual Environment and Teleoperator Systems, 2004. HAPTICS '04. Proceedings* (pp. 146–153). https://doi.org/10.1109/HAPTIC.2004.1287190

Salimi, I., Brochier, T., & Smith, A. M. (1999a). Neuronal Activity in Somatosensory Cortex of Monkeys Using a Precision Grip. I. Receptive Fields and Discharge Patterns. *Journal of Neurophysiology*, *81*(2), 825–834.

Salimi, I., Brochier, T., & Smith, A. M. (1999b). Neuronal Activity in Somatosensory Cortex of Monkeys Using a Precision Grip. II. Responses to Object Texture and Weights. *Journal of Neurophysiology*, *81*(2), 835–844.

Salimi, I., Brochier, T., & Smith, A. M. (1999c). Neuronal Activity in Somatosensory Cortex of Monkeys Using a Precision Grip. III. Responses to Altered Friction Perturbations. *Journal of Neurophysiology*, *81*(2), 845–857.

Seizova-Cajic, T., Karlsson, K., Bergstrom, S., McIntyre, S., & Birznieks, I. (2014). Lateral Skin Stretch Influences Direction Judgments of Motion Across the Skin. In *EuroHaptics (1)* (pp. 425–431). Retrieved from https://www.researchgate.net/profile/Tatjana_Seizova-Cajic/publication/264121418_Lateral_Skin_Stretch_Influences_Direction_Judgments_of_Motion_Across_the_Skin/links/53cee7600cf2fd75bc59abf7/Lateral-Skin-Stretch-Influences-Direction-Judgments-of-Motion-Across-the-Skin.pdf

Sinclair, R. J., & Burton, H. (1991). Neuronal activity in the primary somatosensory cortex in monkeys (Macaca mulatta) during active touch of textured surface gratings: responses to groove width, applied force, and velocity of motion. *Journal of Neurophysiology*, *66*(1), 153–169.

Song, W., & Francis, J. T. (2013). Tactile information processing in primate hand somatosensory cortex (S1) during passive arm movement. *Journal of Neurophysiology*, *110*(9), 2061–2070. https://doi.org/10.1152/jn.00893.2012

Srinivasan, M. A., Whitehouse, J. M., & LaMotte, R. H. (1990). Tactile detection of slip: surface microgeometry and peripheral neural codes. *Journal of Neurophysiology*, *63*(6), 1323–1332.

Strick, P. L., & Preston, J. B. (1982a). Two representations of the hand in area 4 of a primate. I. Motor output organization. *Journal of Neurophysiology*, *48*(1), 139–149.

Strick, P. L., & Preston, J. B. (1982b). Two representations of the hand in area 4 of a primate. II. Somatosensory input organization. *Journal of Neurophysiology*, *48*(1), 150–159.

Tallon-Baudry, C., & Bertrand, O. (1999). Oscillatory gamma activity in humans and its role in object representation. *Trends in Cognitive Sciences*, *3*(4), 151–162.

Tallon-Baudry, C., Bertrand, O., Delpuech, C., & Pernier, J. (1996). Stimulus Specificity of Phase-Locked and Non-Phase-Locked 40 Hz Visual Responses in Human. *Journal of Neuroscience*, *16*(13), 4240–4249.

Tallon-Baudry, C., Bertrand, O., Delpuech, C., & Pernier, J. (1997). Oscillatory γ-Band (30–70 Hz) Activity Induced by a Visual Search Task in Humans. *The Journal of Neuroscience*, *17*(2), 722–734.

Tan, D., Schieffer, M. A., Graczyk, E., Keith, M., Anderson, J. R., & Tyler, D. J. (2014). Restoring Sensation in Amputees: Chronic Stability of Implanted Cuff Electrodes. In *Proc Myoelectric Controls/Powered Prosthetics Symp*. Fredericton, New Brunswick, Canada.

Tan, D. W., Schiefer, M. A., Keith, M. W., Anderson, J. R., & Tyler, D. J. (2015). Stability and selectivity of a chronic, multi-contact cuff electrode for sensory stimulation in human amputees. *Journal of Neural Engineering*, *12*(2), 026002. https://doi.org/10.1088/1741-2560/12/2/026002

Taylor, M. M., & Lederman, S. J. (1975). Tactile roughness of grooved surfaces: A model and the effect of friction. *Perception & Psychophysics*, *17*(1), 23–36. https://doi.org/10.3758/BF03203993

Tecchio, F., Zappasodi, F., Porcaro, C., Barbati, G., Assenza, G., Salustri, C., & Maria Rossini, P. (2008). High-gamma band activity of primary hand cortical areas: A sensorimotor feedback efficiency index. *NeuroImage*, *40*(1), 256–264. https://doi.org/10.1016/j.neuroimage.2007.11.038

Thonnard, J., Saels, P., Van den Bergh, P., & Lejeune, T. (1999). Effects of chronic median nerve compression at the wrist on sensation and manual skills. *Experimental Brain Research*, *128*(1–2), 61–64.

Tremblay, F., Ageranioti-Belanger, S. A., & Chapman, C. E. (1996). Cortical mechanisms underlying tactile discrimination in the monkey. I. Role of primary somatosensory cortex in passive texture discrimination. *Journal of Neurophysiology*, *76*(5), 3382–3403.

van Ede, F., Szebényi, S., & Maris, E. (2014). Attentional modulations of somatosensory alpha, beta and gamma oscillations dissociate between anticipation and stimulus processing. *NeuroImage*, *97*, 134–141. https://doi.org/10.1016/j.neuroimage.2014.04.047

Walker, C. F., Lockhead, G. R., Markle, D. R., & McElhaney, J. H. (1977). Parameters of stimulation and perception in an artificial sensory feedback system. *Journal of Bioengineering*, *1*(3), 251–256.

Wang, Q., & Hayward, V. (2007). In vivo biomechanics of the fingerpad skin under local tangential traction. *Journal of Biomechanics*, *40*(4), 851–860. https://doi.org/10.1016/j.jbiomech.2006.03.004

Ward, L. M., Doesburg, S. M., Kitajo, K., MacLean, S. E., & Roggeveen, A. B. (2006). Neural synchrony in stochastic resonance, attention, and consciousness. *Canadian Journal of Experimental Psychology/Revue Canadienne de Psychologie Expérimentale*, *60*(4), 319.

Webster, R. J., III, Murphy, T. E., Verner, L. N., & Okamura, A. M. (2005). A Novel Two-dimensional Tactile Slip Display: Design, Kinematics and Perceptual Experiments. *ACM Trans. Appl. Percept.*, *2*(2), 150–165. https://doi.org/10.1145/1060581.1060588

Westling, G., & Johansson, R. S. (1984). Factors influencing the force control during precision grip. *Experimental Brain Research*, *53*(2), 277–284. https://doi.org/10.1007/BF00238156

Westling, G., & Johansson, R. S. (1987). Responses in glabrous skin mechanoreceptors during precision grip in humans. *Experimental Brain Research*, *66*(1), 128–140. https://doi.org/10.1007/BF00236209

Wheat, H. E., & Goodwin, A. W. (2000). Tactile discrimination of gaps by slowly adapting afferents: effects of population parameters and anisotropy in the fingerpad. *Journal of Neurophysiology*, *84*(3), 1430–1444.

Winterer, G., Ziller, M., Dorn, H., Frick, K., Mulert, C., Wuebben, Y., … Coppola, R. (2000). Schizophrenia: reduced signal-to-noise ratio and impaired phase-locking during information processing. *Clinical Neurophysiology*, *111*(5), 837–849. https://doi.org/10.1016/S1388-2457(99)00322-3

Witney, A. G., Wing, A., Thonnard, J.-L., & Smith, A. M. (2004). The cutaneous contribution to adaptive precision grip. *Trends in Neurosciences*, *27*(10), 637–643. https://doi.org/10.1016/j.tins.2004.08.006

Wolfe, J., Hill, D. N., Pahlavan, S., Drew, P. J., Kleinfeld, D., & Feldman, D. E. (2008). Texture Coding in the Rat Whisker System: Slip-Stick Versus Differential Resonance. *PLOS Biology*, *6*(8), e215. https://doi.org/10.1371/journal.pbio.0060215

Wood, C. C., Allison, T., Goff, W. R., Williamson, P. D., & Spencer, D. D. (1980). On the Neural Origin of P300 in Man. *Progress in Brain Research*, *54*, 51–56. https://doi.org/10.1016/S0079-6123(08)61605-2

Xerri, C., Coq, J., Merzenich, M., & Jenkins, W. (1996). Experience-induced plasticity of cutaneous maps in the primary somatosensory cortex of adult monkeys and rats. *Journal of Physiology-Paris*, *90*(3–4), 277–287. https://doi.org/10.1016/S0928-4257(97)81438-6

Yamaguchi, S., & Knight, R. T. (1991). P300 generation by novel somatosensory stimuli. *Electroencephalography and Clinical Neurophysiology*, *78*(1), 50–55. https://doi.org/10.1016/0013-4694(91)90018-Y

Yang, J., & Zhang, Q. (2009). P300 as an index of implicit self-esteem. *Neurological Research*. https://doi.org/10.1179/174313209X431138

Yau, J. M., Connor, C. E., & Hsiao, S. S. (2013). Representation of tactile curvature in macaque somatosensory area 2. *Journal of Neurophysiology*, *109*(12), 2999–3012. https://doi.org/10.1152/jn.00804.2012

Yordanova, J., Kolev, V., & Tamer, D. (1997, December). The Phase-Locking of Auditory Gamma Band Responses in Humans is Sensitive to Task Processing [Journal (Paginated)]. Retrieved July 18, 2017, from http://cogprints.org/49/

Zhang, Z. G., Hu, L., Hung, Y. S., Mouraux, A., & Iannetti, G. D. (2012). Gamma-Band Oscillations in the Primary Somatosensory Cortex—A Direct and Obligatory Correlate of Subjective Pain Intensity. *Journal of Neuroscience*, *32*(22), 7429–7438. https://doi.org/10.1523/JNEUROSCI.5877-11.2012

APPENDIX A

ANIMAL PROTOCOLS

Institutional Animal Care and Use Committee (IACUC)
Office of Research Integrity and Assurance
Arizona State University
660 South Mill Avenue, Suite 315
Tempe, Arizona 85287-6111
Phone: (480) 965-4387 *FAX:* (480) 965-7772

Animal Protocol Review

ASU Protocol Number: **12-1206R**
Protocol Title: **Sensory Representations and Learning in Skilled Motor Tasks**
Principal Investigator: **Stephen Helms Tillery**
Date of Action: **07/28/2011**

The animal protocol review was considered by the Committee and the following decisions were made:

- ☐ The original protocol was APPROVED as presented.
- ☒ The revised protocol was APPROVED as presented.
- ☐ The protocol was APPROVED with RESTRICTIONS or CHANGES as noted below. The project can only be pursued, subject to your acceptance of these restriction or changes. If you are not agreeable, contact the IACUC Chairperson immediately.
- ☐ The Committee requests CLARIFICATIONS or CHANGES in the protocol as described in the attached memorandum. The protocol will be considered when these issues are clarified and the revised protocol is submitted.
- ☐ The protocol was approved, subject to the approval of a WAIVER of provisions of NIH policy as noted below. Waivers require written approval from the granting agencies.
- ☐ The protocol was DISAPPROVED for reasons outlined in the attached memorandum

Institutional Animal Care and Use Committee (IACUC)
Office of Research Integrity and Assurance
Arizona State University
660 South Mill Avenue, Suite 315
Tempe, Arizona 85287-6111
Phone: (480) 965-4387 *FAX:* (480) 965-7772

Animal Protocol Review

ASU Protocol Number: **15-1427R**
Protocol Title: **Dexterous Hand Control through Fascicular Targeting (DEFT)**
Principal Investigator: **Stephen Helms Tillery**
Date of Action: **4/24/2015**

The animal protocol review was considered by the Committee and the following decisions were made:

The protocol was approved as presented.

If you have not already done so, documentation of Level III Training (i.e., procedure-specific training) will need to be provided to the IACUC office before participants can perform procedures independently. For more information on Level III requirements see https://researchintegrity.asu.edu/training/animals/levelthree.

Total # of Animals: 4

APPENDIX B

CUSTOM TRANSCUTANEOUS ELECTRODE HOUSING

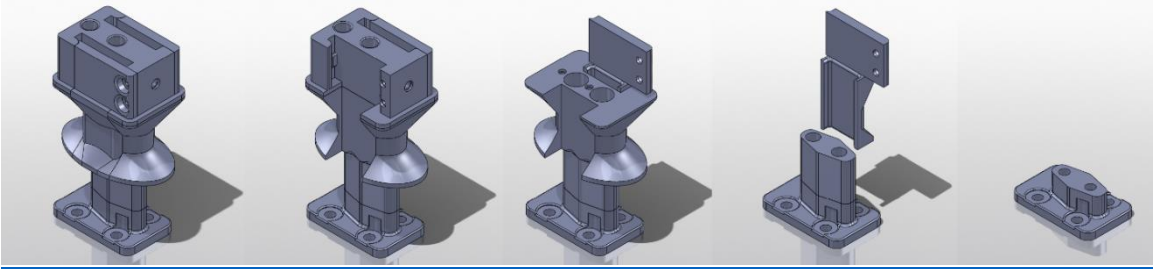

Custom designed transcutaneous pedestal with slotted walls that securely mount of the connector and wires of the electrode array. Manufactured from laser sintered titanium with a resolution of 20 microns. The bottom mounted onto a previously implanted osteo-integrated bone plate and the rest is sequentially installed and secured.

APPENDIX C

PERIPHERAL ELECTRODES STABILITY MEASUREMENTS

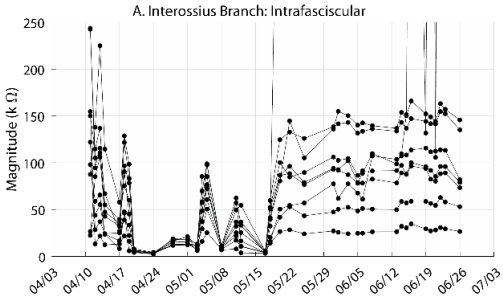
A. Interossius Branch: Intrafasciscular
Magnitude (k Ω)
0
50
100
150
200
250
04/03
04/10
04/17
04/24
05/01
05/08
05/15
05/22
05/29
06/05
06/12
06/19
06/26
07/03

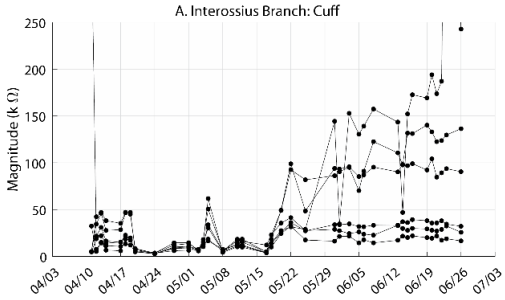
A. Interossius Branch: Cuff
Magnitude (k Ω)
0
50
100
150
200
250
04/03
04/10
04/17
04/24
05/01
05/08
05/15
05/22
05/29
06/05
06/12
06/19
06/26
07/03

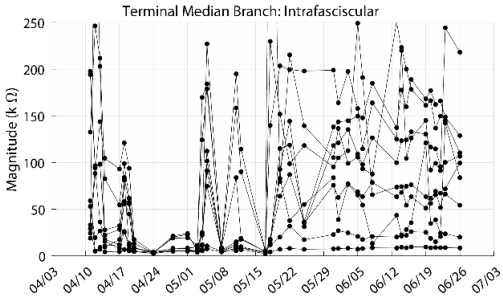
Terminal Median Branch: Intrafasciscular
Magnitude (k Ω)
0
50
100
150
200
250
04/03
04/10
04/17
04/24
05/01
05/08
05/15
05/22
05/29
06/05
06/12
06/19
06/26
07/03

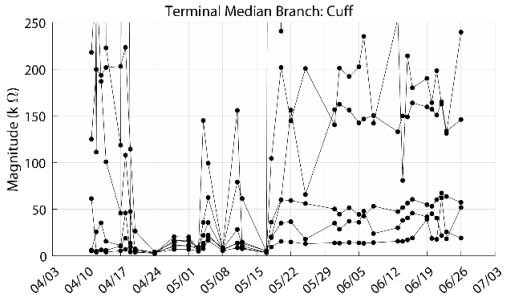
Terminal Median Branch: Cuff
Magnitude (k Ω)
0
50
100
150
200
250
04/03
04/10
04/17
04/24
05/01
05/08
05/15
05/22
05/29
06/05
06/12
06/19
06/26
07/03

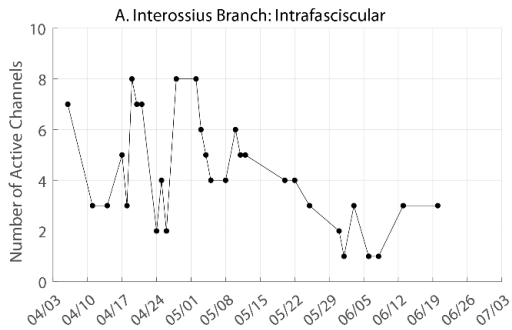
A. Interossius Branch: Intrafasciscular
Number of Active Channels
0
2
4
6
8
10
04/03
04/10
04/17
04/24
05/01
05/08
05/15
05/22
05/29
06/05
06/12
06/19
06/26
07/03

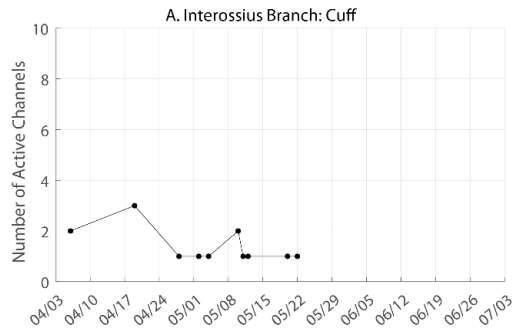
A. Interossius Branch: Cuff
Number of Active Channels
0
2
4
6
8
10
04/03
04/10
04/17
04/24
05/01
05/08
05/15
05/22
05/29
06/05
06/12
06/19
06/26
07/03

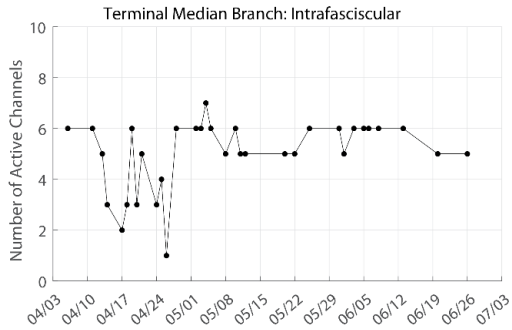
Terminal Median Branch: Intrafasciscular
Number of Active Channels
0
2
4
6
8
10
04/03
04/10
04/17
04/24
05/01
05/08
05/15
05/22
05/29
06/05
06/12
06/19
06/26
07/03

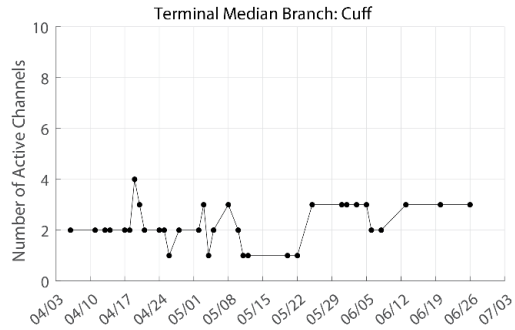
Terminal Median Branch: Cuff
Number of Active Channels
0
2
4
6
8
10
04/03
04/10
04/17
04/24
05/01
05/08
05/15
05/22
05/29
06/05
06/12
06/19
06/26
07/03

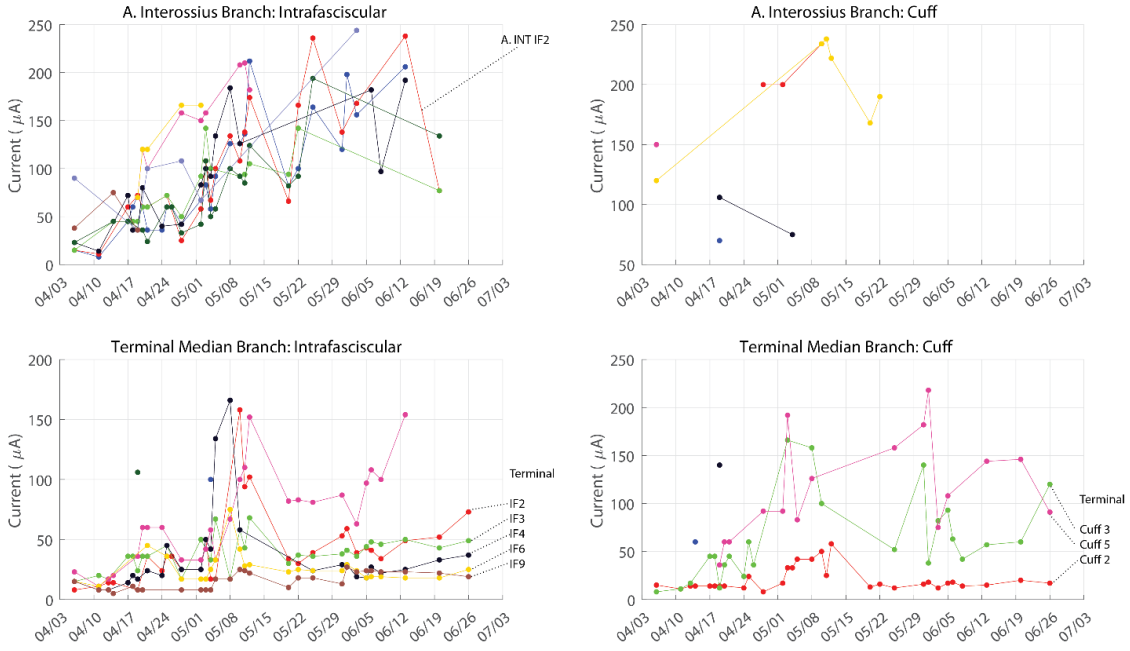
A. Interossius Branch: Intrafasciscular
A. INT IF2
A. Interossius Branch: Cuff
Terminal Median Branch: Intrafasciscular
Terminal
IF2
IF3
IF4
IF6
IF9
Terminal Median Branch: Cuff
Terminal
Cuff 3
Cuff 5
Cuff 2
Current (μA)
04/03
04/10
04/17
04/24
05/01
05/08
05/15
05/22
05/29
06/05
06/12
06/19
06/26
07/03

APPENDIX D

EVOKED POTENTIALS AND GAMMA FOR EACH STIMULATION ELECTRODE

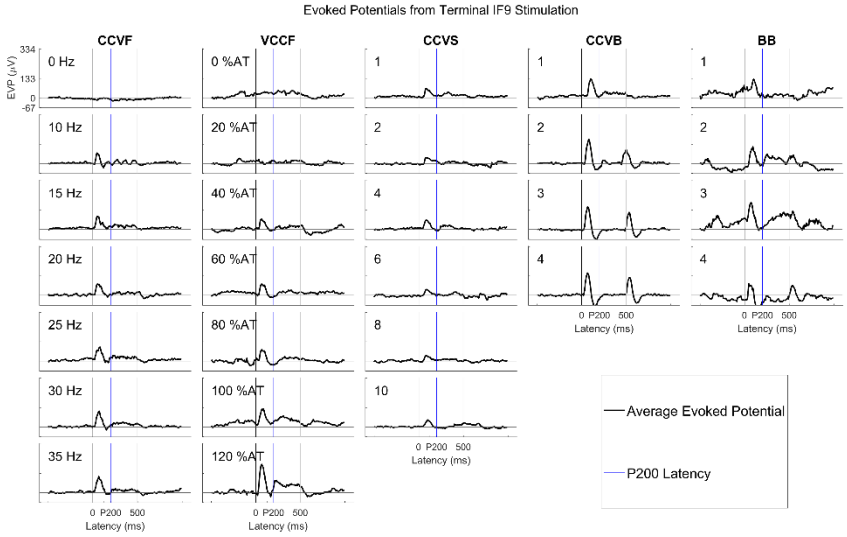
Evoked Potentials from Terminal IF9 Stimulation
CCVF
VCCF
CCVS
CCVB
BB
EVP (μV)
334
133
0
-67
0 Hz
10 Hz
15 Hz
20 Hz
25 Hz
30 Hz
35 Hz
0 %AT
20 %AT
40 %AT
60 %AT
80 %AT
100 %AT
120 %AT
1
2
4
6
8
10
3
0 P200 500
Latency (ms)
Average Evoked Potential
P200 Latency

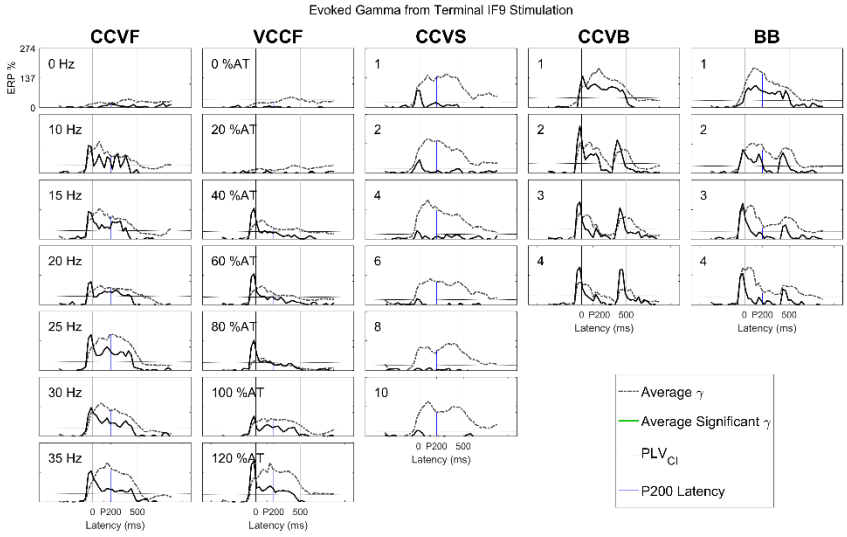
Evoked Gamma from Terminal IF9 Stimulation
CCVF
VCCF
CCVS
CCVB
BB
ERP %
274
137
0
0 Hz
10 Hz
15 Hz
20 Hz
25 Hz
30 Hz
35 Hz
0 %AT
20 %AT
40 %AT
60 %AT
80 %AT
100 %AT
120 %AT
1
2
4
6
8
10
3
0 P200 500
Latency (ms)
Average γ
Average Significant γ
PLV_CI
P200 Latency

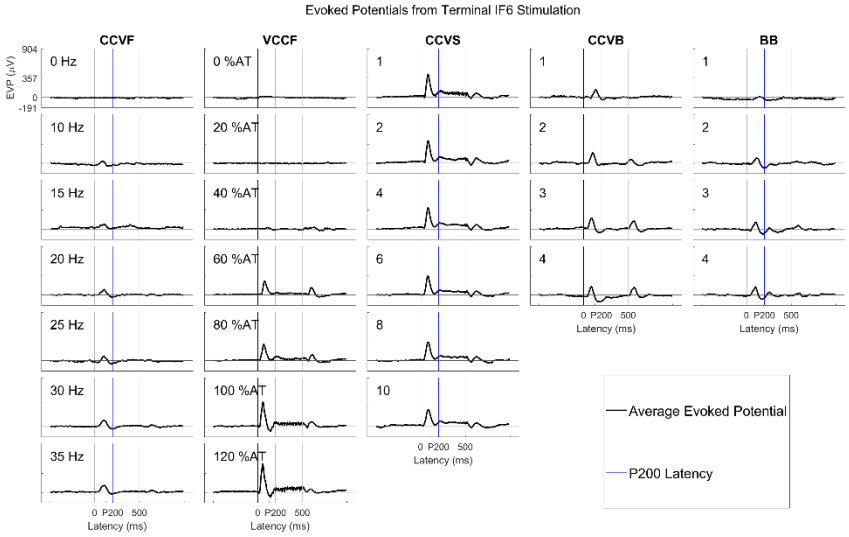
Evoked Potentials from Terminal IF6 Stimulation
CCVF
VCCF
CCVS
CCVB
BB
EVP (μV)
904
357
0
-191
0 Hz
10 Hz
15 Hz
20 Hz
25 Hz
30 Hz
35 Hz
0 %AT
20 %AT
40 %AT
60 %AT
80 %AT
100 %AT
120 %AT
1
2
4
6
8
10
3
0 P200 500
Latency (ms)
Average Evoked Potential
P200 Latency

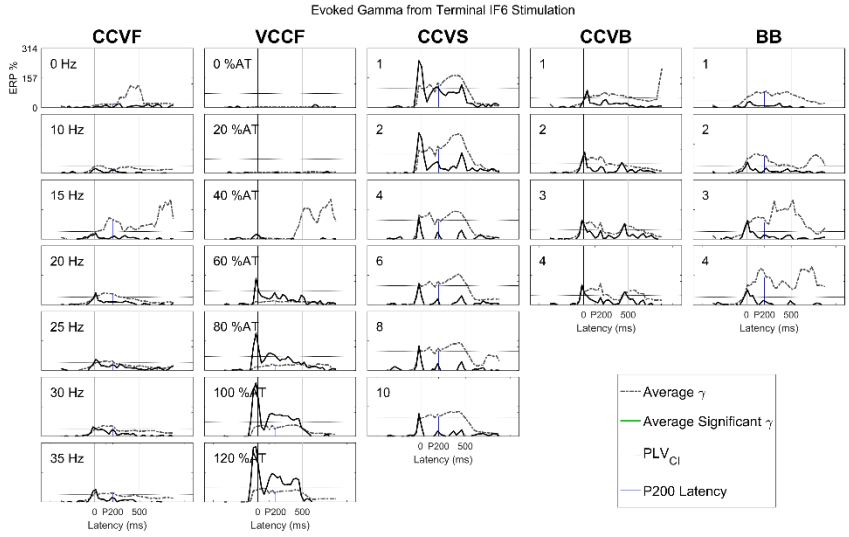
Evoked Gamma from Terminal IF6 Stimulation
CCVF
VCCF
CCVS
CCVB
BB
ERP %
314
157
0
0 Hz
10 Hz
15 Hz
20 Hz
25 Hz
30 Hz
35 Hz
0 %AT
20 %AT
40 %AT
60 %AT
80 %AT
100 %AT
120 %AT
1
2
4
6
8
10
3
0 P200 500
Latency (ms)
Average γ
Average Significant γ
PLV_CI
P200 Latency

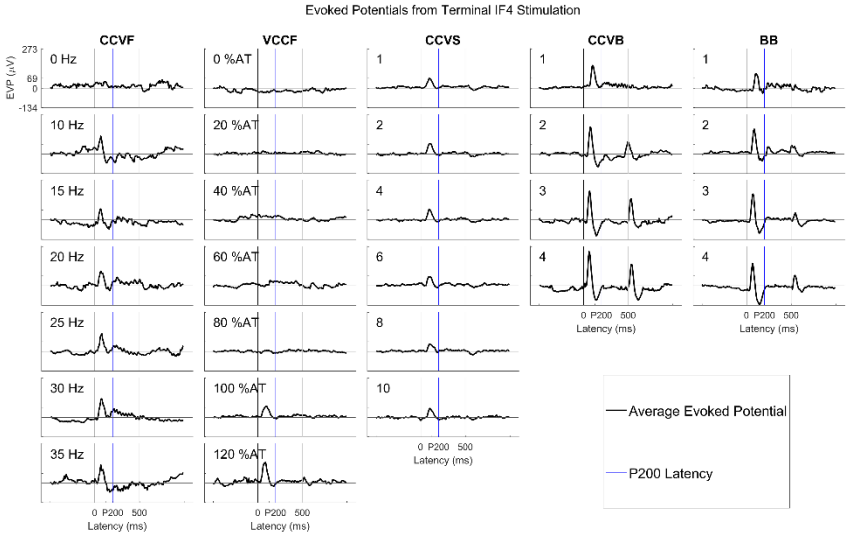
Evoked Potentials from Terminal IF4 Stimulation
CCVF
VCCF
CCVS
CCVB
BB
EVP (μV)
273
69
0
-134
0 Hz
10 Hz
15 Hz
20 Hz
25 Hz
30 Hz
35 Hz
0 %AT
20 %AT
40 %AT
60 %AT
80 %AT
100 %AT
120 %AT
1
2
4
6
8
10
3
0 P200 500
Latency (ms)
Average Evoked Potential
P200 Latency

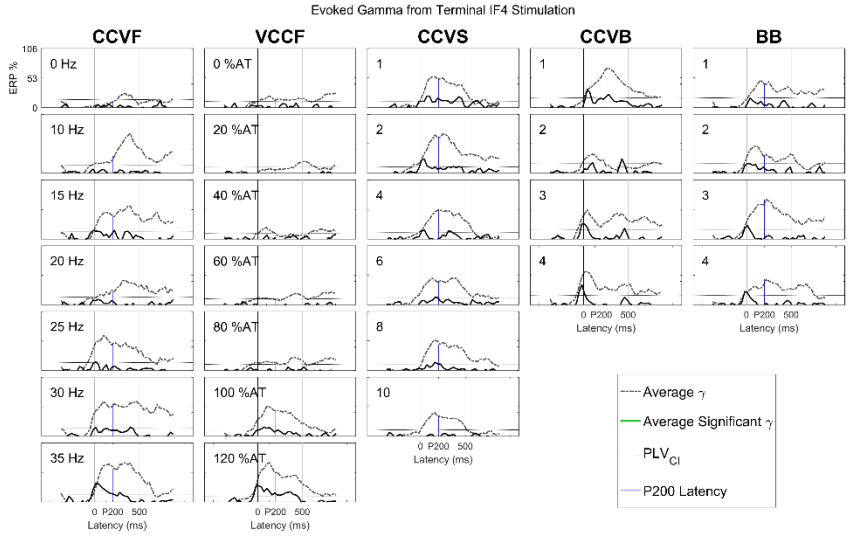
Evoked Gamma from Terminal IF4 Stimulation
CCVF
VCCF
CCVS
CCVB
BB
ERP %
106
53
0
0 Hz
10 Hz
15 Hz
20 Hz
25 Hz
30 Hz
35 Hz
0 %AT
20 %AT
40 %AT
60 %AT
80 %AT
100 %AT
120 %AT
1
2
4
6
8
10
3
0 P200 500
Latency (ms)
Average γ
Average Significant γ
PLV_CI
P200 Latency

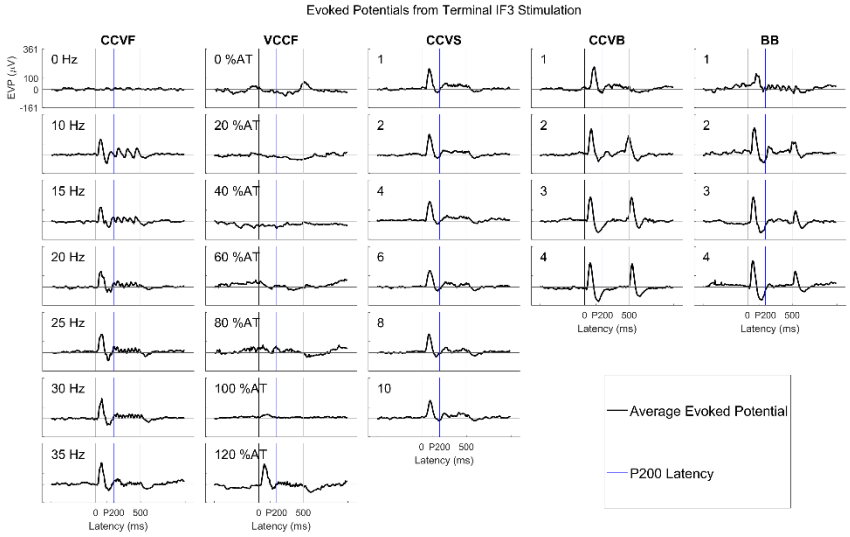
Evoked Potentials from Terminal IF3 Stimulation
CCVF
VCCF
CCVS
CCVB
BB
EVP (μV)
361
100
0
-161
0 Hz
10 Hz
15 Hz
20 Hz
25 Hz
30 Hz
35 Hz
0 %AT
20 %AT
40 %AT
60 %AT
80 %AT
100 %AT
120 %AT
1
2
4
6
8
10
3
0 P200 500
Latency (ms)
Average Evoked Potential
P200 Latency

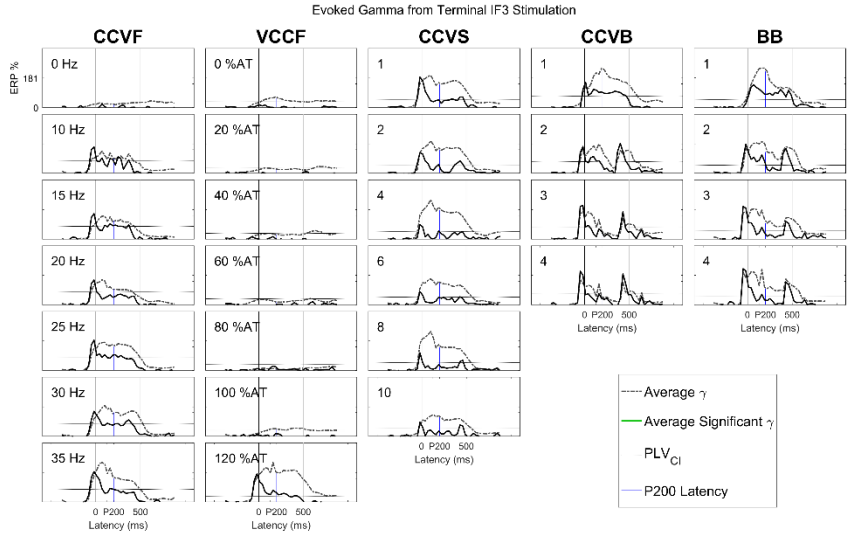
Evoked Gamma from Terminal IF3 Stimulation
CCVF
VCCF
CCVS
CCVB
BB
ERP %
181
0
0 Hz
10 Hz
15 Hz
20 Hz
25 Hz
30 Hz
35 Hz
0 %AT
20 %AT
40 %AT
60 %AT
80 %AT
100 %AT
120 %AT
1
2
4
6
8
10
3
0 P200 500
Latency (ms)
Average γ
Average Significant γ
PLVCI
P200 Latency

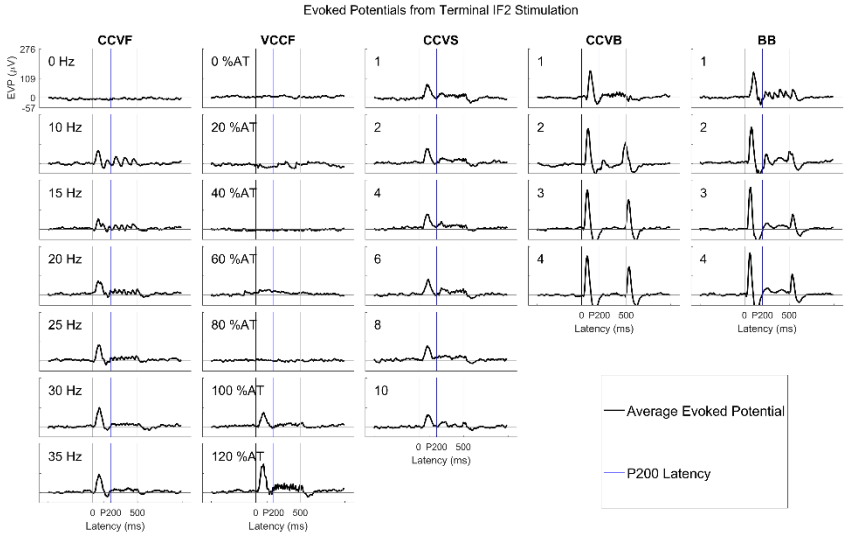
Evoked Potentials from Terminal IF2 Stimulation
CCVF
VCCF
CCVS
CCVB
BB
EVP (μV)
276
109
0
-57
0 Hz
10 Hz
15 Hz
20 Hz
25 Hz
30 Hz
35 Hz
0 %AT
20 %AT
40 %AT
60 %AT
80 %AT
100 %AT
120 %AT
1
2
4
6
8
10
3
0 P200 500
Latency (ms)
Average Evoked Potential
P200 Latency

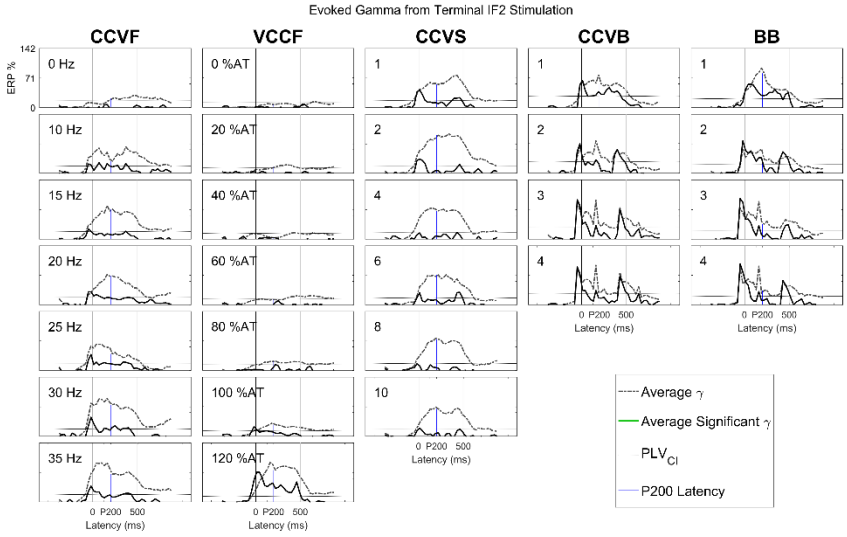
Evoked Gamma from Terminal IF2 Stimulation
CCVF
VCCF
CCVS
CCVB
BB
ERP %
142
71
0
0 Hz
10 Hz
15 Hz
20 Hz
25 Hz
30 Hz
35 Hz
0 %AT
20 %AT
40 %AT
60 %AT
80 %AT
100 %AT
120 %AT
1
2
4
6
8
10
3
0 P200 500
Latency (ms)
Average γ
Average Significant γ
PLV_CI
P200 Latency

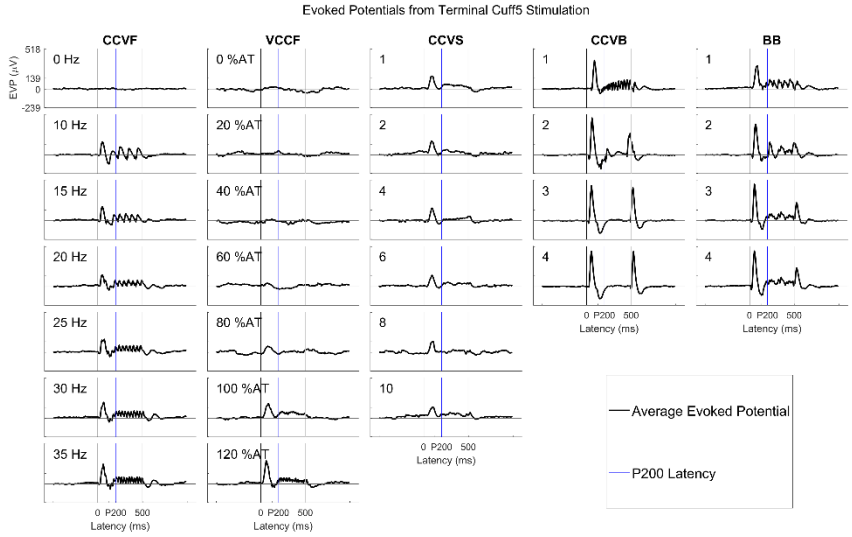
Evoked Potentials from Terminal Cuff5 Stimulation
CCVF
VCCF
CCVS
CCVB
BB
EVP (μV)
518
139
0
-239
0 Hz
10 Hz
15 Hz
20 Hz
25 Hz
30 Hz
35 Hz
0 %AT
20 %AT
40 %AT
60 %AT
80 %AT
100 %AT
120 %AT
1
2
4
6
8
10
3
0 P200 500
Latency (ms)
Average Evoked Potential
P200 Latency

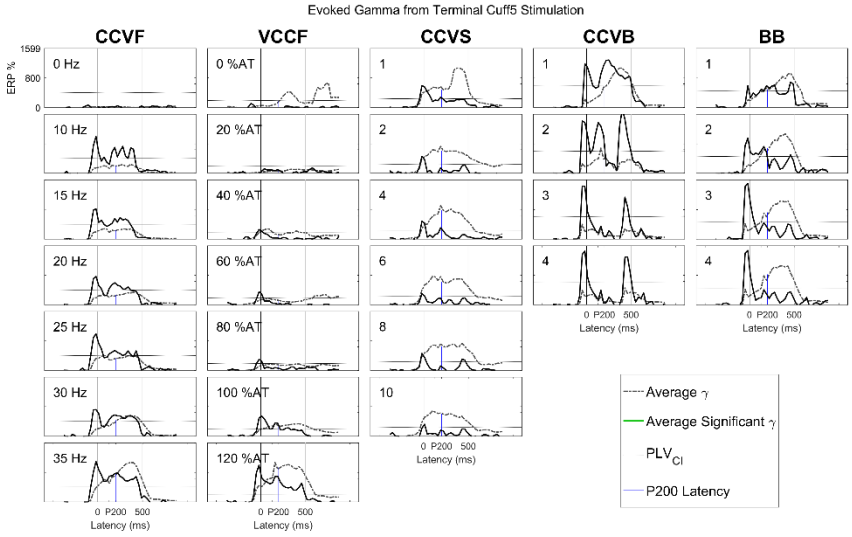
Evoked Gamma from Terminal Cuff5 Stimulation
CCVF
VCCF
CCVS
CCVB
BB
ERP %
1599
800
0
0 Hz
10 Hz
15 Hz
20 Hz
25 Hz
30 Hz
35 Hz
0 %AT
20 %AT
40 %AT
60 %AT
80 %AT
100 %AT
120 %AT
1
2
4
6
8
10
3
0 P200 500
Latency (ms)
Average γ
Average Significant γ
PLV_CI
P200 Latency

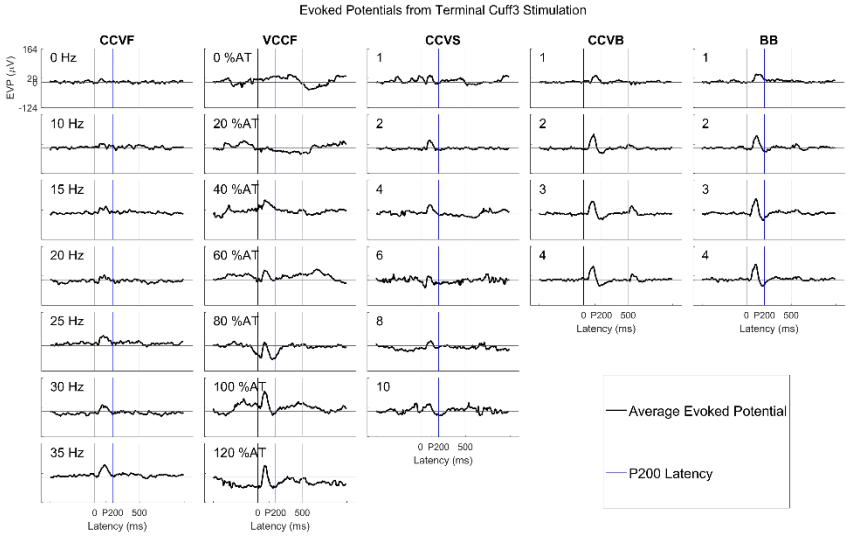
Evoked Potentials from Terminal Cuff3 Stimulation
CCVF
VCCF
CCVS
CCVB
BB
EVP (μV)
164
28
-124
0 Hz
10 Hz
15 Hz
20 Hz
25 Hz
30 Hz
35 Hz
0 %AT
20 %AT
40 %AT
60 %AT
80 %AT
100 %AT
120 %AT
1
2
4
6
8
10
3
0 P200 500
Latency (ms)
Average Evoked Potential
P200 Latency

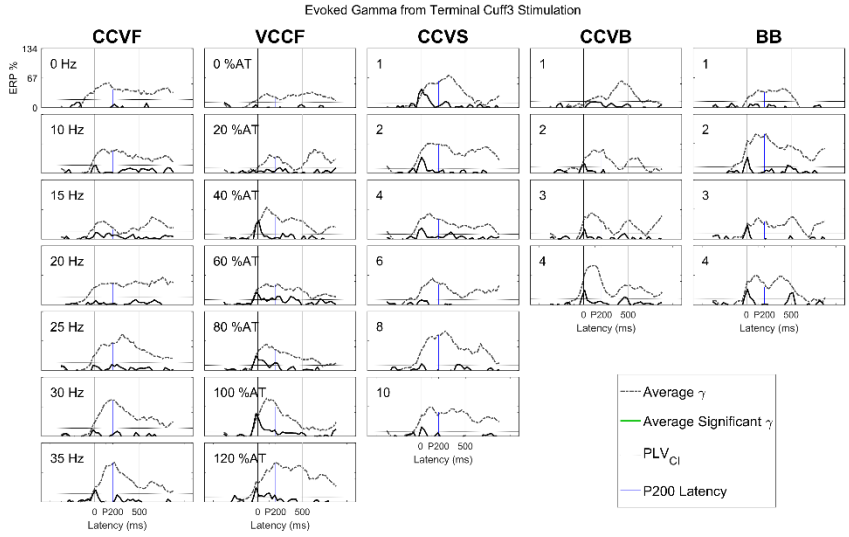
Evoked Gamma from Terminal Cuff3 Stimulation
CCVF
VCCF
CCVS
CCVB
BB
ERP %
134
67
0
0 Hz
10 Hz
15 Hz
20 Hz
25 Hz
30 Hz
35 Hz
0 %AT
20 %AT
40 %AT
60 %AT
80 %AT
100 %AT
120 %AT
1
2
4
6
8
10
3
0 P200 500
Latency (ms)
Average γ
Average Significant γ
PLV$_{CI}$
P200 Latency

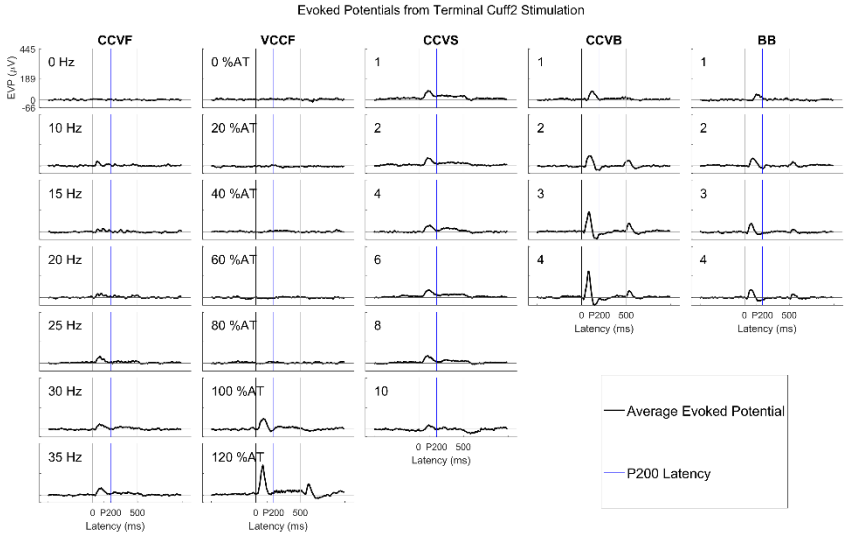
Evoked Potentials from Terminal Cuff2 Stimulation
CCVF
VCCF
CCVS
CCVB
BB
EVP (μV)
445
189
0
-66
0 Hz
10 Hz
15 Hz
20 Hz
25 Hz
30 Hz
35 Hz
0 %AT
20 %AT
40 %AT
60 %AT
80 %AT
100 %AT
120 %AT
1
2
4
6
8
10
3
0 P200 500
Latency (ms)
Average Evoked Potential
P200 Latency

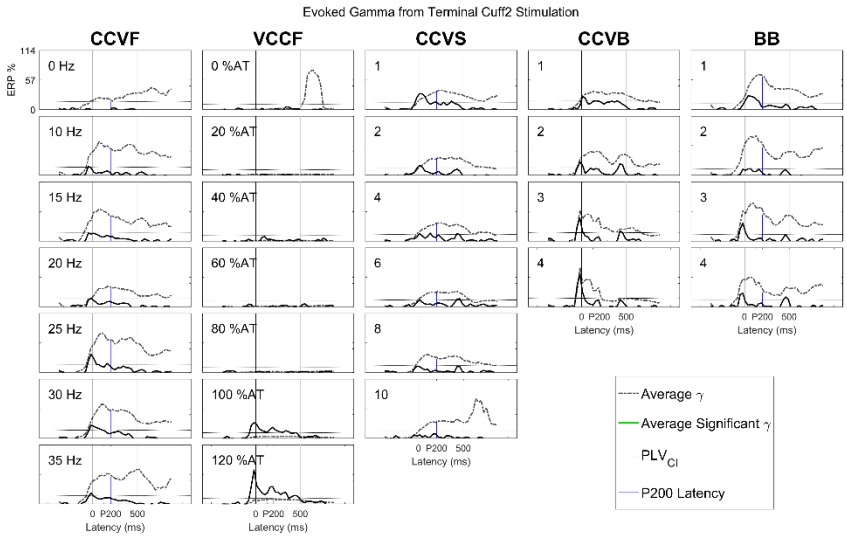
Evoked Gamma from Terminal Cuff2 Stimulation
CCVF
VCCF
CCVS
CCVB
BB
ERP %
114
57
0
0 Hz
10 Hz
15 Hz
20 Hz
25 Hz
30 Hz
35 Hz
0 %AT
20 %AT
40 %AT
60 %AT
80 %AT
100 %AT
120 %AT
1
2
4
6
8
10
3
0 P200 500
Latency (ms)
Average γ
Average Significant γ
PLV_CI
P200 Latency

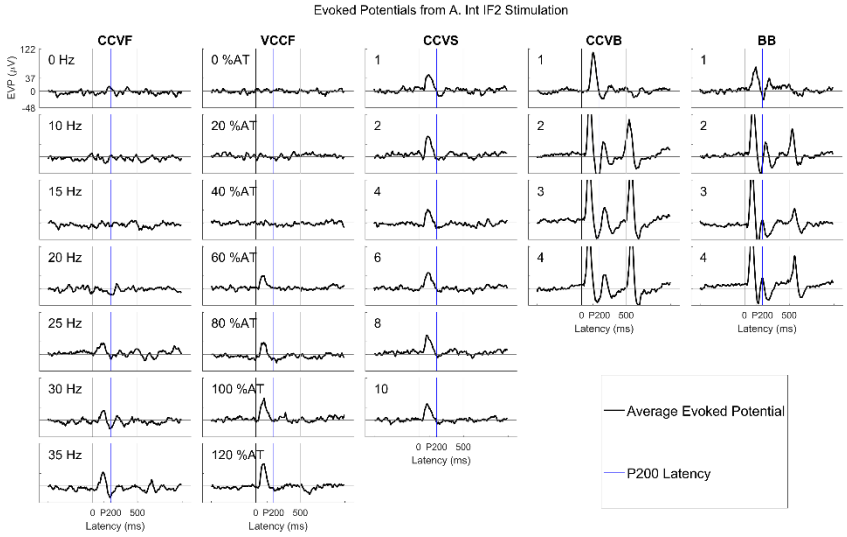
Evoked Potentials from A. Int IF2 Stimulation
CCVF
VCCF
CCVS
CCVB
BB
EVP (μV)
122
37
0
-48
0 Hz
10 Hz
15 Hz
20 Hz
25 Hz
30 Hz
35 Hz
0 %AT
20 %AT
40 %AT
60 %AT
80 %AT
100 %AT
120 %AT
1
2
4
6
8
10
3
0 P200 500
Latency (ms)
Average Evoked Potential
P200 Latency

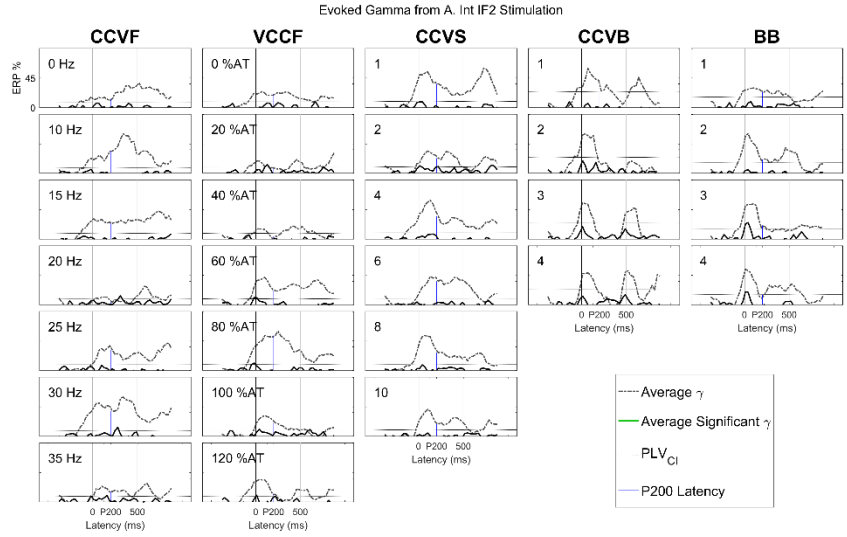
Evoked Gamma from A. Int IF2 Stimulation
CCVF
VCCF
CCVS
CCVB
BB
ERP %
45
0
0 Hz
10 Hz
15 Hz
20 Hz
25 Hz
30 Hz
35 Hz
0 %AT
20 %AT
40 %AT
60 %AT
80 %AT
100 %AT
120 %AT
1
2
4
6
8
10
3
0 P200 500
Latency (ms)
Average γ
Average Significant γ
PLV_CI
P200 Latency

BIOGRAPHICAL SKETCH

Justin Tanner earned dual BS in Bioengineering and Neuroscience from Washington State University in 2010. Entering the Biomedical Engineering PhD program immediately after, he has been working under Stephen Helms Tillery in the Sensory Motor Research Group. Using peripheral nerve stimulation based on dynamics of complex grip responses, Justin's work focuses on mimicking cortical representations of touch in order to recreate appropriate tactile sensation. His research builds on psychophysical experiments for tactile information, single unit and LFP neural recording in primate cortex, and peripheral nerve stimulation in primates and humans.